ADMINISTRATIVE DRAFT

MODESTO SUBBASIN GROUNDWATER SUSTAINABILITY PLAN (GSP)

STANISLAUS AND TUOLUMNE RIVERS GROUNDWATER BASIN ASSOCIATION GROUNDWATER SUSTAINABILITY AGENCY (STRGBA GSA) and TUOLUMNE GSA

July 2020

TODD GROUNDWATER

2490 Mariner Square Loop, Suite 215
Alameda, CA 94501
510.747.6920
www.toddgroundwater.com

SIGNATURE PAGE

First Author Name, Credentials

First Author Title

Second Author Name, Credentials

Second Author Title

Third Author Name, Credentials

Third Author Title

ACKNOWLEDGMENTS

Funding for this project has been provided in full or in part from the Water Quality, Supply, and Infrastructure Improvement Act of 2014 and through an agreement with the State Department of Water Resources.

Table of Contents

List of Tables

List of Figures

Acronyms

CDFW	California Department of Fish and Wildlife
CDPH	California Department of Public Health
COC	Constituents of Concern
CV-SALTS	Central Valley Salinity Alternatives for Long-term Sustainability
DBCP	Dibromochloropropane
DNAPL	Dense Non-Aqueous Phase Liquid
DO	Dissolved Oxygen
DOGGR	California Department of Oil, Gas and Geothermal Resources
DWR	Department of Water Resources, State of California
ESA	European Space Agency
ft/day	feet per day
GAMA	Groundwater Ambient Monitoring and Assessment
GDE	Groundwater Dependent Ecosystem
gpd/ft	gallons per day per foot
gpm	gallons per minute
INSAR	Interferometric Synthetic Aperture Radar
mg/L	milligrams per liter
MID	Modesto Irrigation District
MRWTP	Modesto Regional Water Treatment Plant
MSL	Mean Sea Level
NED	National Elevation Dataset
NL	Notification Level
NWIS	National Water Information System
PCE	Tetrachloroethylene
ppm	parts per million
PRISM	Parameter-elevation Relationships on Independent Slopes Model

QA/QC	Quality Assurance/Quality Control
SMCL	California Secondary Maximum Contaminant Level
T	Transmissivity
TCP	1,2,3-Trichloropropane
TDS	Total Dissolved Solids
TNC	The Nature Conservancy
TRE	TRE ALTAMIRA Inc.
USDA	United States Department of Agriculture
umhos/cm	micromohs per centimeter
USGS	United States Geological Survey
VOCs	Volatile Organic Compounds
WDR	Waste Discharge Requirements
WY	Water Year

3. BASIN SETTING

The Modesto Subbasin of the San Joaquin Valley Groundwater Basin (DWR Basin 5-22.02) is approximately 247,000 acres (385 square miles) and located in the northern San Joaquin Valley in Stanislaus County. It is bordered by the Stanislaus River on the north, Tuolumne River on the south, San Joaquin River on the west and the foothills of the Sierra Nevada on the east. The Subbasin is categorized as high priority in DWR's 2019 Basin Prioritization (DWR, 2019) based on its:

- number of public supply wells: 194 or 0.5 per square mile (DWR prioritization score of 4 out of 5);
- number of production wells: 4,009 or 10.5 per square mile (score of 4 out of 5);
- irrigated acreage: 119,066 acres or 311 acres per square mile, covering approximately 48 percent of the Subbasin (score of 4 out of 5);
- groundwater use: 216,522 AF or 0.88 AF per acre (score of 5 out of 5); and
- declining groundwater levels: long term hydrographs show groundwater level decline.

Although categorized as high priority, the Subbasin is not one of the 21 groundwater basins determined by DWR to be critically overdrafted[1]. To mitigate potential future overdraft and provide a foundation for sustainable groundwater management in this high priority Subbasin, the physical conditions associated with the groundwater system, referred to as the Basin Setting, are documented and described herein. The Basin Setting consists of three interrelated analyses:

1. Hydrogeologic Conceptual Model, which provides a physical description of the groundwater Subbasin including the geologic and hydrogeologic setting, basin geometry and principal aquifers.
2. Groundwater Conditions, which describes groundwater occurrence and flow, groundwater levels and quality, and interconnected surface water.
3. Water Budgets, which provide an accounting of inflows and outflows of the surface water and groundwater systems for historical, current, and future conditions.

Because the water budget analysis is relatively complex, water budgets are presented in a separate **Section 4** of this GSP. The hydrogeologic conceptual model and groundwater conditions are described in the following sections.

[1] Two adjacent subbasins, Delta-Mendota and Eastern San Joaquin, have been designated as critically overdrafted.

3.1. HYDROGEOLOGIC CONCEPTUAL MODEL

The development of the hydrogeologic conceptual model is based on an analysis of the regional geologic and structural setting, physical setting, basin boundaries, and principal aquifers and aquitards. Key building blocks of the hydrogeologic conceptual model include the development of new hydrogeologic cross sections and analyses conducted by others, including published technical studies, data, and maps, along with data provided by member agencies of the STRGBA GSA.

3.1.1. Regional Geologic and Structural Setting

The Modesto Subbasin is in the northeastern San Joaquin Valley where valley-fill sediments overlie consolidated, westward-dipping sedimentary units and basement rock of the Sierra Nevada. Older units crop out in the eastern subbasin and dip west-southwest into the San Joaquin Valley below younger units. The surface geology of the Modesto Subbasin, showing relatively older units in the east and younger units in the west, is shown on **Figure 3-1**.

The San Joaquin Valley is a large northwest-trending structural trough in the southern Central Valley, up to 200 miles long and 70 miles wide and filled with marine and continental sediments up to 6 miles thick (Burow et al., 2004). It evolved during the Cenozoic era from tectonic activity and changes in sea level and climate (Bartow, 1991). Tectonic processes included basin subsidence, uplift of the Sierra Nevada and Coast Ranges, and associated deformation (Burow et al., 2004).

Bartow (1991) divides the San Joaquin Valley into five regions based on structural style. The Modesto Subbasin is within the northern Sierran block, which extends from the Stockton arch on the north to Fresno on the south This region is the least deformed area of the San Joaquin Valley (Bartow, 1991). Deformation in this region consists mostly of a southwest tilt and minor late Cenozoic normal faulting (Bartow, 1991). The normal faulting is mostly within the foothills, a result of the valley side of the Sierra block subsiding faster than the Sierra Nevada was rising (Bartow, 1991). Faults in the foothills, east of the Subbasin, are shown on **Figure 3-1**.

Geologic units along the eastern subbasin boundary represent the oldest units in the Subbasin and include the Valley Springs Formation of Late Miocene age and the underlying Ione Formation of Middle Eocene age. These two formations are labeled Tvs and Ei on **Figure 3-1**, respectively. These consolidated units were formed from mostly non-marine sediments and represent both the eastern lateral extent and the local bottom of the groundwater basin. Jurassic-age metamorphic and volcanic rocks of the Sierra Nevada are in contact with these formations to the east and underlie them locally. In general, the eastern groundwater basin boundary is coincident with the base of the Ione Formation, which crops out along the eastern boundary (**Figure 3-1**).

The Mehrten Formation (late Miocene) crops out along a small portion of the northeastern Subbasin boundary, but primarily crops out as remnant hills in the eastern Subbasin (Tm on **Figure 3-1**). This consolidated unit includes fluvial deposits (sandstone and conglomerates) consisting of eroded andesite and other rocks associated with volcanic eruptions in the adjacent Sierra Nevada. The re-working of andesite has produced distinctive black sands, which are locally well-sorted with relatively high permeability. These zones represent the primary aquifer system in the eastern Subbasin, especially in areas where the younger overlying sediments (discussed below) are unsaturated.

The younger geologic units in the Subbasin include alluvial sediments of Neogene (Pliocene) and Quaternary (Pleistocene and Holocene) age, including Quaternary alluvium deposited along the Stanislaus and Tuolumne rivers (shown in light yellow and labeled Q on **Figure 3-1**) and other alluvial/riverbank/terrace deposits. These additional deposits are also identified on **Figure 3-1** where they occur at the surface, and are listed below from oldest to youngest:

- Laguna Formation (Pl) of Pliocene age,
- Turlock Lake Formation (Qtl) of Early Pleistocene age,
- Riverbank Formation (Qr) of Middle Pleistocene age and
- Modesto Formation (Qm) of Late Pleistocene age.

The Corcoran Clay represents a regional aquitard in the upper part of the Turlock Lake Formation. The Corcoran Clay is a laterally-extensive clay unit deposited by an ancient lake that covers over 4,000 square miles in the San Joaquin Valley. It occurs beneath the western Subbasin and pinches out in the subsurface near Highway 99. The Corcoran Clay does not crop out and, as such, does not appear on **Figure 3-1**.

The Modesto Formation (Qm) is the primary surficial geologic unit in the western Subbasin. Younger alluvium (Q) is present along the Stanislaus and Tuolumne rivers and the Dos Palos Alluvium (Qdp) is present along the San Joaquin River.

The younger geologic units, including the Modesto Formation (Qm), Turlock Lake Formation (Qtl), Riverbank Formation (Qr), and Mehrten Formation (Tm) have been associated with high quality groundwater as characterized by total dissolved solids (TDS). The underlying older units of the Valley Springs Formation (Tvs) and the Ione Formation (Ei) have been associated with higher mineral and salt content. The hydrogeology and groundwater conditions in the Modesto Subbasin aquifer units are described in more detail in subsequent sections of the Basin Setting.

3.1.2. Physical Setting

3.1.2.1. Precipitation and Average Hydrologic Conditions

The Modesto Subbasin is characterized as a Mediterranean-type climate with hot, dry summers and cool, wet winters, with most of the precipitation occurring between November and March.

Figure 3-2 illustrates annual precipitation in the Modesto Subbasin on a water year (WY) basis from WY 1990 through 2017 as measured at the Modesto Irrigation District weather station in Modesto. The chart on **Figure 3-2** illustrates the variability in precipitation, from approximately 7.0 inches in WY 2014 to more than 24 inches in WY 1998. The long-term average rainfall in the Modesto Subbasin is about 12.6 inches per year based on data from 1961 – 2015. A Study Period from WY 1991 through WY 2015 has been selected for GSP analyses that is representative of average hydrologic conditions. The Study Period also overlaps the time period of a regional groundwater model being develop for the GSP and is associated with a relatively large amount of available data. As indicated on **Figure 3-2**, the average annual precipitation during the Study Period is 12.8 inches per year, which is within two percent of the long-term average.

Annual precipitation data on **Figure 3-2** is color-coded based on water year type using the San Joaquin Valley WY hydrologic classification indices (CDEC, 2018): wet (blue), above normal (green), below normal (brown), dry (yellow), and critically dry (red). The San Joaquin Valley WY indices do not always correlate directly with precipitation measured in the Modesto Subbasin because the indices are based on runoff from several rivers, including the Stanislaus, Tuolumne, Merced, and San Joaquin Rivers. However, the indices are a useful benchmark for establishing consistent water year types across numerous subbasins in the San Joaquin Valley.

Figure 3-2 shows that the wettest water years, with precipitation above 15 inches per year, occurred in water years 1993, 1995, 1996, 1998, 2000, 2005, 2010, 2011, 2016 and 2017 (all of which are designated as wet or above normal water year types, except water year 2016). The driest years, with precipitation less than 9 inches per year, occurred in water years 1990, 1991, 2004, 2007, 2009 and 2014 (all of which are designated as critically dry or dry water year types, except 2009).

Data from the PRISM Climate Group were compiled to evaluate spatial variability of precipitation across the Subbasin. These data are based on application of an interpolation model, *Parameter-elevation Relationships on Independent Slopes Model* (PRISM), to detailed datasets from 1895 to present as developed by Oregon State University and the U.S. Department of Agriculture. A PRISM isohyetal map showing 30-year average annual precipitation from 1981 – 2010 across the Subbasin is presented on **Figure 3-3**. This period is slightly wetter than the long-term average but provides the most complete data set for evaluation across the Subbasin.

As shown on **Figure 3-3**, the average annual precipitation varies across the Subbasin, increasing with topography from west to east. Average precipitation ranges from approximately 11 inches per year along the western Subbasin boundary to approximately 21 inches per year along the eastern boundary.

3.1.2.2. Topography

The Modesto Subbasin extends from the Sierra Nevada foothills to the San Joaquin Valley floor. Ground surface elevations dip to the west, from approximately 650 feet mean sea level (msl) in the foothills to less than 20 feet msl along the San Joaquin River. A Digital Elevation Map (DEM) of Subbasin topography based on the United States Geological Society (USGS) National Elevation Dataset (NED) is provided on **Figure 3-4** and illustrates these ground surface elevations.

The western Subbasin is relatively flat. Ground surface elevations rise from about 20 feet msl along the San Joaquin River to about 200 feet msl near the center of the Subbasin. The topography in the eastern Subbasin is hilly and dissected by small drainages and by Dry Creek, a larger drainage and tributary of the Tuolumne River (**Figure 3-4**). The topography in the eastern Subbasin represents the transition from San Joaquin Valley floor to the Sierra Nevada foothills.

To better illustrate the ground surface elevations, four topographic profiles were generated from the NED. These profiles are illustrated on **Figure 3-5**. Profile 1-1' is along the center of the Subbasin from southwest to northeast and profiles 2-2', 3-3' and 4-4' extend from northwest to southeast across the Subbasin in the western, central and eastern Subbasin.

Profile 1-1' illustrates the rise in ground surface elevations from the San Joaquin River to the eastern Subbasin. Ground surface elevations range from about 20 to 500 feet msl along this profile. This profile illustrates the relatively gradual and uniform elevation gain in the western Subbasin and the hilly, dissected terrain in the east.

Profile 2-2' illustrates the Stanislaus and Tuolumne river channels and the flat topography between these channels in the western Subbasin. The ground surface elevations along this profile are relatively flat, sloping from approximately 100 feet msl near the Stanislaus River to approximately 90 feet msl along the Tuolumne River. On this profile, the Stanislaus River channel is wider and shallower than the Tuolumne River channel.

Profile 3-3' illustrates the ground surface elevations in the central Subbasin On this profile, the ground surface slopes from about 170 feet msl along the Stanislaus River to approximately 135 feet msl along Dry Creek. The ground surface between Dry Creek and the Tuolumne River is relatively flat. The topography along this profile is more variable, marking the transition from the flat western Subbasin to the hilly eastern Subbasin. On this profile, the Stanislaus River channel is wider and deeper than the Tuolumne River channel.

Profile 4-4' illustrates the higher elevations and more topographic relief in the eastern Subbasin. The dissected nature of the eastern hills is evident on the northern portion of the profile. Ground surface elevations along this profile vary from approximately 200 feet msl near the Stanislaus River to almost 500 feet msl between the Stanislaus River and Dry Creek. Ground surface elevations decline to about 200 feet msl at Dry Creek and remain relatively flat between Dry Creek and the Tuolumne River. On this profile, the Tuolumne River channel is wider and deeper than the Stanislaus River channel.

3.1.2.3. Soils

Soil textures from the Soil Survey Geographic (SSURGO) database for Stanislaus County, as developed by the U.S. Department of Agriculture Natural Resources Conservation Service (USDA), are illustrated on **Figure 3-6**. Soil textures are color-coded and listed in the legend by increasing grain size (texture). Most of the Subbasin is covered by silty sands (brown shading), clayey sands (dark blue shading), and clayey, silty sands (grayish blue shading). There are coarser-grained soils along the Stanislaus and Tuolumne rivers in the form of gravel and sand (red shading) along the upstream reaches and poorly graded sand and silt (yellow shading) along the middle reaches. The eastern Subbasin is dominated by clay (black shading), clay and silt (brown shading) and coarser-grained silty gravels (pink shading). Fine grained soils are present along the San Joaquin River in the form of clayey and silty sands (blue shading) and clay and silt (dark brown shading). The clay-rich soils in the west along the San Joaquin River limit infiltration and create localized perched conditions.

The USDA soil data shows that the eastern Subbasin is widely covered by low permeability surficial zones, generally referred to as "hardpan." These are considered restrictive layers in that they restrict or prevent surface water infiltration and serve to reduce groundwater recharge from precipitation or streamflow. The surficial occurrence of these materials is illustrated on **Figure 3-6** by cross hatching. Except for small areas near the Stanislaus and Tuolumne rivers and Dry Creek, most of the eastern Subbasin is covered by restrictive layers.

3.1.2.4. Surface Water Bodies and Water Conveyance

The Modesto Subbasin is bounded by rivers on three sides: the Stanislaus River on the north, the Tuolumne River on the south and the San Joaquin River on the west. The Modesto Subbasin is also internally drained by numerous small drainageways, the largest of which is Dry Creek. The Stanislaus and Tuolumne rivers originate in the Sierra Nevada and are tributaries of the San Joaquin River.

The Stanislaus River drains a watershed of about 1,051 square miles to the confluence of the San Joaquin River near Vernalis (Burow et al., 2004). Streamflow on the Stanislaus River ranges between 100 cubic feet per second (cfs) and 10,000 cfs (Phillips et al., 2015). The Tuolumne River drains a watershed of approximately 1,635 square miles and flows to the confluence of the San Joaquin River near Grayson (Burow et al., 2004). Typical average monthly streamflow in the Tuolumne River ranges from 100 to 400 cfs during low streamflow to more than 1,000 cfs, and sometimes more than 10,000 cfs, during high streamflow (Phillips et al., 2015).

The San Joaquin River is the primary drainage for the northern San Joaquin Valley and flows north into the Sacramento-San Joaquin River Delta and San Francisco Bay. Streamflow on the San Joaquin River from 1960 to 2004 ranged from less than 100 cfs upstream of the Merced River to more than 40,000 cfs downstream of the Stanislaus River (Phillips et al., 2015).

Water is diverted from both the Stanislaus and Tuolumne rivers for irrigation and municipal supply within the Subbasin. OID diverts water from the Stanislaus River at the Goodwin Dam into the South Main Canal, which serves agricultural irrigation water throughout OID within the Modesto Subbasin (Davids Engineering, Inc, 2016). Water flows from these canals through a system of unlined earthen ditches, concrete-lined canals, low-head pipelines and gates. Irrigation tailwater is reclaimed by OID using reclamation pumps or discharged to other landowners or irrigation districts via drainage canals. MID diverts water from the Tuolumne River at the La Grange Diversion Dam into the MID Upper Main Canal and onto the Modesto Reservoir (Provost & Pritchard, 2015). Most of the diverted water is used for irrigation, but approximately 20 percent is treated at the Modesto Regional Water Treatment Plan and delivered to the City of Modesto. MID delivers water through a network of lined and unlined canals, pipelines and drains.

3.1.3. Basin Boundaries

In order to define the subsurface lateral and bottom boundaries of the Modesto Subbasin, numerous features of the Subbasin are considered including the surficial river boundaries, the physical contact between the alluvial aquifers and basement rocks of the Sierra Nevada, and groundwater quality changes with depth. These considerations are discussed in the following sections.

3.1.3.1. Lateral Boundaries

Although the surficial river boundaries along the Stanislaus, Tuolumne, and San Joaquin rivers do not represent the extent of the Subbasin aquifers in the subsurface, they do represent important institutional boundaries and authorities for groundwater management. Accordingly, these boundaries are projected vertically in the subsurface to define the Subbasin lateral boundaries for groundwater management purposes.

The eastern Subbasin boundary generally follows the contact of Subbasin sedimentary deposits with the crystalline basement rocks of the Sierra Nevada, specifically the Jurassic-age Gopher Ridge Volcanics (Jgo) **Figure 3-1**. The eastern Subbasin boundary is primarily coincident with the base of the Ione Formation (Ei), which crops out along the boundary and overlies the crystalline basement rocks. The extent of this lateral boundary contact into the subsurface is not known with certainty but is assumed to be relatively steep. The northeastern Subbasin boundary is coincident with outcrops of both the Mehrten Formation (Tm) and the Table Mountain Latite (Mtm) volcanic rocks. Increasing salinity with depth may control the extent of this lateral boundary as discussed in more detail below.

3.1.3.2. Basin Bottom

The sedimentary units of the Modesto Subbasin likely extend several thousand feet into the subsurface. Therefore, using the contact between these units and crystalline basement rocks may not be appropriate for defining a basin bottom for management purposes. It has been well-documented by USGS (Page, 1973) and others that groundwater salinity in the San Joaquin Valley increases significantly with depth, often creating an operational bottom of the basin. The base of fresh water has been mapped by USGS and used in Central Valley subbasins to define the basin bottom. This map has been incorporated and extended by DWR in support of its regional central valley model C2VSim, the same model being revised and applied for the Modesto Subbasin GSP. Because the analysis for C2VSim provides a base of fresh water over the entire Subbasin, this model surface has been selected as a tentative basin bottom for GSP management purposes. Elevations defining that surface are reproduced on **Figure 3-7** and explained in more detail below.

A base of fresh water map was first developed on a San Joaquin Valley-wide basis by the USGS in 1973 (Page, 1973). The map was based on a specific conductance value of 3,000 micromohs per centimeter (umhos/cm), which is equivalent to a TDS range of about 2,000 to 2,880 milligrams per liter (mg/L), or parts per million (ppm), varying with temperature and differences in water chemistry. The map was highly detailed in some areas of the valley but only sparsely controlled in others, including the Modesto Subbasin. The few contours from the Page (1973) map that are near or within the Modesto Subbasin are reproduced in red on **Figure 3-7**. These contours are along the western Subbasin boundary and indicate that the elevation of the base of fresh water is between -400 and -600 feet mean sea level[2] (ft msl). The elevation of the base of fresh water continues to decline west of the western Subbasin boundary to an elevation of -800 feet msl.

Figure 3-8 illustrates the layers of the C2VSim model. As shown, the model is composed of five layers representing four aquifer layers and one aquitard: the unconfined aquifer (L1), Corcoran Clay (A2), primary shallow pumping layer (L2), deeper pumping layer (L3), and saline aquifer (L4). The base of the deeper pumping layer (L3) represents the base of fresh water. **Figure 3-7** shows elevation contours of the base of fresh water (base of L3) from C2VSim. The Page (1973) contours along the western Subbasin boundary are about 100 to 300 feet higher than in C2VSim. However, the elevation of the base of fresh water used in the C2VSim model represents the best available information for the base of fresh water and the operational bottom of the Subbasin.

As indicated on **Figure 3-7**, this Subbasin operational bottom is an undulating surface with the deepest portion occurring in the central Subbasin. Along the eastern Subbasin boundary, the bottom of the Subbasin is at approximately -600 feet msl. It rises slightly and then dips westward to an elevation of approximately -1,000 ft msl in the central Subbasin. The Subbasin bottom then gradually rises to an elevation of approximately -700 ft msl along the western Subbasin boundary.

3.1.3.3. Areas of Recharge and Discharge

Prior to groundwater use in the Modesto Subbasin, groundwater was recharged primarily in the eastern Subbasin where the Stanislaus and Tuolumne rivers entered the Subbasin. Groundwater flowed from these areas to the west (Burow et al., 2004). Artesian conditions occurred in the western Subbasin from upward movement of groundwater from the confined aquifer (Burow et al., 2004).

Since groundwater use began, deep percolation from irrigation is the primary source of recharge to the Subbasin and pumping (municipal, domestic, agricultural and drainage) is the primary source of discharge (Burow et al., 2004). Currently, there is apparent downward flow of groundwater in the western Subbasin where artesian conditions were historically documented. Downward gradients are apparently created from pumping beneath the Corcoran Clay, including areas on the west side of the San Joaquin River (Burow et al., 2004).

Other sources of recharge include deep percolation of precipitation, underflow from the foothills, Modesto Reservoir leakage, leakage from unlined canals, and seepage from rivers

[2] Elevations represented as negative numbers in this GSP represent elevations below mean sea level and are denoted as -400 ft msl, for example.

and streams. Modesto Reservoir leakage was estimated by Modesto Irrigation District to be approximately 24,000 acre-feet per year (Phillips et al., 2015). Other sources of discharge include flow into the downstream (western) reaches of the Stanislaus and Tuolumne rivers, flow into the San Joaquin River, underflow beneath the western Subbasin boundary, flow out of subsurface drains and consumption by riparian vegetation.

3.1.4. Principal Aquifers and Aquitards

As mentioned previously, the Corcoran Clay represents the primary aquitard in the Subbasin and separates the alluvial aquifers above and below the clay, creating confined conditions at depth in the western Subbasin where the Corcoran Clay occurs. The Corcoran Clay does not extend into the eastern Subbasin and no additional regional aquitard has been defined in this area. Accordingly, the Corcoran Clay defines two aquifer systems in the western Subbasin, but aquifers are more hydraulically connected in the eastern Subbasin where the regional clay is absent.

Recognizing these conditions, , three principal aquifers are defined in the Subbasin for the purposes of this GSP and future management of groundwater under SGMA. These three aquifers are defined as follows:

- Western Upper Principal Aquifer – unconfined aquifer above the Corcoran Clay.
- Western Lower Principal Aquifer – confined aquifer below the Corcoran Clay.
- Eastern Principal Aquifer – unconfined to semi-confined aquifer system east of the extent of the Corcoran Clay.

The definition of these three Principal Aquifers is consistent with the Principal Aquifer definitions for the Turlock Subbasin GSP, allowing for consistent interpretations along the shared Tuolumne River boundary. The Principal Aquifers in the Eastern San Joaquin Subbasin are different because the Corcoran Clay is only found in the southwest corner of the Subbasin. The Eastern San Joaquin GSP defines one principal aquifer the provides water from three production zones: a Shallow Zone, Intermediate Zone and Deep Zone.

The Western Upper Principal Aquifer and the Eastern Principal Aquifer are composed of Plio-Pleistocene- to Holocene- age alluvial sediments of the Modesto, Riverbank, Turlock Lake formations, and younger alluvium (where saturated). Not all of these alluvial sediments are present everywhere within the Eastern Principal Aquifer due to erosion or non-deposition. The base of the Western Principal Aquifer is the Corcoran Clay. The Eastern Principal Aquifer (east of the Corcoran Clay) also includes the Laguna, Mehrten and older formations that extend to the operational bottom of the Subbasin (i.e., base of fresh water).

The Modesto, Riverbank and Turlock Lake formations form sequences of overlapping terrace and alluvial fan deposits in response to cycles of alluviation, soil formation and channel incision influenced by changes in climate and glacial stages in the Sierra Nevada (Jurgens et al., 2008). The Modesto Formation forms a thin veneer at the surface, approximately 20 feet thick (Jurgens et al., 2008) throughout most of the western Subbasin (Burow et al., 2004). The Modesto Formation is composed of fluvially-deposited arkosic sand, gravel and silt and its lithology is similar to the underlying Riverbank, Turlock Lake, and Laguna formations (Burow et al., 2004). Where saturated, the Modesto Formation yields moderate amounts of water (Burow et al., 2004).

The Riverbank Formation is also composed of fluvial arkosic sand, gravel and silt and varies in thickness from approximately 150 to 250 feet (Burow et al., 2004). Its depositional dip is slightly steeper than the Modesto Formation, resulting in westward thickening of the deposits. The formation yields moderate quantities of water.

The Turlock Lake Formation is the most developed aquifer in the western Subbasin, both within the Western Upper Principal Aquifer and the Eastern Principal Aquifer, yielding up to 2,000 gallons per minute (gpm) from gravel and sand units (Burow et al., 2004). Similar to the Modesto and Riverbank formations, the Turlock Lake Formation is composed of a coarsening-upward sequence of silt, arkosic sand, and gravel layers (Burow et al., 2004).

The Western Lower Principal Aquifer consists of the Turlock Lake Formation below the Corcoran Clay, the Laguna Formation and the underlying Mehrten Formation. Both the Western Lower Principal Aquifer and the Eastern Principal Aquifer extend to the base of fresh water, which is located within or below the Mehrten Formation, respectively.

The Laguna Formation is composed of alluvial deposits of gravel, sand, and silt in at least two coarsening-upwards sequences (Burow et al., 2004). Laguna Formation sediments are more consolidated than the younger overlying formations (Jurgens et al., 2008) and yield variable amounts of water (Burow et al., 2004). The Laguna Formation is commonly mapped as part of the Turlock Lake Formation in the Modesto area (Burow et al., 2004). The Laguna Formation is not clearly identifiable from adjacent units in areas to the east where it crops out at the surface (Burow et al., 2004).

USGS indicates that the Eastern Principal Aquifer is unconfined and becomes semi-confined with depth due to numerous discontinuous clay lenses and extensive paleosols (Burow et al., 2004). In addition, the Mehrten Formation is more consolidated than the overlying formations and the sand beds are generally thin, so the degree of hydraulic connection between the Mehrten and overlying deposits is not well understood (Burow et al., 2004). However, many wells in the Eastern Principal Aquifer are screened in both the Mehrten Formation and overlying younger formations, where present, providing for some hydraulic connection in wells. Further, these wells provide average water levels across these zones and would represent a combined aquifer system for managing water levels. In the absence of a defined aquitard, it is likely that there is hydraulic connection among the formations, especially where the shallow formations thin to the east.

The Corcoran Clay is defined in this GSP as the only principal aquitard, which delineates the base of the Western Upper Principal Aquifer and the top of the Western Lower Principal Aquifer. The eastern edge of the Corcoran Clay is oriented from northwest to southeast, approximately parallel to the axis of the Valley (Burow et al., 2004). Where present, the blue lacustrine Corcoran Clay is up to 100 feet thick and occurs at depths ranging from 80 to

210 feet (Burow et al., 2004). The Corcoran Clay is generally well sorted clay to silty clay but becomes siltier and grades into coarser textures along the edges (Burow et al., 2004).

The Corcoran Clay surface from the C2VSim Model within the Modesto Subbasin was replaced with the Corcoran Clay surface from the USGS MERSTAN model (Phillips et al., 2015). During analysis for this GSP, it was discovered that the top of the Corcoran Clay surface from C2VSim suggested a mounded area in the western Subbasin where the top of the clay was higher than anticipated and not supported by well logs or USGS texture data. This anomaly was discussed with DWR staff, who supported revision of the surface in the model. The Corcoran Clay surface used in the USGS MERSTAN model (Phillips et al., 2015) is based on USGS hydrogeologic characterization of the Modesto Area (Burow et al., 2004) and represents the most detailed mapping of the Corcoran Clay in the Modesto Subbasin.

The elevation contours of the top and base of the revised Corcoran Clay surface within the Modesto Subbasin is shown on **Figures 3-9 and 3-10**, respectively. The Corcoran Clay generally dips to the west, with some irregularities. The eastern edge of the top of the Corcoran Clay slopes from an elevation of approximately -70 ft msl along the southern Subbasin boundary to -110 ft msl along the northern Subbasin boundary. The top of the Corcoran Clay is deepest in the northwestern Subbasin, at an elevation of approximately -210 ft msl. The elevation contours of the base of the Corcoran Clay generally mimic the top surface, ranging in elevation from approximately -120 to -140 ft msl along its eastern boundary to -260 ft msl in the northwestern Subbasin.

3.1.4.1. Cross Section Development

Five hydrogeologic cross sections (A through E) were developed to illustrate the hydrostratigraphy of the principal aquifers in the Modesto Subbasin, with a focus on aquifer textures and geometry. Cross section locations are shown on **Figures 3-11**. Cross section A-A' extends from southwest to northeast along the length of the Subbasin, cross sections B-B', C-C', and D-D' are perpendicular to A-A', oriented northwest to southeast. Cross section E-E' is a local cross section parallel to A-A' in the vicinity of Oakdale and along the Stanislaus River.

Cross sections were developed based on USGS texture data, DWR well completion reports, California Department of Oil, Gas and Geothermal Resources (DOGGR) geophysical logs, and localized cross sections in the City of Modesto as part of a previous study (Todd, 2016). Cross sections are presented on **Figures 3-12** through **3-18**.

The cross sections present generalized interpretations of coarse-grained (sands and gravels) and fine-grained (silts and clays) textures based on data from the USGS and DWR Well Completion Reports, along with interpretations of specific formations including the Corcoran Clay and Mehrten Formation. **Figure 3-11** shows the cross section locations, wells that were used to construct the cross sections (red dots), and the wells in the USGS texture database (black dots). Most of the cross section texture data are from wells in the USGS texture database (red dots with black dots). DWR Well Completion Reports were used in areas where USGS texture data were not available (red dots without black dots). In addition, geophysical logs from deep oil and gas wells used for cross section development are shown as green dots. **Figure 3-11** also shows the Corcoran Clay extent defined by the USGS (Burow et al., 2004). Ground surface elevations shown on the cross sections were generated from the National Elevation Dataset (NED, 10m) developed by the USGS, as illustrated on **Figure 3-4**.

The texture data were developed by the USGS for a hydrogeologic investigation (Burow et al., 2004) and incorporated into the USGS MERSTAN groundwater flow model (Phillips, et al., 2015). As part of the hydrogeologic investigation (Burow et al., 2004), the USGS reviewed over 10,000 well logs in the region and compiled a texture database using approximately 3,500 of these logs. There are approximately 900 wells in the Modesto Subbasin that are in the texture database. As illustrated on **Figure 3-11**, the USGS texture data does not extend into the eastern Subbasin because the MERSTAN model does not extend east of the Modesto Reservoir.

The USGS used a binary texture classification of either "coarse grained" (100 percent coarse) or "fine grained" (0 percent coarse) to categorize each interval on the well logs. Coarse-grained texture was defined as consisting primarily of sand or gravel while fine grained texture was defined as consisting primarily of silt or clay (Burow et al., 2004). Once this binary texture classification was complete, the coarse-grained percentage was averaged at 1-meter intervals along the depth of the well. This simplification of the lithology on a well basis allows identification of regions and/or depths of the groundwater basin that contain higher percentages of sand-rich zones, likely representing more permeable aquifers and large quantities of groundwater in storage.

The cross sections were created using the ESRI ArcHydro module for ArcGIS. The ArcHydro module allows import and three-dimensional plotting of geologic data from boreholes and topological surfaces. ArcHydro analysis tools include projection of borehole and surface data along cross-sections at selected orientations for analysis and geologic correlation.

DWR Well Completion Reports were available for most USGS texture database wells on the cross sections. The lithologic descriptions on the Well Completion Reports were used to define marker beds, such as black sands (Mehrten Formation) or blue clays (Corcoran Clay). The Well Completion Reports were also used to identify the screened intervals in the wells.

Where USGS texture data were not available, Well Completion Reports were used to interpret the lithology. Without the binary method used by USGS, the texture categories from the Well Completion Reports were defined on the cross sections at the same depth and thickness for which they were described on the Well Completion Reports. In this manner, the texture detail on each Well Completion Report is preserved. In areas with several closely-spaced wells, only higher-quality Well Completion Reports (i.e., most detailed data) were used.

The cross sections honor the texture information from the USGS and Well Completion Reports at well locations. Between well locations, the coarse-grained units were generally correlated based on elevation and thickness. Thick sand lenses were assumed to be more continuous and more likely to be interconnected than thinner sand lenses. The surficial geologic map (Wagner et al., 1991) presented as **Figure 3-1** was used to estimate surface contacts of the geologic formations on the cross sections when appropriate.

3.1.4.2. Cross Sections

Interpretations and observations for each of the five cross sections are described below.

Cross Section A-A'

Cross section A-A', shown on **Figure 3-12**, illustrates the lithology through the center of the Subbasin from southwest to northeast. The lithology is based on data from 61 wells and incorporates a local cross section (H-H') developed for the City of Modesto associated with a previous hydrogeologic study (Todd, 2016). The local cross section is incorporated into A-A' immediately east of cross section B-B' and extends for about 3 to 4 miles (see H-H' on **Figure 3-12**).

The Corcoran Clay extends from the western edge of A-A' and extends almost to the intersection of B-B'. Its extent agrees with that mapped by USGS (Burow et al., 2004). The top of the Corcoran Clay is approximately 150 feet below ground surface (bgs) at its eastern extent and dips to the west to a depth of approximately 220 feet bgs (equivalent to elevations of approximately -80 feet msl to -185 feet msl. The Corcoran Clay generally thickens to the west, ranging in thickness from about 10 feet in the east to about 70 feet in the west. The depth and thickness of the Corcoran Clay generally agrees with the Corcoran Clay in the USGS MERSTAN model (Phillips et al., 2015) and with the data incorporated into the Modesto Subbasin C2VSim model (**Figures 3-9** and **3-10**).

The top of the Mehrten Formation is estimated on the cross section based on the presence of black sands, which are colored orange on **Figure 3-12**. The Mehrten Formation crops out in the eastern Subbasin and is generally consistent with the geologic map illustrated on **Figure 3-1**. Black sands were not identified in the central and western Subbasin because not many wells extend deep enough to intersect the Mehrten Formation in that area. Based on the interpolated dip of the black sands, the top of the Mehrten Formation is approximately 400 feet below the City of Modesto (H-H' on **Figure 3-12**), east of where cross section B-B' crosses A-A' (**Figure 3-12**).

An offset in the top of the black sands was observed during construction of cross section E-E', located north of and parallel to cross section A-A'. As described in more detail for cross section E-E', this offset suggests vertical movement caused by a geologic fault. An offset in the black sands is also suggested by the data in a similar location on cross section A-A', east of the intersection with cross section C-C' (**Figure 3-12**). The vertical movement – down-dropped eastern block relative to the western block – is also consistent with offset observed on cross section E-E'. The estimated location of the fault plane is shown on cross section A-A'.

Cross section A'A' also illustrates the presence of thick coarse-grained units both above and below the Corcoran Clay, at the western edge of the Corcoran Clay. Thick sand units are also noted in the eastern Subbasin within the Mehrten Formation. Note that the lithology shown below the Corcoran Clay is only based on a few wells and is less certain than other areas with more wells. Wells in the western Subbasin are primarily screened either immediately above or immediately below the Corcoran Clay with some wells screened in both aquifers. Most of the wells in the eastern Subbasin are screened within the black sands of the Mehrten Formation.

Cross Section B-B'

Cross section B-B', shown on **Figure 3-13**, illustrates the lithology from the northern to the southern Subbasin boundary in the western Subbasin, through the City of Modesto. The lithology is based on texture information from 38 wells and incorporates a local cross section (D-D') developed in the City of Modesto from a previous study (Todd, 2016). The local cross section extends from north of the intersections with A-A' to the southern edge of the cross section (at B', **Figure 3-13**).

The Corcoran Clay extends from the southern edge of the cross section to slightly north of the Tuolumne River. At the Subbasin boundary, the top of the Corcoran Clay is at a depth of about 130 feet bgs (about -65 feet msl) and is about 65 feet thick. As shown on the cross section location map (**Figure 3-11**), the edge of the Corcoran Clay is oriented northwest to southeast and only intersects the southern portion of section B-B'. However, the Corcoran Clay does not extend as far east in this area as mapped by USGS (compare the edge of the Corcoran Clay on cross section B-B' to the Corcoran Clay extent mapped by USGS and shown on **Figure 3-11**). This could indicate that the extent is more irregular than previously mapped or extends farther than indicated by well data on this section. Because the cross section interpretation is based only on a few logs, the unit may have been too thin to be identified (or not recorded) on the Well Completion Reports.

Wells present in the southern region of the cross section are screened both above and below the Corcoran Clay. To the north of the Corcoran Clay, wells tend to have long screened intervals that intersect multiple coarse-grained units. The thickest coarse-grained units on cross section B-B' are present along the edge of the Corcoran Clay.

The wells on cross section B-B' are not deep enough to penetrate the Mehrten Formation. Based on where B-B' intersects A-A', the Mehrten Formation is at an elevation of approximately -370 feet msl in this area of the Subbasin (near the bottom of B-B' on **Figure 3-13**). The deepest wells on cross section B-B' extend to about -300 feet msl.

Cross Section C-C'

Cross section C-C', illustrated on **Figure 3-14**, depicts the lithology in the central Subbasin, east of the Corcoran Clay between Riverbank and Oakdale. The cross section is based on geologic information from 43 wells.

Most of the wells on cross section C-C' section are too shallow to encounter the Mehrten Formation. However, a few wells are several hundred feet deep and have sufficiently long screens that intercept the Mehrten Formation black sands. These wells allow the top of the Mehrten Formation to be approximated on the cross section (**Figure 3-14**).

As shown on C'C', the top of the Mehrten Formation is present at an elevation between -100 and -200 feet msl, shallower than in cross section B-B' due to its westward dip. The elevation of the top of the Mehrten Formation dips gently to the south along this cross section, with elevations ranging from approximately -125 feet msl along the northern Subbasin boundary to approximately -220 feet msl at the southern Subbasin boundary. The depth to the Mehrten Formation from the edge of the river channels at the Subbasin boundaries range from about 285 feet bgs in the north to 325 feet in the south. The Mehrten is likely shallower in the northern section because it crops out over a larger area in the northern part of the Subbasin (see **Figure 3-14**).

The thickest and most continuous coarse-grained units on the section are in the center of the Subbasin. Coarse-grained units appear to be thicker and more continuous in the southern Subbasin near Dry Creek and the Tuolumne River than along the northern Subbasin boundary.

Cross Section D-D'

Cross section D-D' (**Figure 3-15**) illustrates the lithology in the eastern Subbasin. The cross section extends from the Stanislaus River to the Tuolumne River and crosses Dry Creek and the Modesto Reservoir. The cross section is based on lithology from 27 wells. Due to the lack of USGS texture data in the eastern Subbasin, most of the lithologic information on this cross section is from DWR Well Completion Reports.

The cross section shows that the Mehrten Formation is shallow or crops out as remnant hills in the eastern Subbasin. The delineation of Mehrten Formation outcrop is based on the presence of black sands and the geologic map (**Figure 3-1**). The cross section is dominated by coarse-grained material and black sands. It should be noted that some Well Completion Reports do not indicate the color of the textures and much of the yellow color on the section may, in fact, also represent black sands.

The cross section shows that most of the wells are hundreds of feet deep and screened within or across the black sands. The black sands and coarse-grained material appear to be thicker and more extensive in the northern half of the Subbasin.

Cross Section E-E'

Cross section E-E', illustrated on **Figure 3-16**, is a local cross section in the northeast Subbasin oriented from southwest to northeast, parallel to cross section A-A'. The cross section is along the northern Subbasin boundary and extends from cross section C-C', through Oakdale, to east of cross section D-D'. The cross section approximately follows the Stanislaus River channel, crossing it in two places, and is based on lithology from 62 wells. Due to the high density of wells on the cross section, well numbers are shown on a separate expanded-scale version of this section, provided as **Figure 3-17**.

The Mehrten Formation is shallow throughout most of the cross section and crops out in the eastern region of the section. Similar to cross section D-D', the delineation of the Mehrten Formation outcrop is based on the presence of black sands and the geologic map (**Figure 3-1**). The Mehrten Formation crops out as remnant hills with the erosional surface roughly corresponding to the ground surface elevation on the cross section. The dip of the Mehrten Formation is visible because the transect is roughly parallel to the dip direction. The coarse-grained material and black sands appear to be the thickest and most continuous at depth, but this interpretation is based on only a few deep wells.

There was some irregularity in the elevation of the top of the black sands in wells in the western region of the section. It appears that the black sands on the western side of this fault are at a significantly higher elevation than on the east side of the fault, suggesting vertical movement possibly associated with a geologic fault as interpreted on E-E'. The eastern block is down-dropped relative to the western block.

The USGS (Marchand, 1980) mapped multiple surface lineaments (trending northwest to southeast) south of the Modesto Subbasin, within the Turlock Subbasin. This mapping included folds and faults with approximately northwest to southeast trends. The faulting, which occurred post-deposition, resulted in a down-dropped eastern block relative to the western block, showing reverse offset because of compressive stresses. The evidence of a fault in the Modesto Subbasin has a similar pattern of offset and trend as the faults mapped in the Turlock Subbasin.

Cross Section A-A' with Hydrogeologic Framework

Cross section A-A' is repeated on **Figure 3-18** with a focus on formations and the geometry of the Principal Aquifers rather than textures. The cross section depicts the formation boundaries and the base of fresh water from C2VSim through the center of the Subbasin from southwest to northeast (**Figure 3-11**). The boundary between the base of the undifferentiated Modesto, Riverbank, and Turlock Lake Formations and the top of the Mehrten Formation is the same as shown on cross section A-A' and is based on the geologic texture data. The base of the Mehrten Formation was approximated from geophysical logs at 13 deep oil and gas wells available from the California Department of Oil, Gas and Geothermal Resources (DOGGR). (The location of the DOGGR geophysical logs is shown on **Figure 3-11**).

The cross section shows the westward dip of the formations and offsets caused by two faults in the central and eastern Subbasin. The fault east of intersection with C-C' was identified based on offset of Mehrten Formation black sands. The fault identified west of intersection with C-C' is based on offset of the base of the Mehrten Formation identified from DOGGR geophysical logs. The fault west of C-C' is not shown on **Figure 3-12** because the wells in this area are not deep enough to intersect the black sands of the Mehrten Formation, and therefore offset could not be identified.

The base of fresh water surface from C2VSim, which represents the bottom of the Subbasin, is overlaid onto the conceptual cross section. The base of fresh water undulates throughout the Subbasin. It is highest in the eastern Subbasin, at an elevation of approximately -550 feet msl, and deepest in the central Subbasin, at an elevation of approximately -1,000 feet msl. In the eastern Subbasin, the base of fresh water is below the Mehrten Formation, within the undifferentiated continental and marine sediments. In the central Subbasin it rises into the base of the Mehrten Formation. The undulations approximately correspond with the locations of the faults.

The conceptual cross section also illustrates the three principal aquifers: the Western Upper Principal Aquifer above the Corcoran Clay, the Western Lower Principal Aquifer below the Corcoran Clay and above the base of fresh water, and the Eastern Principal Aquifer east of the Corcoran Clay and above the base of fresh water.

3.1.4.3. Aquifer Properties

The USGS compiled aquifer property data for the Modesto and Turlock subbasins (Burow et al., 2004). The USGS reported hydraulic conductivity above the Corcoran Clay, in the Western Upper Principal Aquifer, to range from 27 to 54 feet per day (ft/day) (Page, 1977 in Burow et al., 2004). The C2VSim Modesto Model has an average hydraulic conductivity above the Corcoran Clay of 42 ft/day, which is within this published range.

The hydraulic conductivities in the Mehrten Formation, at the base of both the Eastern Principal Aquifer and Western Lower Principal Aquifer, ranged from 0.01 to 67 ft/day (Page and Balding, 1973 in Burow et al., 2004). Average hydraulic conductivity in the lower aquifer of the C2VSIM Modesto Model, which includes the Mehrten Formation, is 25 ft/day, which is within this published range.

In the Eastern Principal Aquifer, the transmissivity (T) in the shallow unconsolidated sediments is estimated to be 9,100 ft^2/day (68,068 gpd/ft). The T in the deeper, partly consolidated sediments of both the Eastern Principal Aquifer and Western Lower Principal Aquifer was lower, approximately 8,000 ft^2/day (59,840 gpd/ft) (Page and Balding, 1973 in Burow et al., 2004).

3.1.5. Hydrogeologic Conceptual Model Representation in Modesto C2VSim Model

The hydrogeologic conceptual model was compared with the Modesto C2VSim Model to ensure that the hydrogeologic system is well represented in the model.

As discussed previously in Section 3.1.4, the original Corcoran Clay surface that was in the model was replaced with the Corcoran Clay surface from the USGS MERSTAN Model (Phillips et al., 2015). This was because an anomaly in the original surface was discovered while comparing the cross sections and well logs to the model. The Corcoran Clay surface in the USGS MERSTAN Model is the most detailed mapping of the Corcoran Clay in the Modesto Subbasin. The depth, thickness and extent of the Corcoran Clay shown on the cross sections generally agrees with the USGS MERSTAN Model, and consequently, with the revised surface in the Modesto C2VSim Model.

The model layers are a good representation of the Principal Aquifers. The primary shallow pumping layer of the model contains most of the pumping wells. As mentioned in the previous section, the average hydraulic conductivity in the model in the Western Upper Principal Aquifer and within the Mehrten Formation were within the range published in the literature.

The hydrogeologic conceptual model is well represented in the Modesto C2VSim Model. Because of this, the model is an effective tool for estimating water levels in areas lacking water level data, such as within the Western Lower Principal Aquifer and in the eastern Subbasin. The model is also an effective tool for developing water budgets, which will be presented in Section 4.

3.1.6. Data Gaps and Uncertainties in the Hydrogeologic Conceptual Model

This section will summarize hydrogeologic data gaps that affect implementation of the Plan and are related to the GSAs ability to sustainably manage groundwater. The Plan Implementation section, when developed, will describe how these data gaps will be addressed in future GSP actions. A summary of the data gaps for the Hydrogeologic Conceptual Model is summarized below.

Table 3-1: Data Gaps for the Hydrogeologic Conceptual Model

Issue	Area	Impacts on Groundwater Management	Actions to Address
Eastern Subbasin Aquifers	East and Northeast of Modesto Reservoir	Sparse number of wells in this area of the Subbasin means more uncertainty regarding the Eastern Principal Aquifer.	• Collect relevant data from landowners, as available. • Install additional monitoring wells. • Examine lithologic logs and other well data when new wells are drilled in this area.
Mehrten Formation	Central and Western Subbasin	Depth to top of Mehrten Formation not well understood in central and western Subbasin due to shallow wells. Impacts understanding of aquifer properties and geometry.	• Examine lithologic logs and other well information as additional deep wells are drilled in central and western Subbasin. • Add testing program, such as geophysical logs, to proposed deep wells where needed.

Exact Base of Fresh Water	Entire Subbasin	Uncertainty in Subbasin geometry, fresh groundwater in storage, and water quality with depth.	Compile TDS data for wells with known screen intervals. Test water quality in all new Subbasin wells.

3.2. GROUNDWATER CONDITIONS

An evaluation of groundwater conditions in the Modesto Subbasin was conducted using water level data obtained from numerous sources, including the DWR Water Data Library (which includes CASGEM data), USGS, MID, OID, and the municipalities and urban communities. There are more than 600 wells in the Subbasin with measured water levels between 1918 and 2018, with most measurements occurring after 1970. The locations of these wells are shown on **Figure 3-19**. As shown on the figure, most water level data are from wells in the western and central Subbasin, with limited data in the eastern Subbasin.

The groundwater analysis focused on data from 1990 to 2018; this water level study period overlaps the water budget study period (WY 1991 – WY 2015, see **Section 3.1.2.1**) while including more recent data to examine current groundwater conditions. During this period, water levels were measured at approximately 450 of these wells.

3.2.1. Groundwater Occurrence

As summarized in **Section 3.1.4**, groundwater is present in unconfined to semi-confined aquifers above and east of the Corcoran Clay and in confined aquifers below the Corcoran Clay. Groundwater is also present in the shallow alluvial unconsolidated to semi-consolidated deposits as well as the underlying consolidated sediments; however, groundwater conditions are not well defined in the deeper aquifers due to a lack of data.

3.2.2. Water Levels and Trends

To examine water level trends over the study period, working hydrographs were constructed for each of the approximately 450 wells with water level measurements since 1990. Representative hydrographs were chosen for discussion from wells in each principal aquifer based on data availability and on levels, fluctuations, and trends consistent with other hydrographs in a certain area. The locations of selected wells with representative hydrographs are shown on **Figure 3-20** and are color-coded based on the principal aquifer in which they are screened.

Representative hydrographs are presented on **Figures 3-21** through **3-25**. These hydrographs have consistent horizontal scales (1990 to 2018) and vertical scales (0 to 160 feet msl) to facilitate comparisons across the Subbasin. The ground surface elevation is shown as a black line on the hydrographs unless it is greater than 160 ft msl, in which case it is noted at the top of the hydrograph. If known, the depth of the screened intervals for each well are noted on the hydrograph. Representative hydrographs include data measured at MID wells, City of Modesto wells, City of Oakdale wells, CASGEM wells and DWR Water Data Library wells.

Eight representative hydrographs from the Western Upper Principal Aquifer are illustrated on **Figures 3-21** and **3-22**. As shown on **Figure 3-21**, groundwater elevations in the western and central regions of the Western Upper principal aquifer are shallow. Depth to water in the northwest Subbasin (hydrograph 1) is within ten feet of ground surface and deepens to the south (hydrograph 2) and east (hydrographs 3, 4 and 5). Water levels are relatively stable, especially along the western Subbasin boundary near the San Joaquin River (hydrographs 1 and 2). Water levels fluctuate more to the east. Hydrographs 3, 4 and 5 show slightly more pronounced water level declines during the recent drought. The declines are greater in the center of the Subbasin (hydrograph 4, approximately 13 feet) than near the rivers (hydrographs 3 and 5, approximately 5 or less feet).

Three hydrographs from the eastern edge of the Western Upper Principal Aquifer are shown on **Figure 3-22** and illustrate a similar historical water level trend. Water levels between 1990 and 1995 are relatively low and rise after 1995 when the City of Modesto began receiving water from the Modesto Regional Water Treatment Plant (MRWTP) and pumping less groundwater. Water levels were relatively steady from 2000 to the recent drought, when declines up to 10 feet (hydrograph 7) and 15 feet (hydrograph 6) occurred. Water levels have recovered slightly since the end of the drought.

Hydrograph 8 illustrates water levels from a City of Modesto pumping well (Well 17). In 1994, shortly before the City of Modesto began receiving water from the MRWTP, water levels were the lowest of the study period. Between 1995 and 2000, after the City began receiving water from the MRWTP, water levels rose almost 50 feet. Since 2000, water levels indicate significant seasonal pumping variation, but overall have remained relatively steady.

Three hydrographs from the Western Lower Principal Aquifer are shown on **Figure 3-23**. Each of these hydrographs are from City of Modesto pumping wells (Well 290, Well 313 and Well 56). Each of these hydrographs illustrate significant seasonal pumping variations. When compared to Well 17, in the Wester Upper Principal Aquifer (hydrograph 8 on **Figure 3-22**), it appears that the water level variation below the Corcoran Clay is more significant than above the Corcoran Clay, consistent with pumping in a confined aquifer. Water levels in City of Modesto Well 56 (hydrograph 11) depict the historical trend of water level recovery between 1995 and 2000 followed by relatively stable water levels with seasonal pumping fluctuations.

Representative hydrographs from ten wells east of the edge of the Corcoran Clay in the Eastern Principal Aquifer are illustrated on **Figures 3-24** and **3-25**. Hydrographs from wells in the western side of the Eastern Principal Aquifer are shown on **Figure 3-24** and include three MID wells, one City of Modesto well and one well from the DWR WDL. These hydrographs indicate a deeper water table as ground surface elevations rise to the east. Hydrographs illustrate depths to water ranging from approximately 40 feet bgs in MID-208 to more than 80 feet bgs in MID-197 (**Figure 3-24**). The water levels in the MID wells are relatively steady until declines during the most recent drought. Those declines increase to the east, ranging from about 12 feet in MID-208 to 27 feet in MID-214. Some recovery occurred after the drought, but water levels remain approximately 20 feet below pre-drought levels in the two easternmost wells, MID-214 and MID-197.

The City of Modesto well 37 (hydrograph 13), located in the center of the Subbasin close to the edge of the Corcoran Clay, has a similar water level pattern to other City of Modesto wells in the western principal aquifers. The water level in City of Modesto Well 37 rose approximately 50 feet between 1995 and 2000 and remained relatively steady, with pumping cycles, since then. There is a slight downward water level trend since about 2005 that was less pronounced in the City of Modesto wells in the western principal aquifers.

Five hydrographs from the eastern region of the Eastern Principal Aquifer are illustrated on **Figure 3-25**. These hydrographs are from a City of Oakdale well (Well 5), two MID wells and two wells from the DWR WDL. Although the City of Oakdale Well 5 (hydrograph 17) has missing data between 1995 and 2009, the measured record illustrates up to 40 feet of seasonal pumping variations and an overall slightly declining trend. The other four hydrographs show historical declining trends since about the mid-2000s. For example, water levels in MID-228 (hydrograph 19, near the Tuolumne River), declined approximately 30 feet from the late 1990s to present. Most of the declines occur during the recent drought (2013 – 2016) and appear most significant in the eastern Subbasin. Water levels during the drought declined approximately 25 feet in MID-228 (hydrograph 19) and MID-223 (hydrograph 21) and about 40 feet in the DWR WDL well 02S12E32P01M (hydrograph 18), north of Modesto Reservoir. In that well, recent water levels have not recovered or stabilized substantially, even during the wet year of 2017.

In general, hydrographs in the Eastern Principal Aquifer indicate that water levels in the eastern Subbasin have declined since about 2000 and have significant declines during the most recent drought. The historical declining trends and the magnitude of decline during the recent drought are most pronounced in the eastern region of the Eastern Principal Aquifer. Due to a lack of data, water level trends east of the Modesto Reservoir and in the northeastern region of the Subbasin are not known.

3.2.3. Groundwater Flow

3.2.3.1. Groundwater Elevation Contour Maps

Groundwater elevation contour maps were developed at three different times within the study period: the wettest year (1998), a dry year during the recent drought (2015), and the most recent year with a sufficient set of measured data (2017). These contour maps are shown on **Figures 3-26, 3-27 and 3-28**. Each groundwater elevation contour map includes water levels measured in the unconfined Western Upper Principal Aquifer and unconfined to semi-confined Eastern Principal Aquifer. Water levels from these two principal aquifers are shown and contoured on the same map as representative of water table conditions.

Maps illustrating the available water level data in the Western Lower Principal Aquifer were developed for each time period and are shown on **Figures 3-29, 3-30 and 3-31**. Water levels in the Western Lower Principal Aquifer cannot be contoured due to limited data. Although many wells in the western Subbasin were drilled below the Corcoran Clay, most have screened intervals both above and below the clay. Wells shown on these figures are screened only below the Corcoran Clay.

Groundwater Flow in Spring 1998 (March and April)

Groundwater elevations measured in spring 1998 are illustrated on **Figure 3-26**. As shown on **Figure 3-2**, water year 1998 is the wettest year between 1990 and 2017. With almost 25 inches of rain, precipitation during water year 1998 was almost double the long term average (12.6 inches) and study period average (12.8 inches). As shown on the hydrographs, water levels throughout most of the Subbasin rebounded between 1995 and 2000 in response to the reduction of groundwater pumping within the City of Modesto as a result of the delivery of water from the MRWTP. For this and other reasons, 1998 water levels do not always represent the highest water levels in all parts of the Subbasin.

Groundwater elevations in spring 1998 ranged from about 150 feet msl near the Modesto Reservoir to approximately 35 feet msl in the western Subbasin. The lowest groundwater elevations occurred along the western edge of the Subbasin and within the City of Modesto along the Tuolumne River. Groundwater flow is generally to the southwest with flatter hydraulic gradients in the west. There is a southerly component of flow towards the Tuolumne River in the western Subbasin caused by a pumping depression in the City of Modesto. Groundwater elevations in this region are between about 30 and 40 feet msl, which is similar to the groundwater elevations along the western edge of the Subbasin next to the San Joaquin River. There is a general area of higher groundwater elevations in the central Subbasin, with elevations slightly over 100 feet msl. Additional localized areas of higher or lower groundwater elevations also occur in the Subbasin. As illustrated on **Figure 3-26**, there is a lack of measured water level data in the eastern Subbasin.

Groundwater elevations in the Western Lower Principal Aquifer are available in only two wells during spring 1998 (**Figure 3-29**). The wells are along the eastern edge of the aquifer and have similar water levels (41 and 44 ft msl); levels are also similar to water levels in the Western Upper Principal Aquifer.

Groundwater Flow in October 2015

Figure 3-27 illustrates groundwater elevations measured in October 2015. Water year 2015 was the third consecutive critically dry year during the recent drought and water levels reached historical lows in many areas of the Subbasin. January 2015 is defined in the Water Code as the SGMA baseline, so this map generally represents baseline conditions for the Subbasin.

As shown on **Figure 3-27**, groundwater elevations ranged from approximately 130 feet msl in the eastern Subbasin to 14 feet msl in the western Subbasin along the Tuolumne River in Modesto. In October 2015, more water level data are available in the eastern Subbasin than in spring 1998 and the highest water level (132 feet msl) was measured in the northeastern Subbasin.

Groundwater flow patterns in October 2015 are similar to spring 1998, with groundwater flow to the southwest, with a southerly component towards the Tuolumne River, especially within the City of Modesto. Hydraulic gradients are steeper in the eastern Subbasin and become flatter to the west. Even though flow directions are the same as 1998, groundwater levels in October 2015 are generally lower throughout the Subbasin.

Increased municipal pumping during the drought has created a pumping depression within the City of Modesto, with water levels approximately 20 feet lower than in spring 1998. Similarly, increased irrigation pumping has created a pumping depression east of the City of Modesto in the central Subbasin, with water levels approximately 20 to 30 feet lower than in spring 1998. Water levels in the Western Upper Principal Aquifer appear to have the least amount of decline, on the order of 10 to 20 feet lower than in spring 1998. The magnitude of water level declines between these two time periods is larger in the east. For example, water levels in October 2015 near the Modesto Reservoir are approximately 30 to 40 feet lower than they were in spring 1998.

Groundwater elevations are available in four wells in the Western Lower Principal Aquifer for October 2015 (**Figure 3-30**). The wells, located along the eastern edge of the aquifer, have elevations ranging from 26 to 41 feet msl; although there are more wells with 2015 data, elevations for the same wells are between 3 feet and 10 feet lower than in spring 1998.

Groundwater Flow in Spring 2017 (February through May)

Groundwater elevations measured in spring 2017 are illustrated on **Figures 3-28 and 3-31**. Water year 2017 was a wet year with above average precipitation; as such, water levels are higher throughout the Subbasin than in October 2015.

As shown on **Figure 3-28**, groundwater elevations range from 110 feet msl north of the Modesto Reservoir to about 20 feet msl within the City of Modesto near the Tuolumne River. Groundwater flow patterns are similar to spring 1998 and October 2015. Flow is to the southwest with a southerly component towards the Tuolumne River, most notably in the vicinity of the City of Modesto, but also in other areas.

Groundwater elevations have recovered more in the western Subbasin than they have in the eastern Subbasin. For example, water levels within the City of Modesto are about 10 to 20 feet higher than in October 2015. Groundwater elevations in the central Eastern Principal Aquifer are less than 10 feet higher than in October 2015. Although data are limited, it appears that water levels have continued to decline further to the east. Two wells north of the Modesto Reservoir show water level declines of 13 feet (from 118 to 105 feet msl) and 3 feet (from 113 to 110 feet msl) since October 2015.

Water levels at four wells in the Western Lower Principal aquifer are shown on **Figure 3-31**. As in 1998 and 2015, the wells are along the eastern edge of the aquifer. Groundwater elevations are higher than they were in October 2015, ranging from 44 to 53 feet msl.

3.2.3.2. Vertical Groundwater Flow

The USGS has found that vertical groundwater movement within the extent of the Corcoran Clay is downward, from the Western Upper Principal Aquifer to the Western Lower Principal Aquifer (Burow et al., 2004). An analysis of groundwater elevation data in the Modesto Subbasin supports this.

The analysis of vertical gradients is based on water levels from a USGS well cluster and a group of nearby wells that are screened above and below the Corcoran Clay. The location of these wells is shown on **Figure 3-32** and hydrographs are shown on **Figures 3-33 and 3-34**. The extent of the Corcoran Clay, as defined by the USGS (Burow et al., 2004), is shown on **Figure 3-32**.

In 2004, USGS installed a cluster (MRWA) of three wells in the southwestern Subbasin. Two of the wells are screened above the Corcoran Clay (MRWA-1 and MRWA-2) and one is screened below the Corcoran Clay (MRWA-3). MRWA-1 is screened at a depth of 25 to 30 feet bgs (37 to 32 feet msl), in the shallow portion of the Western Upper Principal Aquifer. MRWA-2 is screened in the deeper portion of the Western Principal Aquifer just above the Corcoran Clay, at a depth of 174 to 179 feet bgs (-112 to -117 feet msl). MRWA-3 is screened in the Western Lower Principal Aquifer, at a depth of 269 to 274 feet bgs (-207 to -212 feet msl). According to data provided by the USGS, the Corcoran Clay was encountered from 195 to 240 feet bgs (-133 to -178 feet msl) at this location. The USGS collected water levels from these wells between 2004 and 2006 and again in 2009. These water levels are shown on **Figure 3-33**.

Water levels measured in the MRWA cluster show that groundwater elevations are higher in the Western Upper Principal Aquifer than the Western Lower Principal Aquifer. Groundwater elevations above the Corcoran Clay in MRWA-1 and MRWA-2 are similar to one another and are between about 1.5 and 6 feet higher than in MRWA-3, below the Corcoran Clay. Therefore, groundwater flow is downward from the Western Upper Principal Aquifer to the Western Lower Principal Aquifer (**Figure 3-33**).

Groundwater elevations in the shallow and deep regions of the Western Upper Principal Aquifer (MRWA-1 and MRWA-2) are similar except when steep declines occur below the Corcoran Clay. These declines are likely associated with pumping increases below the Corcoran Clay. The shallow unconfined aquifer does not appear to be affected (MRWA-1). The water levels show consistent downward groundwater flow from the Western Upper Principal Aquifer to the Western Lower Principal Aquifer, which is increased with pumping in the Western Lower Principal Aquifer (**Figure 3-33**).

The second set of wells used for the vertical groundwater flow analysis includes one MID well (MID-103), screened above the Corcoran Clay from 53 to 81 feet bgs, and two City of Modesto wells (MOD-63 and MOD-313), screened below the Corcoran Clay at multiple intervals ranging from 171 to 456 feet bgs. Well depths in relation to the Corcoran Clay were verified with the cross sections and the base elevation of the Corcoran Clay in the model. These wells, shown on **Figure 3-32**, are in close proximity to one another near the eastern edge of the Corcoran Clay.

Hydrographs for these three wells are shown on **Figure 3-34**. The City of Modesto wells show cyclic seasonal pumping fluctuations of up to 30 feet, while the MID well is relatively steady, with fluctuations of 10 or less feet. Groundwater elevations below the Corcoran Clay in the two City of Modesto wells are very similar to one another and consistently lower than the elevations in the MID well above the Corcoran Clay. Groundwater elevations above the Corcoran Clay are about 10 to 40 feet higher than below the Corcoran Clay. The biggest differences occurred during the recent drought (2014 to 2016) due to increased pumping. Water levels in this group of wells indicate consistent downward groundwater flow from the Western Upper Principal Aquifer to the Western Lower Principal Aquifer in this area of the Subbasin.

3.2.4. Changes of Groundwater in Storage

Recognizing water levels trends and fluctuations observed throughout the Subbasin, along with the significant water level declines during drought conditions, it is clear that significant changes in groundwater in storage are occurring over time in the Modesto Subbasin. One accepted method of estimating groundwater in storage changes is to construct groundwater elevation contour maps during seasonal highs for various water years and develop change in water level maps between them. By applying storage parameters to these water level changes, a change in groundwater in storage can be estimated.

To develop accurate and reliable change in storage maps associated with this methodology, groundwater elevation contour maps should be developed during each time period over the entire Plan Area for each Principal Aquifer. However, these maps cannot be developed over the entire Modesto Subbasin with the desired level of certainty due to significant data gaps for water levels both within certain areas of the Subbasin as well as for one of the three Principal Aquifers. Specifically, water level data in the eastern third of the Subbasin are not available (see **Figures 3-26** through **3-28**). Further, water level data are insufficient for mapping groundwater elevations in the Western Lower Principal Aquifer (see **Figures 3-29** through **3-31**). As such this methodology would not likely yield sufficiently credible results for an accurate understanding of changes in groundwater in storage over time.

However, refinements to a regional integrated surface water-groundwater model (C2VSim) are in progress to develop a tool for GSP water budget analyses. Early results from the revised C2VSim Modesto Model suggest well-calibrated water levels and reliable water budget data to provide an alternative method for generating groundwater level contour maps and resulting changes in groundwater in storage. The model also has the advantage of providing this information over the entire Subbasin, even where water level data are lacking. Selection, refinements, and calibration of the C2VSim Modesto Model are provided in Appendix X. Water budgets, including change in groundwater in storage over a 25-year Study Period have been developed and are summarized in **Section 4** of this GSP. Those model results represent the best technical data available for determining changes in groundwater in storage over time. Improvements to the monitoring program will support development of more reliable groundwater elevation contour maps in the future.

3.2.5. Groundwater Quality

Historical and current groundwater quality conditions of the Modesto Subbasin have been reviewed to characterize groundwater quality of the principal aquifers including an analysis of any constituents of concern. In particular, the analysis allows identification of groundwater quality issues that may affect the supply and beneficial uses of groundwater, including possible plumes of groundwater contamination. The compilation and analysis of historical and current data is described in the following sections, including the sources of data, screening procedures and quality assurance of the data, selection of constituents to analyze, and characteristics of the resulting data sets. Statistical summaries are also presented for select constituents.

3.2.5.1. Regional Groundwater Quality

Groundwater quality in the San Joaquin Valley is highly variable and reliant on the quality of the water recharging the aquifer, the chemical changes that occur as surface water percolates to groundwater, and chemical changes that occur within the aquifer (Dale et al., 1966). USGS has categorized regional groundwater quality in the San Joaquin Valley into three groups based on geography: east side, west side, and axial trough (Dale et al., 1966).

East side groundwater quality is of the bicarbonate type with low total dissolved solids (TDS). This groundwater is characteristic of the surface waters that drain the granitic Sierra Nevada Range to the east of the San Joaquin Valley groundwater basin (Dale et al., 1966). Groundwater quality in the east side reflects the quality of the quality of the local surface water including the Stanislaus and Tuolumne rivers, the primary sources of recharge to the Modesto Subbasin aquifers.

3.2.5.2. Local Groundwater Quality

Publicly available groundwater quality data for the Modesto Subbasin were used in this analysis. These data sources include STRGBA GSA member agencies (City of Modesto, City of Riverbank, City of Waterford, and Modesto Irrigation District), Eastern San Joaquin Water Quality Coalition, Central Valley Salinity Alternatives for Long-term Sustainability (CV-SALTS), and the California State Water Resources Control Board GeoTracker-GAMA and GAMA database. Water quality data from other GSA member agencies, such as City of Oakdale, Oakdale Irrigation District, Stanislaus County, and Tuolumne County, were either not available or associated with constituents that were not included in this water quality analysis, such as total coliform and E. Coli coliform. The City of Modesto dataset includes >76,000 water quality records consisting of >30 different constituents collected between 1938 and 2018. The Eastern San Joaquin Water Quality Coalition dataset includes 50,696 records of nitrate analyses between 1902 and 2013, and 19,923 records of total dissolved solids (TDS) analyses between 1925 and 2013. The CV-SALTS database includes nitrate and TDS that were collected between 1934 to 2014 from the following five original collection agencies or sources: RWQCB Waste Discharge Requirements (WDR) data per the Dairy CARES program (Dairy); California Department of Public Health (CDPH); Department of Water Resources (DWR); the (USGS) National Water Information System (NWIS) program; and Geotracker Groundwater Ambient Monitoring and Assessment (GAMA) program.

The data compiled here includes all well types, including domestic, public supply, industrial, monitoring, irrigation, and stock wells, and from all local groundwater quality monitoring programs in the Modesto Subbasin. Using these data, a Microsoft Access database was built that includes over 118,203 groundwater quality records that were collected from 1,339 wells between the start of water year 1995 (October 1, 1994) to 2019. The database includes 260 unique water quality constituents. However, only the most relevant water quality constituents for the Modesto Subbasin are analyzed here. Prior to analysis, quality assurance/quality control (QA/QC) steps were performed on the data, including the identification and removal of duplicate samples and cross-checking the correct well location.

3.2.5.3. Constituents of Concern

A list of potential constituents of concern was developed by the technical team based on a preliminary data review, and review of previous water quality analyses developed in the Subbasin. The constituent list was reviewed at two public STRGBA GSA TAC meetings – April and July 2019. Based on input from TAC members, nine potential constituents of concern were identified for the analysis as listed below:

Table 3-2: Potential Constituents of Concern

Nitrate (as N)	Boron	Dibromo-3-chloropropane (DBCP)
Total Dissolved Solids (TDS)	Uranium	Tetrachloroethene (PCE)
Arsenic	Gross Alpha, 1,2-	1,2,3-Trichloropropane (TCP)

The following is a summary of groundwater quality conditions in the Modesto Subbasin during historical (water year 1995 to 2014) and present (2015 to 2019) periods, emphasizing these potential constituents of concern (COCs). Based on a review of water quality and input from the TAC, these COCs are the most likely to affect groundwater quality from irrigated agriculture (i.e., nitrate, TDS, and DBCP), which is the dominant land use across the Modesto Subbasin, from other human point sources (i.e., PCE) and from natural geogenic sources (i.e., arsenic, boron, uranium, and Gross Alpha) in the Subbasin. Nitrate is reported here as nitrate (as N); nitrate values reported in the original data sources as nitrate (as NO_3^-) were converted to nitrate (as N) prior to analysis.

Nitrate

Nitrate is the most common soluble form of nitrogen in natural groundwater and originates from natural and anthropogenic sources. In general, naturally occurring nitrate is found in low concentrations in groundwater and is derived from precipitation, atmospheric deposition, and natural biogeochemical cycling processes in soils, including the decomposition of organic matter. The most common anthropogenic source of nitrate is the application of nitrogen fertilizers, particularly on irrigated agricultural lands (Gurdak and Qi, 2012). As a result, nitrate is the most ubiquitous nonpoint-source COC of groundwater resources worldwide, including the Central Valley in California (Gurdak and Qi, 2012).

Point sources of nitrate in groundwater include feedlot and dairy drainage, leaching from septic systems, wastewater percolation, industrial wastewater, aerospace activities, and food processing waters (Viers et al., 2012). Denitrification is the only natural process that attenuates nitrate concentrations in groundwater. Previous studies have shown that denitrification is promoted in groundwater with anoxic conditions (dissolved oxygen (DO) < 0.5 mg/L) and large amounts of organic carbon (Gurdak and Qi, 2012). However, there are too few measurements of DO (N = 29) in the database to evaluate if oxic or anoxic conditions exist and the potential for denitrification. All of the DO samples except for two have concentrations in the oxic range (>0.5 milligrams per liter (mg/L)), which indicates a limited potential for denitrification. Future groundwater quality monitoring that includes measurements of DO could help characterize the potential for denitrification and explain the vulnerability of groundwater in the Modesto Subbasin to nitrate contamination.

Nitrate in groundwater from municipal wells in the Modesto Subbasin has been detected in concentrations that approach and, in some cases, exceed the MCL for drinking water (JJ&A and Formation Environmental, 2019). Currently, six municipal wells in the City of Modesto have been taken off-line due to elevated nitrate concentrations (JJ&A and Formation Environmental, 2019). Blending of water is being used to reduce nitrate concentrations at other municipal wells. Nitrate is present in the City of Modesto's drinking water aquifers because of historical agricultural and wastewater management activities. Nitrate is often detected in the shallow aquifer system, but in some cases, can be drawn down into the deeper aquifer by pumping or through wells with long screened or perforated intervals (Jurgens et al., 2008). Nitrate migration is influenced by downward hydraulic gradients created by municipal pumping, and elevated nitrate concentrations are being drawn deeper in the aquifer near local cones of depression (JJ&A and Formation Environmental, 2019).

A total of 41,898 groundwater samples in the Modesto Subbasin have nitrate analyses and an average concentration of 5.3 mg/L (as N) and generally meet drinking water quality standards (**Table 3-3)**. The median value (5.0 mg/L) is approximately double of the range of nitrate concentrations (2 to 3 mg/L) that have been established by previous studies as representing relative background concentrations from natural processes (Gurdak and Qi, 2012). Although isotopic analysis on the nitrate are needed to identify the source, the median value of 5.0 mg/L indicates that more than half of the samples are above the relative background concentration and thus have a nitrogen input from mostly human sources, such as fertilizers. The majority (93%) of the nitrate analyses have concentrations that are below the MCL of 10 mg/L (as N) (**Table 3-3**). However, 7% of the nitrate samples have concentrations that exceed the MCL (**Table 3-3**).

Table 3-3: Summary Statistics of Select Groundwater Quality Constituents

Water Quality Constituent	California MCL[1] or SMCL[2]	Number of Samples	Percentage of Samples			Concentrations			
			<0.5MCL	>0.5MCL to MCL	>MCL	Min.	Median	Avg.	Max.
Nutrients									
Nitrate (as N), mg/L	10 mg/L[1]	41,898	50%	42%	7%	0.0	5.0	5.3	490
Pesticides									
DBCP, µg/L	0.2 µg/L[1]	9,636	74%	12%	14%	0.0	0.0	0.1	18
TCP, µg/L	0.005 µg/L[1]	5,004	96%	0%	4%	0.000	0.000	0.008	12
Radionuclides									
Gross Alpha, pCi/L	15 pCi/L[1]	1,369	65%	20%	15%	-0.6	4.1	6.9	47
Uranium, pCi/L	20 pCi/L[1]	3,326	71%	20%	8%	0.0	4.9	7.4	65
Secondary Maxiumum Contaminant Level Constituents									
Total dissolved solids, mg/L	1,000 mg/L[2]	16,288	55%	30%	14%	0.0	450.0	703.2	20,000
Trace Elements									
Arsenic, µg/L	10 µg/L[1]	5,993	72%	20%	7%	0.0	2.9	4.8	300
Boron, mg/L	1 mg/L*	841	98%	1%	1%	0.0	0.0	1.9	200
Volatile Organic Compounds (VOC)									
PCE, µg/L	5 µg/L[1]	8,262	87%	4%	8%	0.0	0.0	10.4	8,860

Notes:

[1]**MCL**: California drinking water Maximum Contaminant Level

[2]**SMCL**: California drinking water Secondary Maximum Contaminant Level

<0.5MCL: percentage of samples with concentrations less than one-half the MCL.

>0.05MCL to MCL: percentage of samples with concentrations between one-half of the MCL to the MCL.

>MCL: percentage of samples with concentrations greater than the MCL.

*California State Notification Level (CA-NL). Boron does not have an MCL.

min.: minimum concentration

avg.: average concentration

max.: maximum concentration

The average and maximum concentrations of nitrate in groundwater from wells in the Modesto Subbasin during the period of water year 1995 to 2019 are shown in **Figures 3-35 and 3-36**. Nitrate concentrations are illustrated as green circles (less than 5 mg/L), yellow circles (between 5 mg/L and the MCL of 10 mg/L), orange circles (between 10 and 15 mg/L), and red circles (greater than 15 mg/L). Wells with average nitrate concentrations below the MCL of 10 mg/L (as N) tend to be located within the central part of the Subbasin, especially within the urban areas surrounding Modesto, Oakdale, Riverbank, and Waterford (**Figure 3-35**). The wells that have average nitrate concentrations that exceed the MCL of 10 mg/L (as N) are mostly located within the agricultural lands to the west and east of Modesto, but there are also clusters of exceedances within the City of Modesto (**Figure 3-35**). The spatial pattern of maximum nitrate concentrations is similar to the spatial pattern of average nitrate concentrations; most wells with maximum nitrate concentrations below the MCL tend to be in urban areas and the maximum nitrate concentrations above the MCL tend to be in the agricultural lands (**Figure 3-36).** However, there are several wells in Modesto and other urban areas of the Subbasin that have maximum nitrate concentrations above the

MCL. The spatial patterns in the average and maximum nitrate concentrations are apparently influenced by the general land-use pattern of the Subbasin.

Summary statistics of nitrate concentrations in groundwater from the Eastern Principal Aquifer, Western Upper Principal Aquifer, and Western Lower Principal Aquifer are shown in **Tables 3-4**, **3-5**, and **3-6**, respectively. The average nitrate concentrations are similar (5.6, 5.9, and 5.8 mg/L) in the Eastern, Western Upper, and Western Lower Principal Aquifers. The percentage of samples that exceed the 10 mg/L MCL in the Western Upper (13%) and Western Lower (22%) is greater than in the Eastern Principal Aquifer (3%). The data indicate that groundwater quality is relatively similar above and below the Corcoran Clay.

Table 3-4: Summary Statistics of Select Groundwater Quality Constituents for the Eastern Principal Aquifer

Water Quality Constituent	California MCL[1] or SMCL[2]	Number of Samples	Percentage of Samples			Concentrations			
			<0.5MCL	>0.5MCL to MCL	>MCL	Min.	Median	Avg.	Max.
Nutrients									
Nitrate (as N), mg/L	10 mg/L[1]	25,425	39%	58%	3%	0.0	5.7	5.6	490
Pesticides									
DBCP, µg/L	0.2 µg/L[1]	8,518	71%	14%	15%	0.0	0.0	0.1	18
TCP, µg/L	0.005 µg/L[1]	4,568	96%	0%	4%	0.000	0.000	0.008	12
Radionuclides									
Gross Alpha, pCi/L	15 pCi/L[1]	920	72%	17%	12%	-0.6	3.6	5.7	31
Uranium, pCi/L	20 pCi/L[1]	2,285	81%	14%	5%	0.0	4.0	5.9	52
Secondary Maxiumum Contaminant Level Constituents									
Total dissolved solids, mg/L	1,000 mg/L[2]	6,963	74%	25%	1%	0.0	380	389	3,000
Trace Elements									
Arsenic, µg/L	10 µg/L[1]	4,245	86%	11%	3%	0.0	2.2	3.1	130
Boron, mg/L	1 mg/L*	606	97%	1%	2%	0.0	0.0	2.6	200
Volatile Organic Compounds (VOC)									
PCE, µg/L	5 µg/L[1]	5,983	86%	5%	9%	0.0	0.0	6.3	8,860

Notes:

[1]**MCL**: California drinking water Maximum Contaminant Level

[2]**SMCL**: California drinking water Secondary Maximum Contaminant Level

<0.5MCL: percentage of samples with concentrations less than one-half the MCL.

>0.05MCL to MCL: percentage of samples with concentrations between one-half of the MCL to the MCL.

>MCL: percentage of samples with concentrations greater than the MCL.

*California State Notification Level (CA-NL). Boron does not have an MCL.

min.: minimum concentration

avg.: average concentration

max.: maximum concentration

Table 3-5: Summary Statistics of Select Groundwater Quality Constituents for the Western Upper Principal Aquifer

Water Quality Constituent	California MCL[1] or SMCL[2]	Number of Samples	Percentage of Samples			Concentrations			
			<0.5MCL	>0.5MCL to MCL	>MCL	Min.	Median	Avg.	Max.
Nutrients									
Nitrate (as NO3), mg/L	10 mg/L[1]	2,326	47%	40%	13%	0.0	5.3	5.9	52
Pesticides									
DBCP, µg/L	0.2 µg/L[1]	434	75%	2%	23%	0.0	0.0	0.1	1.5
TCP, µg/L	0.005 µg/L[1]	118	100%	0%	0%	0.0	0.000	0.000	0.000
Radionuclides									
Gross Alpha, pCi/L	15 pCi/L[1]	153	33%	33%	33%	0.0	11.4	12.4	47.2
Uranium, pCi/L	20 pCi/L[1]	433	29%	52%	20%	0.0	13.0	13.6	32
Secondary Maxiumum Contaminant Level Constituents									
Total dissolved solids, mg/L	1,000 mg/L[2]	1,215	46%	41%	13%	0.0	530	733	20,000
Trace Elements									
Arsenic, µg/L	10 µg/L[1]	1,108	42%	41%	17%	0.0	5.4	9.5	300
Boron, mg/L	1 mg/L*	139	100%	0%	0%	0.0	0.2	0.1	0.3
Volatile Organic Compounds (VOC)									
PCE, µg/L	5 µg/L[1]	1,014	93%	1%	7%	0.0	0.0	0.9	250

Notes:

[1]**MCL**: California drinking water Maximum Contaminant Level

[2]**SMCL**: California drinking water Secondary Maximum Contaminant Level

<0.5MCL: percentage of samples with concentrations less than one-half the MCL.

>0.05MCL to MCL: percentage of samples with concentrations between one-half of the MCL to the MCL.

>MCL: percentage of samples with concentrations greater than the MCL.

***California State Notification Level (CA-NL). Boron does not have an MCL.

min.: minimum concentration

avg.: average concentration

max.: maximum concentration

Table 3-6: Summary Statistics of Select Groundwater Quality Constituents for the Western Lower Principal Aquifer

Water Quality Constituent	California MCL[1] or SMCL[2]	Number of Samples	Percentage of Samples			Concentrations			
			<0.5MCL	>0.5MCL to MCL	>MCL	Min.	Median	Avg.	Max.
Nutrients									
Nitrate (as N), mg/L	10 mg/L[1]	445	50%	28%	22%	0.0	4.8	5.8	17
Pesticides									
DBCP, µg/L	0.2 µg/L[1]	110	100%	0%	0%	0.0	0.0	0.0	0
TCP, µg/L	0.005 µg/L[1]	133	95%	0%	5%	0.000	0.000	0.000	0
Radionuclides									
Gross Alpha, pCi/L	15 pCi/L[1]	30	93%	7%	0%	0.0	0.0	1.7	14
Uranium, pCi/L	20 pCi/L[1]	92	97%	3%	0%	0.0	1.0	1.4	13
Secondary Maxiumum Contaminant Level Constituents									
Total dissolved solids, mg/L	1,000 mg/L[2]	66	100%	0%	0%	45.0	188	192	468
Trace Elements									
Arsenic, µg/L	10 µg/L[1]	222	9%	74%	17%	0.0	9.0	8.3	14
Boron, mg/L	1 mg/L*	13	100%	0%	0%	0.0	0.1	0.1	0
Volatile Organic Compounds (VOC)									
PCE, µg/L	5 µg/L[1]	438	100%	0%	0%	0.0	0.0	0.0	1

Notes:

[1]**MCL**: California drinking water Maximum Contaminant Level

[2]**SMCL**: California drinking water Secondary Maximum Contaminant Level

<0.5MCL: percentage of samples with concentrations less than one-half the MCL.

>0.05MCL to MCL: percentage of samples with concentrations between one-half of the MCL to the MCL.

>MCL: percentage of samples with concentrations greater than the MCL.

*California State Notification Level (CA-NL). Boron does not have an MCL.

min.: minimum concentration

avg.: average concentration

max.: maximum concentration

Total Dissolved Solids

Total dissolved solids (TDS) represents the total concentration of anions and cations in water and is a useful indicator of mineralization, salt content, and overall groundwater quality. The TDS concentrations in groundwater of the Modesto Subbasin generally meet drinking water quality standards (**Table 3-3**) and some irrigation requirements. A total of 16,288 groundwater samples in the Modesto Subbasin have TDS analyses and only 14% of those samples exceed the California Secondary Maximum Contaminant Level (SMCL) of 1,000 mg/L (**Table 3-3**).

TDS can also be used to characterize the salinity of irrigation water, which can affect crop health and yield (Grattan, 2002). It is recommended that TDS concentrations should be below about 450 mg/L for irrigation of salt sensitive crops, and TDS concentrations between about 450 and 1,000 mg/L can represent a salinity hazard for plants if used as irrigation water (Bauder et al., 2014). About half (49%) of the samples have TDS concentrations less than 450 mg/L and would not cause plant stress. However, 36% of samples are between 450 and 1,000 mg/L and 14% of samples are greater than 1,000 mg/L. Therefore, about 51% of groundwater samples have TDS concentrations that could result in plant stress and salinity hazard as irrigation water.

To identify any areas of concern, the median and maximum TDS concentrations in groundwater from wells within the Modesto Subbasin during the period of water year 1995 to 2019 are shown in **Figures 3-37 and 3-38.** TDS concentrations are illustrated as green circles (below 500 mg/L), yellow circles (between 500 and 1,000 mg/L), orange circles (between 1,000 and 1,500 mg/L), and red circles (above 1,500 mg/L). The median and maximum TDS concentrations in groundwater throughout most of the Modesto are below 1,000 mg/L (**Figures 3-37 and 3-38**). Concentrations of TDS are generally lowest (less than 500 mg/L) in the central part of the Subbasin, especially within the urban areas surrounding Modesto, Oakdale, Riverbank, and Waterford (**Figure 3-37 and 3-38**). Concentrations of TDS above the MCL are generally found in wells located in the San Joaquin River National Wildlife Refuge on the western extent of the Subbasin, in southwest Modesto, and to the southeast of Modesto (**Figure 3-37 and 3-38**).

Summary statistics of TDS concentrations in groundwater from the Eastern Principal Aquifer, Western Upper Principal Aquifer, and Western Lower Principal Aquifer are shown in **Tables 3-4**, **3-5**, and **3-6**, respectively. The average TDS concentrations are similar (389 and 192 mg/L) in the Eastern and Western Lower Principal Aquifers. However, the average TDS in the Western Upper Principal Aquifer (733 mg/L) is much higher than in the other two Principal Aquifers. Similarly, 13% of TDS samples from the Western Upper Principal Aquifer exceed the MCL, while only 1 and 0% of the samples from the Eastern and Western Lower exceed the MCL. These results, along with the 20,000 mg/L maximum concentration may indicate a point source affecting TDS concentrations in the Western Upper Principal Aquifer (**Table 3-5**).

Arsenic

Arsenic is a naturally occurring trace element in rocks, soils, and groundwater in some areas of the Central Valley aquifer (Burton et al., 2012). In the Modesto Subbasin, arsenic in groundwater is generally naturally occurring and is largely derived from the Sierran sediments that were transported to the eastern San Joaquin Valley by glacial and fluvial processes (Jurgens et al., 2008). Previous studies of arsenic in the San Joaquin Valley (Belitz et al., 2003; Welch et al., 2006; Izbicki et al., 2008; and Burton et al., 2012) and a literature review of arsenic (Welch et al., 2000) have identified two dominant mechanisms for elevated arsenic in groundwater. The first mechanism is the reductive dissolution of arsenopyrite or other iron or manganese oxyhydroxides under iron- or manganese-reducing conditions. The second mechanism is the pH-dependent desorption of arsenic from aquifer sediments under oxic conditions, which tends to occur in groundwater with pH above 7.5 (Stollenwerk, 2003). Given the general oxic nature of groundwater in the Subbasin, sorption and desorption on iron oxyhydroxides at pH above 7.5 is expected to be the most significant control on arsenic groundwater mobility. Another mechanism that has been identified is the decreased resorption due to increasing pH, competing species, or lack of sorption sites

(Jurgens et al., 2008; Jurgens et al., 2009). Arsenic can also be mobilized from aquitards by dewatering (Smith et al., 2018). The USGS (2008) indicate that migration of arsenic in groundwater in the study area can be facilitated by lateral and vertical gradients created by municipal pumping and by vertical movement through wells with long screened or perforated intervals. Additionally, it has been proposed that geochemical changes in modern recharge water, such as relatively high dissolved organic carbon concentrations could contribute to mobilization of arsenic in the aquifer (JJ&A and Formation Environmental, 2019). Anthropogenic sources of arsenic in groundwater can include the use of wood preservatives, paints and dyes, and from some mining and oilfield operations (Welch et al., 2000).

Groundwater arsenic concentrations in the Subbasin are generally higher in older and deeper groundwater samples (Jurgens et al., 2009). Arsenic in groundwater from municipal wells has been detected in concentrations that approach and, in some cases, exceed the MCL for drinking water (JJ&A and Formation Environmental, 2019). Several municipal wells from the City of Modesto have been taken off-line due to elevated arsenic concentrations (JJ&A and Formation Environmental, 2019).

The concentrations of arsenic are generally low in groundwater of the Modesto Subbasin as compared to the MCL (**Table 3-3**). A total of 5,993 groundwater samples have arsenic analyses and only 7% of those analyses exceed the California MCL of 10 µg/L (**Table 3-3**). The wells with average concentrations of arsenic that exceed the MCL are generally located in the urban area of Modesto and in wells on the western extent of the Subbasin (**Figures 3-39**). Wells with maximum concentrations of arsenic that exceed the MCL are also generally located in the urban areas of Modesto and Riverbank, and wells on the western extent of the Subbasin (**Figure 3-40**).

Summary statistics of arsenic concentrations in groundwater from the Eastern Principal Aquifer, Western Upper Principal Aquifer, and Western Lower Principal Aquifer are shown in **Tables 3-4**, **3-5**, and **3-6**, respectively. The average arsenic concentrations in the Western Upper (9.5 µg/L) and Western Lower (8.3 µg/L) Principal Aquifers are more than double the 3.1 µg/L average concentration in the Eastern Principal Aquifer. Similarly, 17% of the arsenic samples in both the Western Upper and Western Lower exceed the MCL, as compared to only 3% of samples in the Eastern Principal Aquifer. These data indicate important differences may exist in the source(s) and geochemical conditions that control arsenic in groundwater of the Western Upper and Lower Principal Aquifers as compared to the Eastern Principal Aquifer.

Uranium

Uranium in groundwater in the Modesto Subbasin is generally naturally occurring and is largely derived from granitic rocks in the Sierra Nevada rather than sources at land surface (Jurgens et al., 2008). The uranium was weathered from these rocks and oxidized and adsorbed to sediments that were transported to the eastern San Joaquin Valley by glacial and fluvial processes and deposited in the alluvial fans that now make up the Modesto Subbasin (Jurgens et al., 2008). Uranium is a relatively prevalent contaminant in shallow and intermediate depth aquifers in the study area, including beneath the City of Modesto (JJ&A and Formation Environmental, 2019). The mobilization of uranium in the shallow and intermediate aquifer is likely influenced by elevated bicarbonate concentrations in modern and oxic recharge water resulting from agricultural activities (Jurgens et al., 2009). Irrigation return flow that recharges the aquifer can be relatively elevated in bicarbonate concentrations because of the rich and active biomes of the agricultural soils that create elevated carbon dioxide and relatively high partial pressures of carbon dioxide that often result in bicarbonate water type of modern recharge. The uranium is mobilized from the natural sediments when the bicarbonate-rich water flow downward through the aquifer and replaces older groundwater that has relatively lower bicarbonate concentrations (Jurgens et al., 2009). Uranium concentrations have also been observed to be negatively correlated with pH (Burton et al., 2012). Therefore, uranium concentrations are generally higher near the water table and in shallow groundwater and decrease with depth (Jurgens et al., 2008).

Uranium has been detected in municipal wells at concentrations that approach and, in some cases, exceed the MCL for drinking water (JJ&A and Formation Environmental, 2019). Currently, nine municipal wells in the City of Modesto have been taken off-line due to elevated uranium concentrations (JJ&A and Formation Environmental, 2019).

The concentrations of uranium are generally low in groundwater across much of the Modesto Subbasin as compared to the MCL (**Table 3-3**). A total of 3,326 groundwater samples have uranium analyses and 8% of those analyses exceed the California MCL of 20 pCi/L (**Table 3-3**). Most of the uranium samples were collected from supply wells within the urban areas of Modesto, Oakdale, Riverbank, and Waterford. The wells with average (**Figure 3-41**) and maximum (**Figure 3-42**) uranium concentrations that exceed the MCL tend to be located in the City of Modesto.

Summary statistics of uranium concentrations in groundwater from the Eastern Principal Aquifer, Western Upper Principal Aquifer, and Western Lower Principal Aquifer are shown in **Tables 3-4**, **3-5**, and **3-6**, respectively. The uranium concentrations in groundwater are much greater in the Western Upper Principal Aquifer, as compared to the Eastern or Western Lower Principal Aquifers. A total of 20% of uranium samples in the Western Upper exceed the MCL, while only 5 and 0% in the Eastern and Western Lower, respectively, exceed the MCL. These differences in uranium concentration among groundwater of the Principal Aquifers are consistent with the processes of the oxic and bicarbonate rich irrigation return flow that mobilizes uranium in the shallow and intermediate aquifer.

Gross Alpha

Alpha particles (α-particles) are a type of radiation emitted by some radionuclides. The alpha particles consist of two protons and two neutrons. Their travel range is only a few centimeters. Once alpha particles lose energy, they pick up electrons and become helium. Alpha emitting radionuclides are naturally occurring elements, and include radium-226, uranium-238, radium-226, and radon-222. Radium-226 and radon-222 are generally the alpha emitters of greatest interest to drinking water because they are groundwater contaminants widely distributed in the U.S. and associated with granitic rock, including the Sierra Nevada. The California MCL for gross alpha in drinking water is 15 pCi/L.

The concentrations of gross alpha are relatively low in groundwater across much of the Modesto Subbasin as compared to the MCL (**Table 3-3**). A total of 1,369 groundwater samples have gross alpha analyses and 85% of those analyses have concentrations that are less than the California MCL of 15 pCi/L. A total of 15% of the groundwater samples exceed the gross alpha MCL, which is a higher percentage than uranium samples exceeding the MCL (**Table 3-3**). Similar to the uranium samples, most of the gross alpha samples were collected from supply wells within the urban areas of Modesto, Oakdale, Riverbank, and Waterford. The wells with average (**Figure 3-43)** and maximum (**Figure 3-44**) uranium concentrations that exceed the MCL tend to be located in the City of Modesto, especially in the southwest part of Modesto.

Summary statistics of gross alpha in groundwater from the Eastern Principal Aquifer, Western Upper Principal Aquifer, and Western Lower Principal Aquifer are shown in **Tables 3-4**, **3-5**, and **3-6**, respectively. Similar to the pattern of uranium, the gross alpha in groundwater is much greater in the Western Upper Principal Aquifer, as compared to the Eastern or Western Lower Principal Aquifers. A total of 20% of uranium samples in the Western Upper exceed the MCL, while only 5 and 0% in the Eastern and Western Lower, respectively, exceed the MCL. Similar to uranium, these differences in gross alpha among groundwater of the Principal Aquifers are consistent with the processes of the oxic and bicarbonate rich irrigation return flow that mobilizes uranium in the shallow and intermediate aquifer.

Boron

Boron is a naturally occurring trace element in many minerals and rocks, including igneous rocks such as granite and pegmatite, and some evaporite minerals. Borax is a boron-containing evaporite mineral that is mined in California and is used as a cleaning agent and therefore may be present in sewage and industrial wastes (Burton et al., 2012). There is no MCL for boron. However, California has a Notification Level (NL) of 1 mg/L. Boron is an essential element for plant growth in relatively small concentrations. However, for many crops, boron concentrations greater than 1 to 2 mg/L may be toxic (Ayers and Westcot, 1994).

The concentrations of boron are generally very low in groundwater in the Modesto Subbasin as compared to the NL (**Table 3-3**). A total of 841 groundwater samples have boron analyses and 99% of those analyses have concentrations that are less than the California NL of 1.0 mg/L and 1% have concentrations that exceed the NL (**Table 3-3**). The average (**Figures 3-45**) and maximum (**Figures 3-46**) boron concentrations of groundwater in wells that exceed the NL are generally located in Waterford, which may indicate a potential point-source contamination issue. 98% of the boron analyses have concentrations below 0.5 mg/L (**Table 3-3**), and thus the boron concentrations in groundwater of the Modesto Subbasin are well below toxic levels for plants.

Summary statistics of boron concentrations in groundwater from the Eastern Principal Aquifer, Western Upper Principal Aquifer, and Western Lower Principal Aquifer are shown in **Tables 3-4**, **3-5**, and **3-6**, respectively. There are no major differences in boron concentration or percentage of samples that exceed the NL among the three Principal Aquifers.

Pesticides

Pesticides in groundwater can result from the over-application on agricultural lands or from point-source contamination and preferential flow down improperly constructed wells. While pesticides are typically soluble in water, many can be highly sorptive to soils, which can slow their transport to the water table. The analysis is focused on the two widely detected pesticides Dibromochloropropane (DBCP) and 1,2,3-Trichloropropane (TCP).

Dibromochloropropane (DBCP)

Dibromochloropropane (DBCP) was a widely used agricultural nematocide and soil fumigant in parts of the Central Valley that was first detected in California drinking water in 1979 and later banned in the late 1970s. In 1983, a statewide drinking water source monitoring program was initiated and found DBCP to be the most commonly detected pesticide in groundwater (CA Department of Health Services, 1999). DBCP is relatively mobile when dissolved in water and free DBCP may occur as a dense non-aqueous phase liquid (DNAPL). DBCP is toxic to humans at low concentrations, and thus has presented a local concern (JJ&A and Formation Environmental, 2019). The Federal and California MCL for DBCP is 0.2 µg/L. DBCP was detected in at least seven municipal wells in the City of Modesto at concentrations above the MCL that warranted the use of wellhead treatment using granular activated carbon (Jurgens et al., 2008). DBCP has also been detected at lower concentrations below the MCL in water from at least seven municipal wells from the City of Modesto (JJ&A and Formation Environmental, 2019).

The concentrations of DBCP are generally low in groundwater of the Modesto Subbasin as compared to the MCL (**Table 3-3**). A total of 9,636 groundwater samples have DBCP analyses and 86% of those analyses and below the California MCL of 0.2 µg/L (**Table 3-3**). The remaining 14% of samples with DBCP concentrations above the MCL are from wells that are generally located to the north, west, and southeast of the City of Modesto (**Figures 3-47 and 3-48**).

Summary statistics of DBCP concentrations in groundwater from the Eastern Principal Aquifer, Western Upper Principal Aquifer, and Western Lower Principal Aquifer are shown in **Tables 3-4**, **3-5**, and **3-6**, respectively. The percentage of DBCP samples that exceed the MCL are somewhat similar (15 and 23%) in the Eastern and Western Upper and greater than in the Western Lower (0%) Principal Aquifer. Unlike nitrate concentrations that were somewhat similar above and below the Corcoran Clay, relatively higher concentrations of DBCP appears to be more frequently detected in only the Western Upper Principal Aquifer. The relatively longer flow paths and travel times for groundwater below the Corcoran Clay may help to limit DBCP concentrations in the Western Lower Principal Aquifer.

1,2,3-Trichloropropane (TCP)

1,2,3-Trichloropropane (TCP) is a chlorinated hydrocarbon with high chemical stability that often occurs as an intermediate in chemical manufacturing. It is a manmade chemical that is often found at industrial or hazardous waste sites, used as a cleaning and degreasing solvent, and associated with pesticide products (SWRCB, 2019). TCP may be produced as a byproduct of processes used to produce soil fumigant chemicals. TCP is also a major and minor component of several soil fumigants that were used historically in California through most of the 1980s (Burton et al., 2012). Although TCP was banned from pesticides in the 1990s, it has been detected in groundwater beneath agricultural areas of the Central Valley as part of the GAMA sampling program (Shelton et al., 2008). TCP is an emerging contaminant of concern because it is widely detected and is a probable carcinogen to humans (SWRCB, 2019). In 2017, California adopted an MCL of 0.005 µg/L for drinking water, and now many water supply systems are being monitored for TCP. TCP has been detected in several wells throughout the Subbasin at concentrations above the MCL (JJ&A and Formation Environmental, 2019).

The concentrations of TCP in groundwater in the Modesto Subbasin as compared to the MCL are shown in **Table 3-3**. A total of 5,004 groundwater samples have TCP analyses and 4% of those analyses are above the California MCL of 0.005 µg/L (**Table 3-3**). The wells with average (**Figures 3-49**) and maximum (**Figures 3-50**) TCP concentrations that exceed the MCL are located primarily in the urban areas of Modesto, Riverbank and Waterford. As discussed below in the section on historical and present trends, the wells with elevated TCP tend to have concentrations that are sometimes two to three orders of magnitude greater than the MCL. Such high concentrations of TCP may indicate locations of point-source contamination.

Summary statistics of TCP concentrations in groundwater from the Eastern Principal Aquifer, Western Upper Principal Aquifer, and Western Lower Principal Aquifer are shown in **Tables 3-4**, **3-5**, and **3-6**, respectively. TCP exceedances of the MCL occur in 15% of Eastern Principal Aquifer samples, 23% of Western Upper Principal Aquifer samples, and 0% of Western Lower Principal Aquifer samples. These data suggest that relatively lower concentrations of TCP are below the Corcoran Clay.

Tetrachloroethylene (PCE)

Volatile organic compounds (VOCs) have been detected in several wells in and around the City of Modesto and in Oakdale (JJ&A and Formation Environmental, 2019). The source of the VOCs is largely attributed to historical dry-cleaning operations. At least seven City of Modesto wells are currently receiving treatment to remove PCE, trichloroethylene, and (or) Freon-113 (JJ&A and Formation Environmental, 2019). There have been a number of response actions in the Modesto area to the PCE contamination, including site investigations, groundwater extraction to address shallow groundwater contamination, and soil vapor extraction to address source removal and potential vapor intrusion into buildings (JJ&A and Formation Environmental, 2019). Therefore, the VOC analysis here is focused on PCE.

Tetrachloroethylene (PCE) is a manufactured chemical and does not occur naturally in the environment. It is a regulated contaminant with a Federal and California MCL of 5 µg/L. Common sources of PCE include dry cleaning operations, textile operations, and metal degreasing processes. It was also widely used in the production of CFC-113 and other fluorocarbons. PCE is also used in rubber coatings, solvent soaps, printing inks, adhesives and glues, sealants, polishes, lubricants, and pesticides. PCE is a DNAPL and has moderate to high mobility.

The concentrations of PCE are generally low in groundwater in the Modesto Subbasin as compared to the MCL (**Table 3-3**). A total of 8,262 groundwater samples have PCE analyses and 92% of those analyses are below the California MCL of 5 µg/L (**Table 3-3**). Most PCE concentrations above the MCL are from wells located in Modesto and Oakdale, which are likely impacted by historical dry-cleaning operations (**Figures 3-51 and 3-52**).

Summary statistics of PCE concentrations in groundwater from the Eastern Principal Aquifer, Western Upper Principal Aquifer, and Western Lower Principal Aquifer are shown in **Tables 3-4**, **3-5**, and **3-6**, respectively. The percentage of PCE samples that exceed the MCL are somewhat similar (9% and 7%) in the Eastern and Western Upper and greater than in the Western Lower (0%) Principal Aquifer. Similar to patterns in DBCP and TCP concentrations, relatively lower concentrations of PCE appear to be detected below the Corcoran Clay in the Western Lower Principal Aquifer. The low permeability of the clay associated with relatively longer flow paths and travel times for groundwater below the Corcoran Clay may help to limit PCE concentrations in the Western Lower Principal Aquifer.

3.2.5.4. Trends in Historical and Present Groundwater Quality

Statistical tests were used to evaluate if the concentrations of groundwater quality constituents are statistically similar or different between historical (water year 1995 to 2014) and present (2015 to 2019) periods. This analysis will help identify processes that may affect the temporal trends in the groundwater quality of the Modesto Subbasin.

First, the Shapiro-Wilk test for normality was used to test the null hypothesis that the groundwater quality constituents come from a normal distribution. Results of the Shapiro-Wilk test support a rejection of the null hypothesis (α-level = 0.05) and indicate that nitrate, DBCP, TCP, Gross Alpha, Uranium, TDS, arsenic, boron, and PCE all have a non-normal distribution.

Based on the results of the Shapiro-Wilk tests, the nonparametric Wilcoxon rank-sum test was used to test the null hypothesis that the groundwater quality constituents sampled between the historical and present period come from populations that have the same distribution and thus are statistically similar. Results of the Wilcoxon rank-sum test support the decision to fail to reject the null hypothesis (α-level = 0.05) for TCP (p-value = 0.767), gross alpha (p-value = 0.212), and PCE (p-value = 0.981) (**Figure 3-53**), which indicates that these groundwater quality constituents have statistically similar median concentrations during the historical and present periods. However, the results of the Wilcoxon rank-sum test for nitrate (p-value = <0.001), DBCP (p-value = <0.001), uranium (p-value = <0.001), TDS (p-value = 0.001), arsenic (p-value = <0.001), and boron (p-value = <0.001) support the decision to reject the null hypothesis (**Figure 3-54**), which indicates that these groundwater quality constituents have statistically different median concentrations during the historical and present periods. The median concentrations of nitrate, DBCP, arsenic, and boron are statistically lower in the present period than the historical period (**Figure 3-54**). Conversely, the median concentrations for uranium and TDS are statistically higher in the present period than the historical period (**Figure 3-54**).

The temporal linear trends in groundwater quality constituents are evaluated in **Figures 3-55 and 3-56**. Results of the trend analysis indicate statistically significant (α-level = 0.05) increasing trends for TCP (p-value = <0.001) and gross alpha (p-value = <0.001) concentrations, but no statistically significant temporal trend for PCE (p-value = 0.141) (**Figure 3-55**). Results of the trend analysis indicate statistically significant (α-level = 0.05) increasing trends for TDS (p-value = <0.001), nitrate (p-value = <0.001), and uranium (p-value = <0.001) concentrations (**Figure 3-56**). Conversely, there are decreasing trends for DBCP (p-value = <0.001) and arsenic (p-value = 0.002), but no statistically significant trend for boron (p-value = 0.232) (**Figure 3-56**).

These findings indicate that TCP, gross alpha, TDS, nitrate, and uranium concentrations are increasing over time in the Modesto Subbasin, while DBCP and arsenic concentrations are decreasing over time in the Modesto Subbasin.

3.2.6. Land Subsidence

The overdraft conditions exacerbated by the recent drought have resulted in lowered groundwater levels – a condition that can contribute to subsidence of the ground surface. As water levels decline in the subsurface, dewatering and compaction of predominantly fine-grained deposits (such as clay and silt) can cause the overlying ground surface to subside.

This process is illustrated by two conceptual diagrams shown on **Figure 3-57**. The upper diagram depicts an alluvial groundwater basin with a regional clay layer and numerous smaller discontinuous clay layers. Water level declines associated with pumping cause a decrease in water pressure in the pore space (pore pressure) of the aquifer system (Galloway, et al., 1999). Because the water pressure in the pores helps support the weight of the overlying aquifer, the pore pressure decrease causes more weight of the overlying aquifer to be transferred to the grains within the structure of the sediment layer. The difference between the water pressure in the pores and the weight of the overlying aquifer is termed the effective stress. If the effective stress borne by the sediment grains exceeds the structural strength of the sediment layer, then the aquifer system begins to deform. This deformation consists of re-arrangement and compaction of fine-grained units[3], as illustrated on the lower diagram of **Figure 3-57**. The tabular nature of the fine-grained sediments

[3] Although extraction of groundwater by pumping wells causes a more complex deformation of the aquifer system than discussed herein, the simplistic concept of vertical compaction is often used to illustrate the land subsidence process (Galloway, et al., 1999; LSCE et al., 2014).

allows for preferred alignment and compaction. As the sediments compact, the ground surface can sink, as illustrated by the 2nd column on the lower diagram of **Figure 3-57**.

Land subsidence due to groundwater withdrawals can be temporary (elastic) or permanent (inelastic).

Elastic deformation occurs when sediments compress as pore pressures decrease but expand by an equal amount as pore pressures increase. A decrease in water levels from groundwater pumping causes a small elastic compaction in both coarse- and fine-grained sediments; however, this compaction recovers as the effective stress returns to its initial value. Because elastic deformation is relatively minor and fully recoverable, it is not considered an impact.

Inelastic deformation occurs when the magnitude of the greatest pressure that has acted on the clay layer since its deposition (preconsolidation stress) is exceeded. This occurs when groundwater levels in the aquifer reach a historically low water level. During inelastic deformation, or compaction, the sediment grains rearrange into a tighter configuration as pore pressures are reduced. This causes the volume of the sediment layer to reduce, which causes the land surface to subside. Inelastic deformation is permanent because it does not recover as pore pressures increase. Clay particles are often planar in form and more subject to permanent realignment (and inelastic subsidence). In general, coarse-grained deposits (e.g., sand and gravels) have sufficient intergranular strength and do not undergo inelastic deformation within the range of pore pressure changes encountered from groundwater pumping.

The volume of compaction is equal to the volume of groundwater that is expelled from the pore space, resulting in a loss of storage capacity. This loss of storage capacity is permanent but may not be substantial because clay layers do not typically store significant amounts of usable groundwater (LSCE, et al., 2014). Inelastic compaction, however, may decrease the vertical permeability of the clay resulting in minor changes in vertical flow.

The following potential impacts can be associated with land subsidence due to groundwater withdrawals (modified from LSCE, et al., 2014):

- Damage to infrastructure including foundations, roads, bridges, or pipelines;
- Loss of conveyance in canals, streams, or channels;
- Diminished effectiveness of levees;
- Collapsed or damaged well casings; and
- Land fissures.

Land subsidence in the San Joaquin Valley has been documented for more than 90 years and recent investigations using satellite imagery indicate continuing problems in some areas. However, subsidence is not a significant issue in Modesto Subbasin. **Figure 3-58** illustrates the results of a subsidence study conducted by the USGS (Faunt et al., 2015) in the San Joaquin Valley from 2008 to 2010. This study shows that subsidence did not occur within Modesto Subbasin during this time period.

Beginning in June 2015, vertical displacement was estimated throughout many California groundwater basins using Interferometric Synthetic Aperture Radar (InSAR) data. The InSAR data are collected by the European Space Agency (ESA) Sentinel-1A satellite and processed by TRE ALTAMIRA Inc. (TRE), under contract with DWR as part of DWR's SGMA technical assistance. **Figure 3-59** illustrates vertical displacement (in feet) for the Modesto Subbasin from June 2015 to June 2018. Most of the Subbasin is shaded grey on this figure, meaning that ground surface elevations actually rose between 0 and 0.05 feet (0.6 inches). Negative vertical displacement (subsidence), shown by yellow to light brown colors, occurred in the eastern Subbasin, within the Eastern Principal Aquifer (east of the Corcoran Clay). Most of the eastern Subbasin subsided between 0 and 0.05 feet (0.6 inches), as shown by the yellow shading. There are two small areas in the eastern Subbasin with more subsidence. The maximum measured subsidence, shown by the small brown shaded area, is 0.14 feet (1.7 inches). This is a minimal amount of measured subsidence possibly due to the abundance of clay surficial soils (see black shading on **Figure 3-6**) that have the potential to shrink. This subsidence is not likely to impact critical infrastructure in this area. There is a higher potential for subsidence in the western Modesto Subbasin if groundwater levels are lowered below the Corcoran Clay.

3.2.7. Interconnected Surface Water

Analysis awaiting modeling results

3.2.8. Groundwater Dependent Ecosystems

To support identification of groundwater dependent ecosystems (GDEs), DWR created the Natural Communities Commonly Associated with Groundwater dataset. This Natural Communities dataset is a compilation of 48 publicly available State and federal agency datasets that map vegetation, wetlands, springs, and seeps in California. The resultant mapping of natural vegetation communities and wetlands commonly associated with groundwater has been reviewed by DWR, California Department of Fish and Wildlife (CDFW), and The Nature Conservancy (TNC) and provided online for California groundwater basins. The data included in the Natural Communities dataset do not necessarily represent GDEs but can be used as a starting point in identifying GDEs within a groundwater basin.

Figure 3-60 is the mapping for the Subbasin, which shows wetlands and vegetation along the three major rivers (Stanislaus, Tuolumne and San Joaquin rivers), along Dry Creek and areas between Dry Creek and the Tuolumne River, and within the San Joaquin River Natural Wildlife Refuge.

A groundwater dependent ecosystem (GDE) is defined under SGMA as "ecological communities of species that depend on groundwater emerging from aquifers or on groundwater occurring near the ground surface" (23 CCR § 351(m)). The presence of vegetation and wetlands does not necessarily indicate the presence of a GDE.

The discussion of GDEs will be continued after the analysis of interconnected surface water is complete.

3.2.9. Data Gaps and Uncertainties for Groundwater Conditions

This section will summarize groundwater condition data gaps that affect implementation of the Plan and are related to the GSAs ability to sustainably manage groundwater. The Plan Implementation section, when developed, will describe how these data gaps will be addressed in future GSP actions. A summary of the data gaps for the Groundwater Conditions is summarized below.

Table 3-7: Data Gaps for the Groundwater Conditions

Issue	Area	Impacts on Groundwater Management	Actions to Address
Water Levels in Western Lower Principal Aquifer	Western Lower Principal Aquifer	Groundwater levels and flow; vertical gradients; evaluation for potential future land subsidence; insufficient wells for groundwater elevation mapping.	• Install monitoring wells screened solely in the Western Lower Principal Aquifer. • Locate existing wells to incorporate into monitoring program, if available.
Groundwater Conditions in Eastern Subbasin	East and Northeast of Modesto Reservoir	Groundwater flow and quality of Eastern Principal Aquifer	• Install monitoring wells in eastern Subbasin. • Obtain water level data from landowners.
Interconnected Surface Water	River boundaries	Groundwater levels and flow, surface water availability, water budgets	• Analyze with Modesto C2VSim Model. • Calibrate model to local surface water data.
Groundwater Dependent Ecosystems (GDEs)	River boundaries	Groundwater levels and flow	Verify presence of GDEs based on DWR's Natural Communities Commonly Associated with Groundwater dataset.

References

Ayers, R.S., and Westcot, D.W., 1994, Water Quality for Agriculture, Chapter 4: Toxicity Problems, Food and Agriculture Organization (FAO) of the United Nations, FAO Irrigation and Drainage Paper, 29 Rev.1.

Bartow, A., 1991, The Cenozoic Evolution of the San Joaquin Valley, California, U.S. Geological Survey Professional Paper 1501.

Bauder, T.A., Waskom, P.L., Sutherland, P.L., Davis, J.G., Irrigation Water Quality Criteria, Irrigation Water Quality Criteria, Fact Sheet No. 0506, Crop Series / Irrigation, Colorado State University Extension.

Belitz, K., Dubrovsky, N.M., Burow, K.R., Jurgens, B., and Johnson, T., 2003, Framework for a ground-water quality monitoring and assessment program for California: U.S. Geological Survey Water-Resources Investigations Report 03-4166, 78 p. Available at http://pubs.usgs.gov/wri/wri034166/.

Burow, K.R., Shelton, J.L., Hevesi, J.A., and Weissmann, G.S., 2004, Hydrogeologic Characterization of the Modesto Area, San Joaquin Valley, California: U.S. Geological Survey Scientific Investigations Report 2004-5232, 54 p.

Burton, C.A., Shelton, J.L., and Belitz, Kenneth, 2012, Status and understanding of groundwater quality in the two southern San Joaquin Valley study units, 2005–2006—California GAMA Priority Basin Project: U.S. Geological Survey Scientific Investigations Report 2011–5218, 150 p.

California Data Exchange Center (CDEC), 2018, http://cdec.water.ca.gov/cgi-progs/iodir/WSIHIST

California Department of Health Services, 1999, MCL Evaluation for 1,2-dibromo-3-chloropropane (DBCP), Division of Drinking Water and Environmental Management, Final Draft, Available at https://www.waterboards.ca.gov/drinking_water/certlic/drinkingwater/documents/mclreview/DBCP-MCLevaluation.pdf.

California Department of Water Resources (DWR), 2019, Sustainable Groundwater Management Act, 2019 Basin Prioritization, December.

California Department of Water Resources (DWR), 1974, Evaluation of Ground Water Resources: Sacramento County, Bulletin 118-3, July.

Dale, R.H., French, J.J., and Gordon, G.V., 1966, Ground-Water Geology and Hydrology of the Kern River Alluvial-Fan Area, California, USGS Open-File Report, June 20.

Davids Engineering, Inc, 2006, 2015 Agricultural Water Management Plan, Oakdale Irrigation District, March.

Faunt, C.C., Sneed, M., Traum, J., Brandt, J.T., 2015, Water Availability and Land Subsidence in the Central Valley, California, USA, Hydrogeol J, November 15.

Galloway, D., Jones, D.R., Ingebritsen, S.E., 1999, Land Subsidence in the United States, U.S. Geological Survey Circular 1182.

Grattan, S, 2002, Irrigation water salinity and crop production. Farm Water Quality Planning.

Gurdak, J.J., and Qi, S.L., 2012, Vulnerability of recently recharged groundwater in principal aquifers of the United States to nitrate contamination, Environmental Science and Technology, 46, pgs. 6004-6012, doi:10.1021/es300688b.

Izbicki, J.A., Stamos, C.L., Metzger, L.F., Halford, K.J., Kulp, T.R., and Bennett, G.L., 2008, Source, distribution, and management of arsenic in water from wells, eastern San Joaquin ground-water subbasin, California: U.S. Geological Survey Open-File Report 2008–1272, 8 p.

Jacobson James & Associates, Inc. (JJ&A) and Formation Environmental, 2019, Draft remedial investigation feasibility study workplan, City of Modesto Well Field RIFS, Prepared for City of Modesto Utilities Department by JJ&A and Formation Environmental, April 26, 2019.

Jurgens, B.C., Fram, M.S., Belitz, K., Burow, K.R., and Landon, M.K., 2009. Effects of Groundwater Development on Uranium: Central Valley, California, USA: *Groundwater 48(6), 10.1111/j.1745-6584.2009.00635.x, pages 913-928.*

Jurgens, B.C., Burow, K.R., Dalgish, B.A., and Shelton, J.L., 2008, Hydrogeology, water chemistry, and factors affecting the transport of contaminants in the zone of contribution of a public-supply well in Modesto, eastern San Joaquin Valley, California: U.S. Geological Survey Scientific Investigations Report 2008-5156, 78 p.

Landon, M.K., Belitz, K., Jurgens, B.C., Kulongoski, J.T., and Johnson, T.D., Status and understanding of groundwater quality in the Central–Eastside San Joaquin Basin, 2006: California GAMA Priority Basin project. Scientific Investigations Report (SIR) 2009–5266.

Luhdorff & Scalmanini Consulting Engineers (LSCE), James Borchers, and Michael Carpenter, 2014, Report of Findings: Land Subsidence from Groundwater Use in California, April.

Marchand, D.E., 1980, Preliminary Geologic Maps Showing Quaternary Deposits of the Ceres, Denair and Montpelier 7 ½ Quadrangles, Stanislaus and Merced Counties, California, United States Department of the Interior Geological Survey Open-file report 80-607.

Page, R.W., 1977, Appraisal of ground-water conditions in Merced, California, and vicinity; U.S. Geological Survey Open-File Report 77-454, 43 p.

Page, R.W. and Balding, G.O., 1973. Geology and Quality of Water in the Modesto-Merced Area, San Joaquin Valley, California, with a Brief Section on Hydrology. U.S. Geological Survey, prepared in cooperation with the California Department of Water Resources. Water-Resources Investigation 6-73. September 1973.

Phillips, S.P., Rewis, D.L., and Traum, J.A., 2015. Hydrologic Model of the Modesto Region, California, 1960-2004. U.S. Geological Survey Scientific Investigations Report (SIR), 2015-5045.

Provost & Pritchard, 2015, Agricultural Water Management Plan, 2015 Update for the Modesto Irrigation District, December.

Shelton, J.L., Pimentel, I., Fram, M.S., and Belitz, K., 2008, Ground-Water Quality Data in the Kern County Subbasin Study Unit, 2006—Results from the California GAMA Program, U.S. Geological Survey in cooperation with the California State Water Resources Control Board, USGS Data Series 337, 75 p., Available at http://pubs.usgs.gov/ds/337/.

Smith, R., Knight, R., and Fendorf, S., 2018. *Overpumping leads to California groundwater arsenic threat,* Nature Communications 9(1), December.

State Water Resources Control Board (SWRCB) of California, 2019, 1,2,3-Trichloropropane, Available at: https://www.waterboards.ca.gov/drinking_water/certlic/drinkingwater/123TCP.html

State Water Resources Control Board (SWRCB) of California, 2017, Groundwater Information Sheet – Tetrachloroethylene (PCE), Division of Water Quality, GAMA Program, 8 p., Available at: https://www.waterboards.ca.gov/water_issues/programs/gama/docs/coc_pce.pdf

Stollenwerk, K.G., 2003, Geochemical processes controlling transport of arsenic in groundwater, a review of adsorption, *in* Welch, A.H., and Stollenwerk, K.G., eds., Arsenic in groundwater—geochemistry and occurrence: Boston, Kluwer Academic Publishers, 488 p.

Todd Groundwater, 2016, Groundwater Characterization and Recharge Study, June.

Viers, J.H., Liptzin, D., Rosenstock, T.S., Jensen, V.B., Hollander, A.D., McNally, A., King, A.M., Kourakos, G., Lopez, E.M., De La Mora, N., Fryjoff-Hung, A., Dzurella, K.N., Canada, H.E., Laybourne, S., McKenney, C., Darby, J., Quinn, J.F. & Harter, T., 2012, Nitrogen Sources and Loading to Groundwater. Technical Report 2 in: Addressing Nitrate in California's Drinking Water with a Focus on Tulare Lake Basin and Salinas Valley Groundwater. Report for the State Water Resources Control Board Report to the Legislature. Center for Watershed Sciences, University of California, Davis, July.

Wagner, D.L., Bortugno, E.J., and McJunking, R.D., 1991, Geologic Map of the San Francisco-San Jose Quadrangle, California, 1:250,000.

Welch, A.H., Oremland, R.S., Davis, J.A., and Watkins, S.A., 2006, Arsenic in groundwater—A review of current knowledge and relation to the CALFED solution area with recommendations for needed research: San Francisco Estuary and Watershed Science, v. 4, no. 2, Article 4, 32 p.

Welch, A.H., Westjohn, D.B., Helsel, D.R., and Wanty, R.B., 2000, Arsenic in ground water of the United States—Occurrence and geochemistry: Ground Water, v. 38, no. 4, p. 589–604.

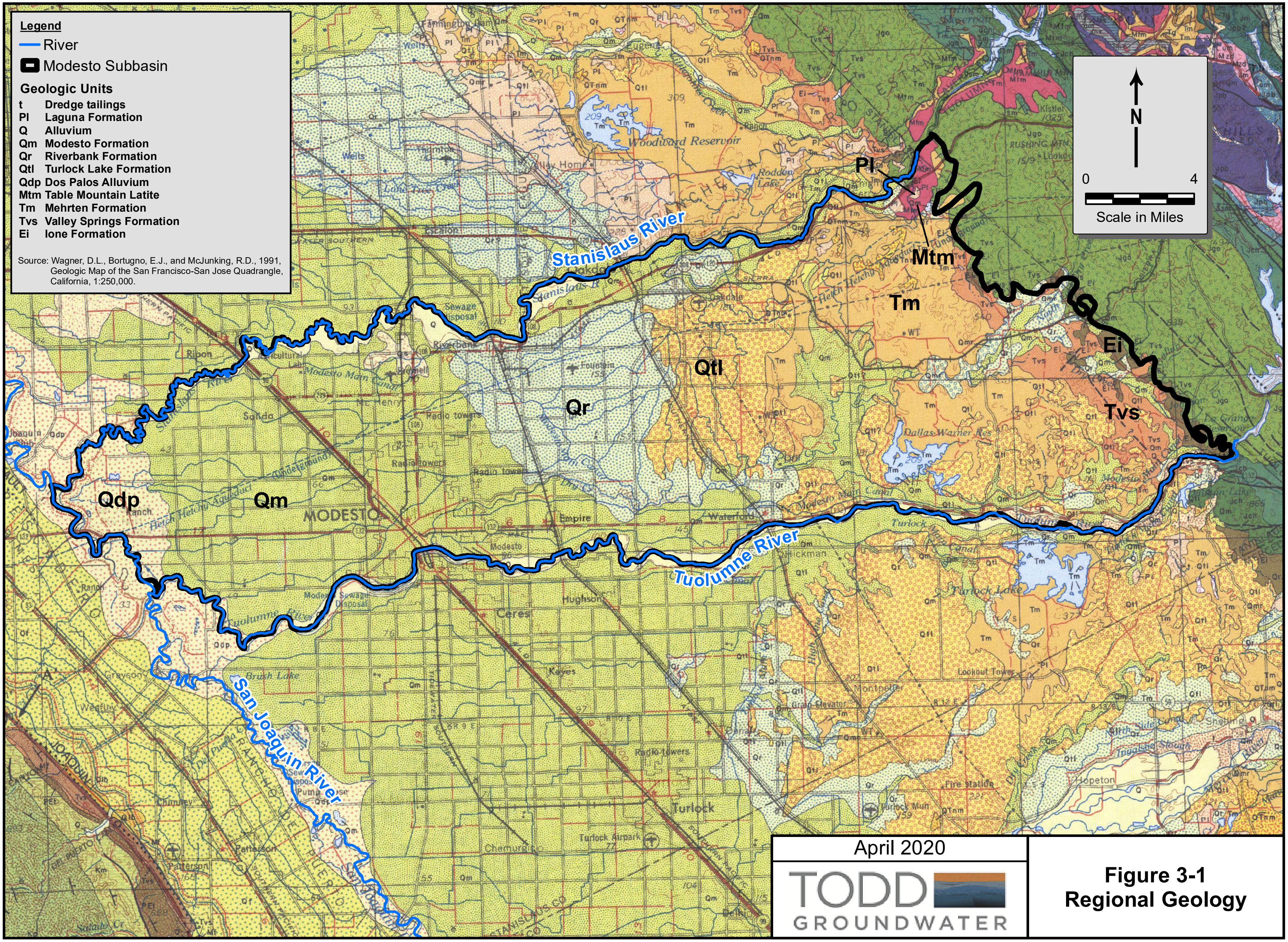

April 2020

TODD GROUNDWATER

Figure 3-1
Regional Geology

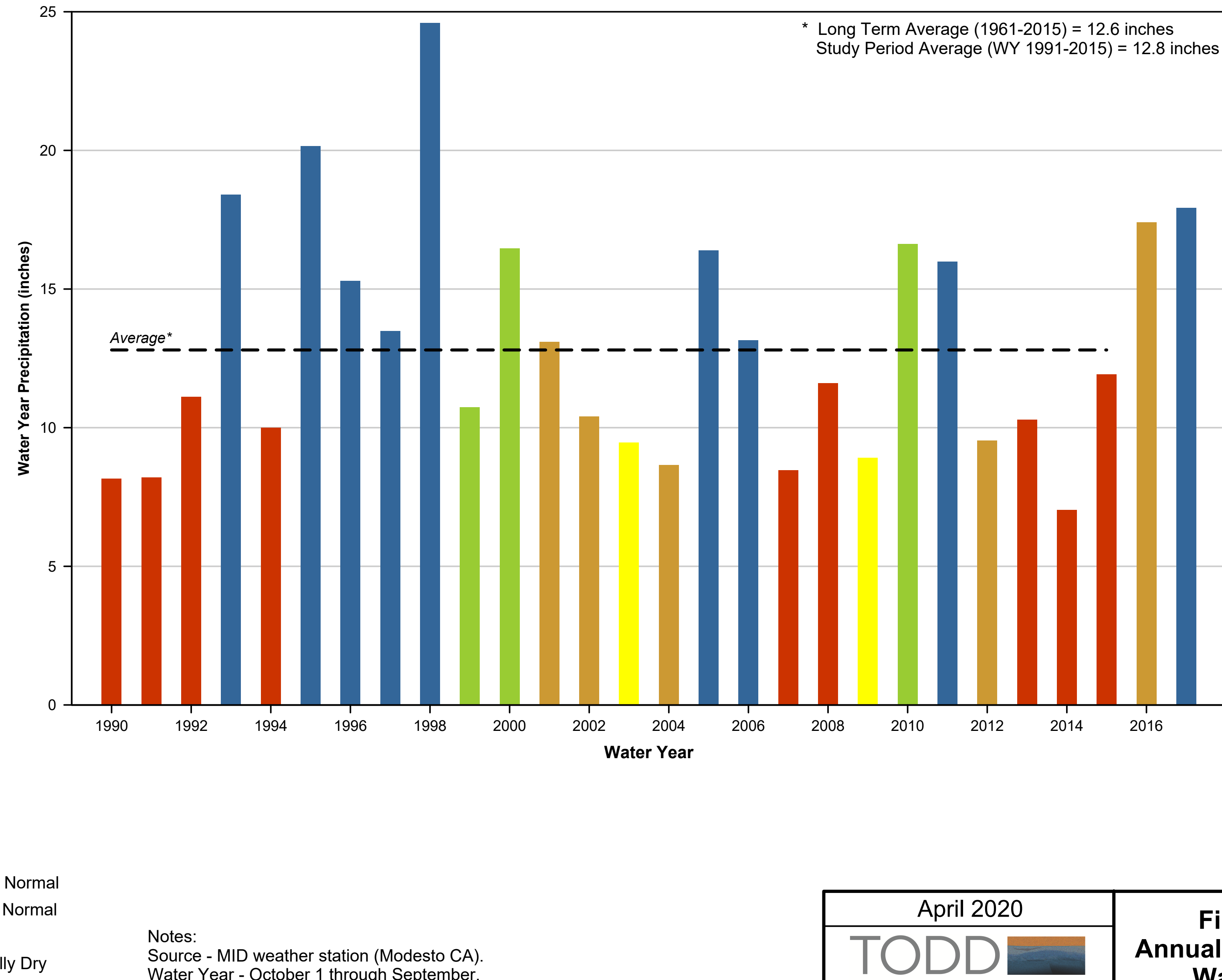

Notes:
Source - MID weather station (Modesto CA).
Water Year - October 1 through September.

April 2020

TODD GROUNDWATER

Figure 3-2
Annual Precipitation
Water Year

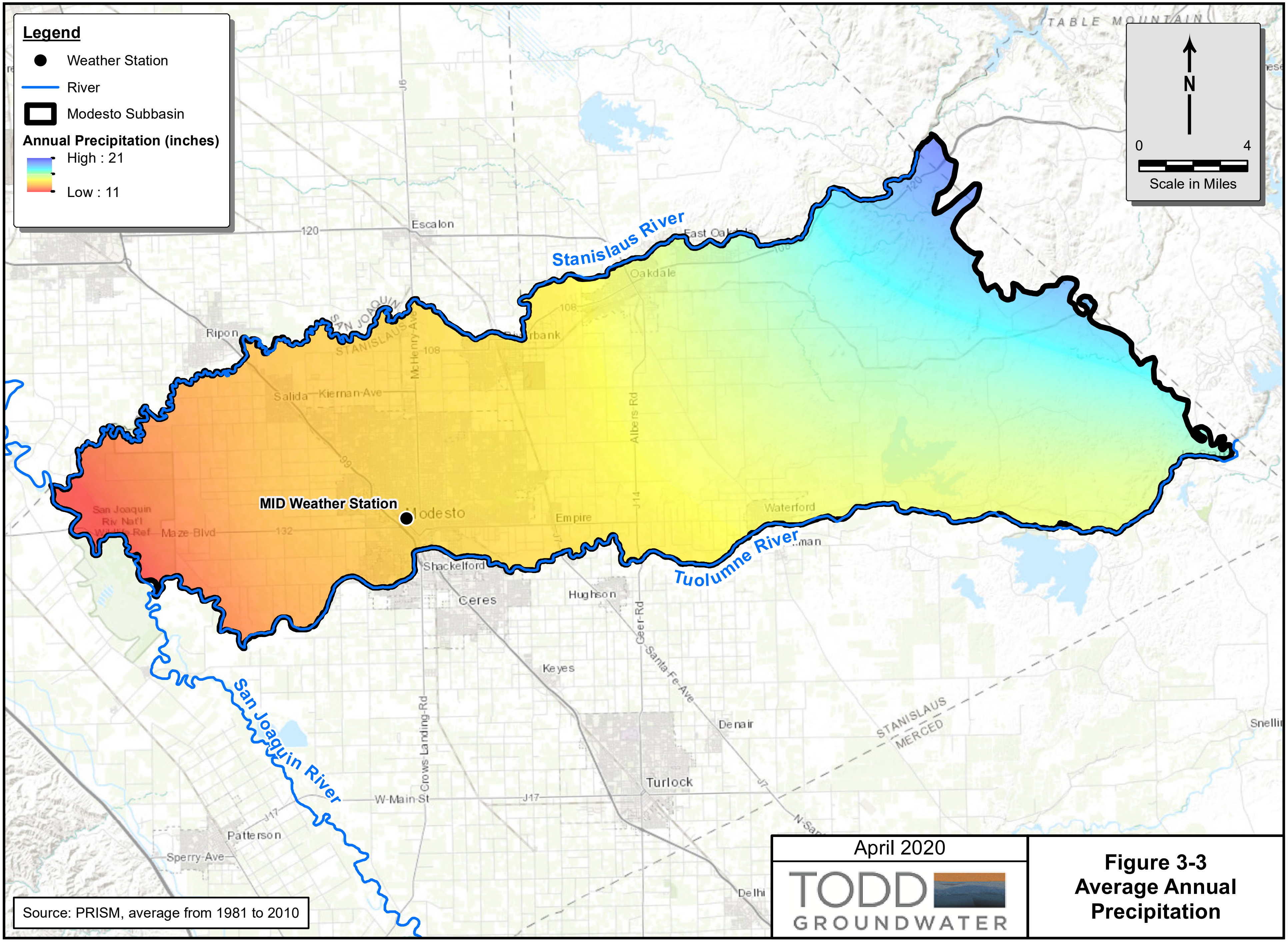

April 2020

TODD GROUNDWATER

Figure 3-3
Average Annual Precipitation

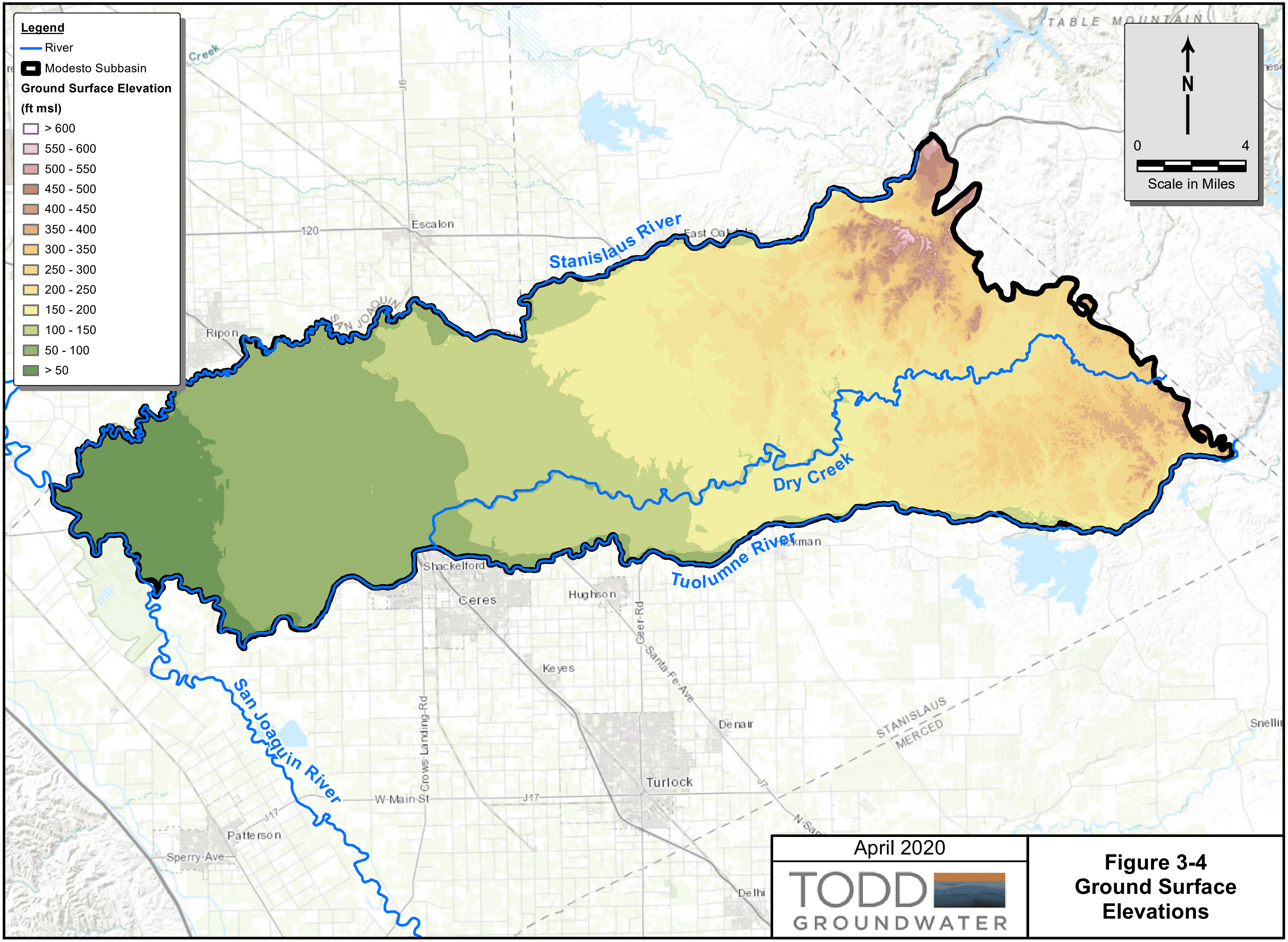

April 2020

TODD GROUNDWATER

Figure 3-4
Ground Surface Elevations

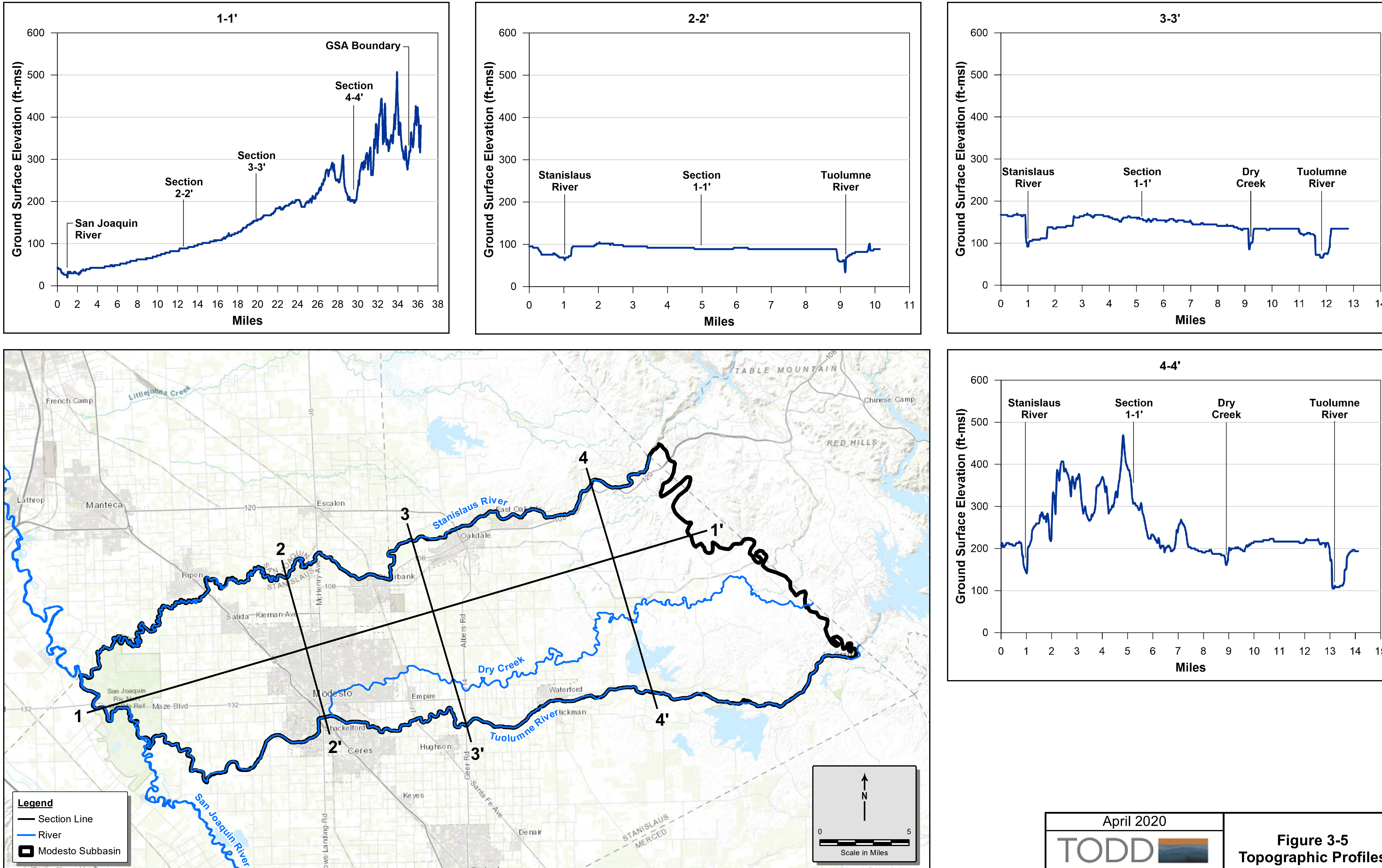

April 2020

TODD GROUNDWATER

Figure 3-5
Topographic Profiles

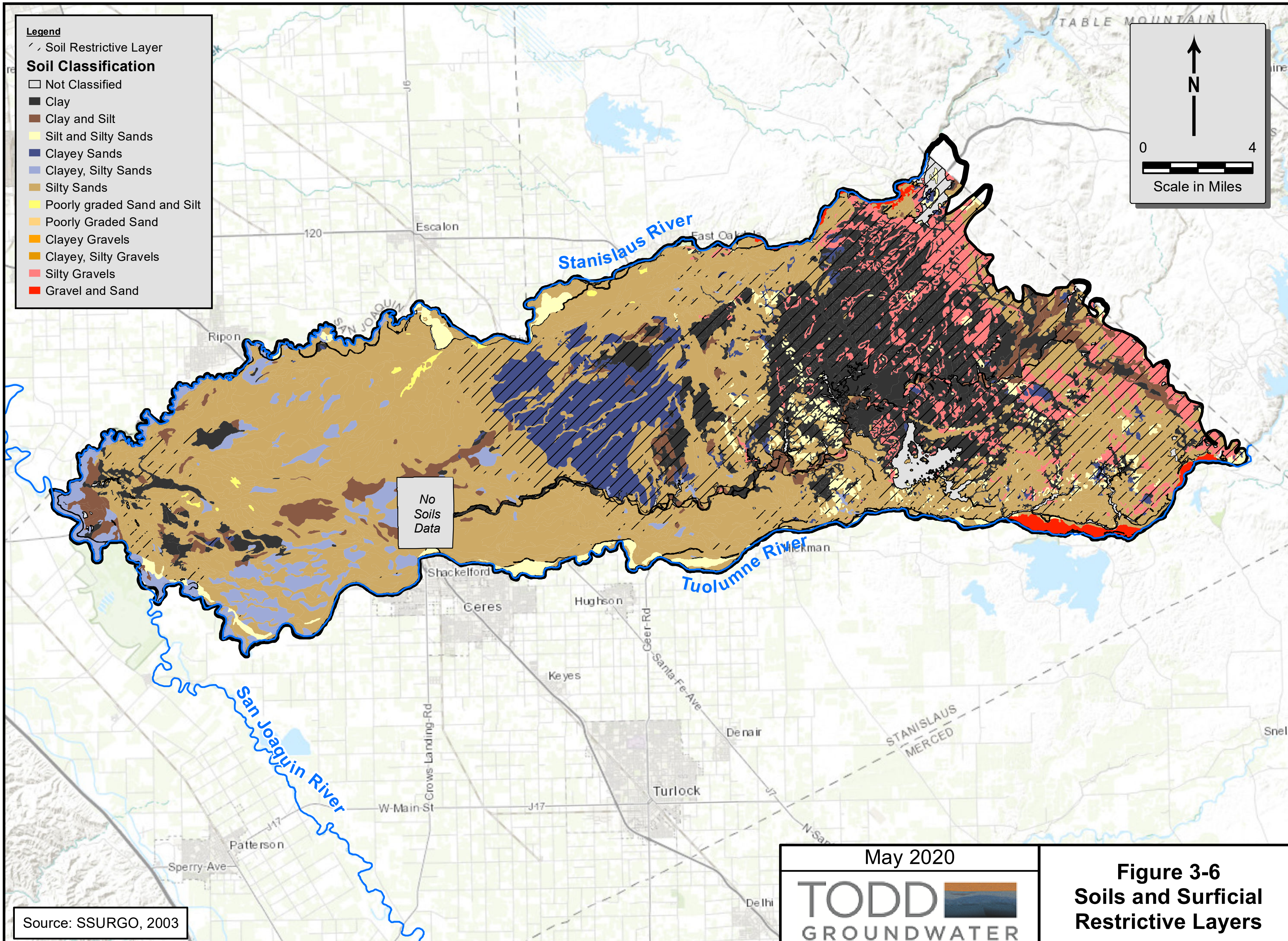

May 2020

TODD GROUNDWATER

Figure 3-6
Soils and Surficial Restrictive Layers

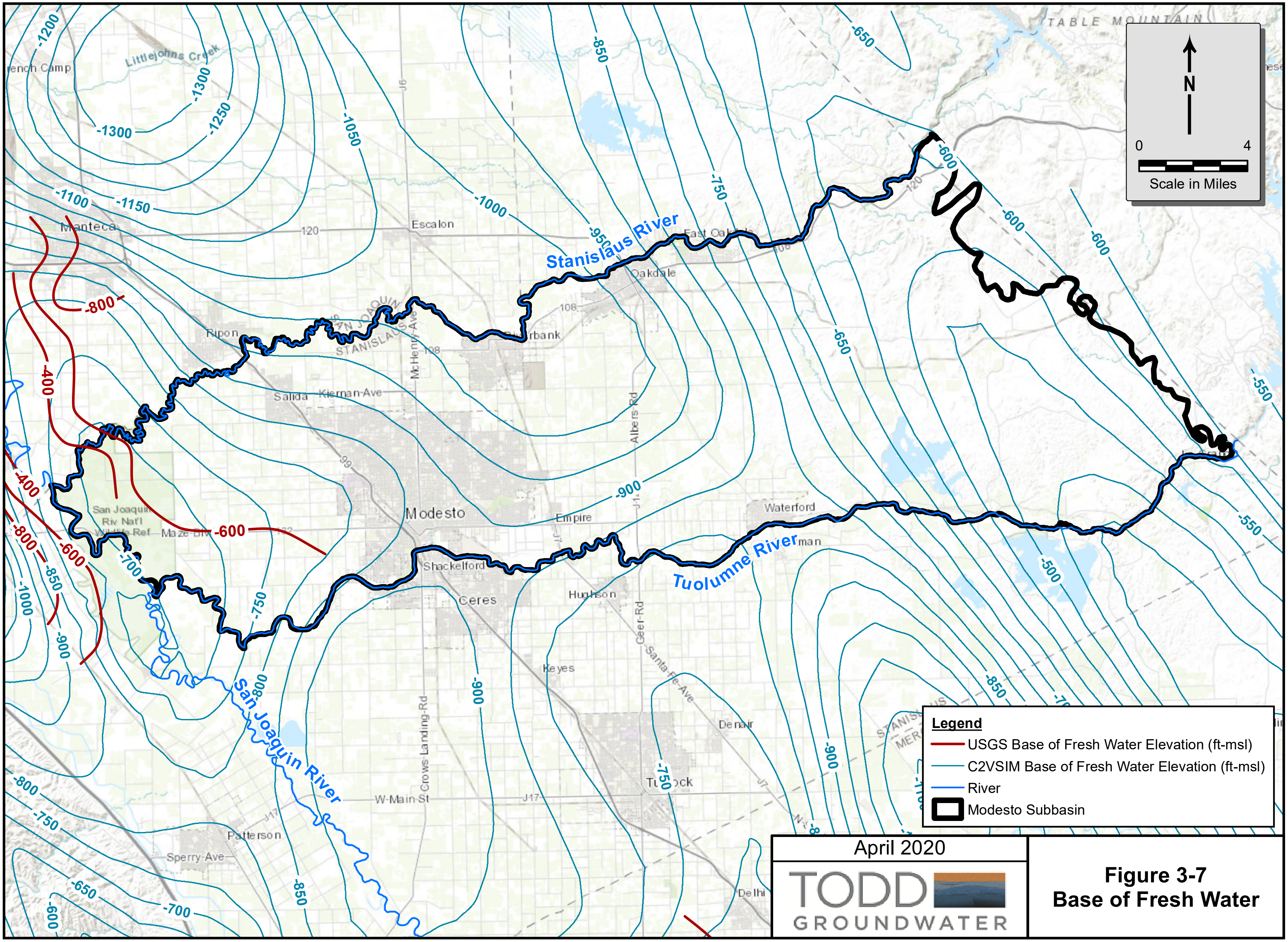

Figure 3-7
Base of Fresh Water

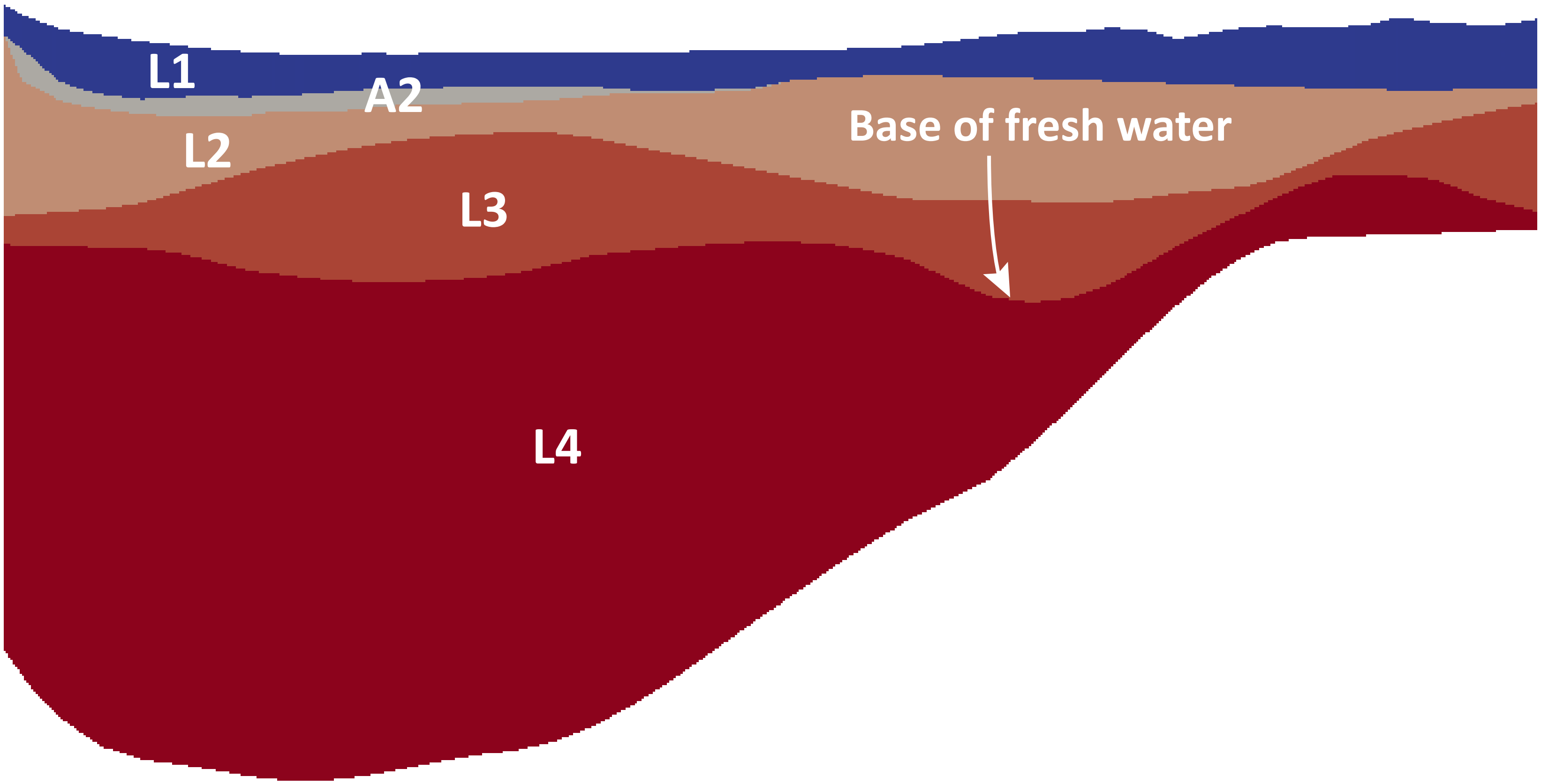

L1: Aquifer ranging from the ground surface to the top of the pumping layer
A2: Corcoran Clay
L2: Primary shallow pumping layer
L3: Deeper pumping layer (bottom of layer is the base of fresh water)
L4: Saline aquifer (bottom of layer is the base of continental deposits)

April 2020

TODD GROUNDWATER

Figure 3-8
C2VSIM
Model Layers

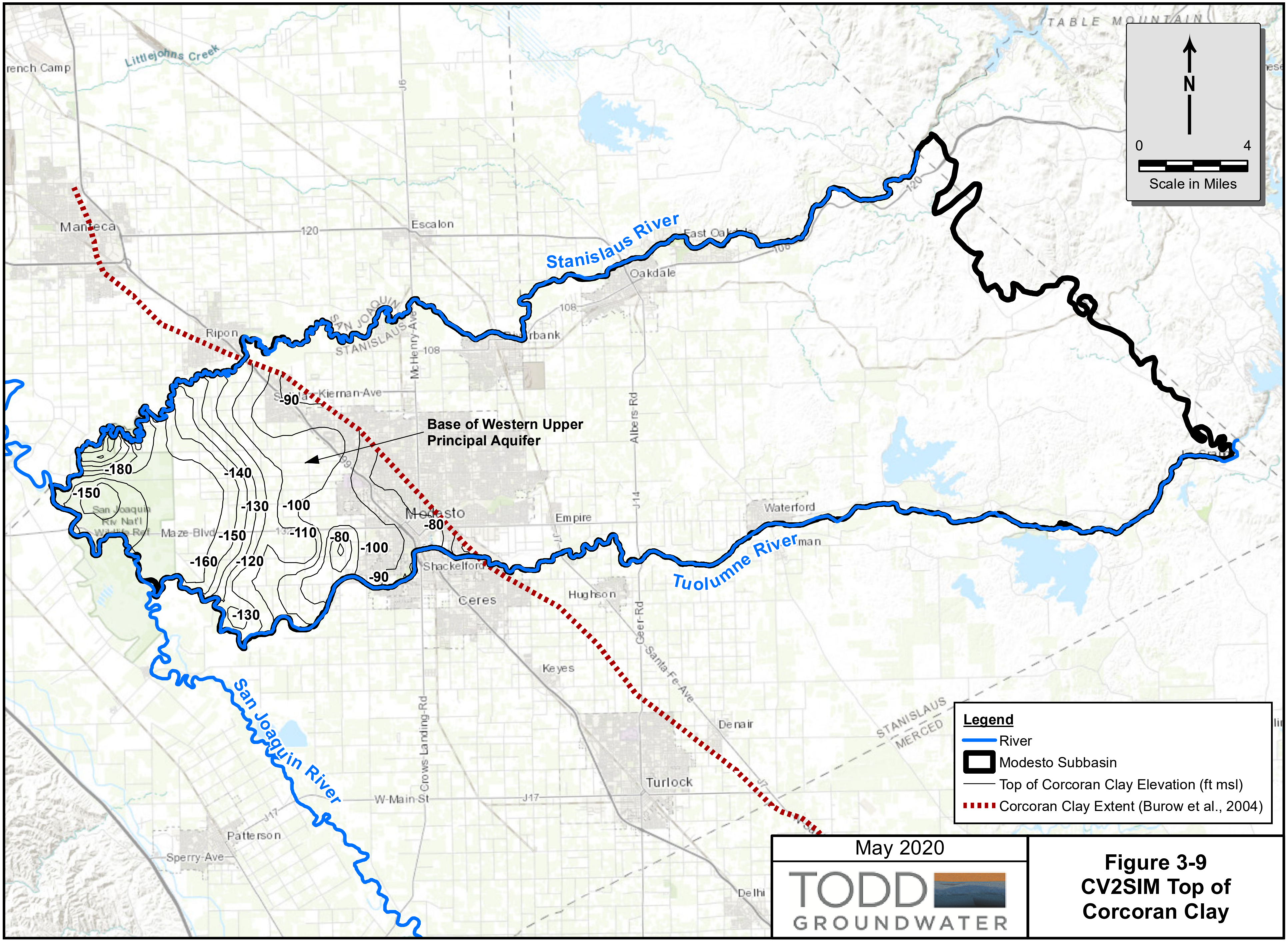

Figure 3-9
CV2SIM Top of Corcoran Clay

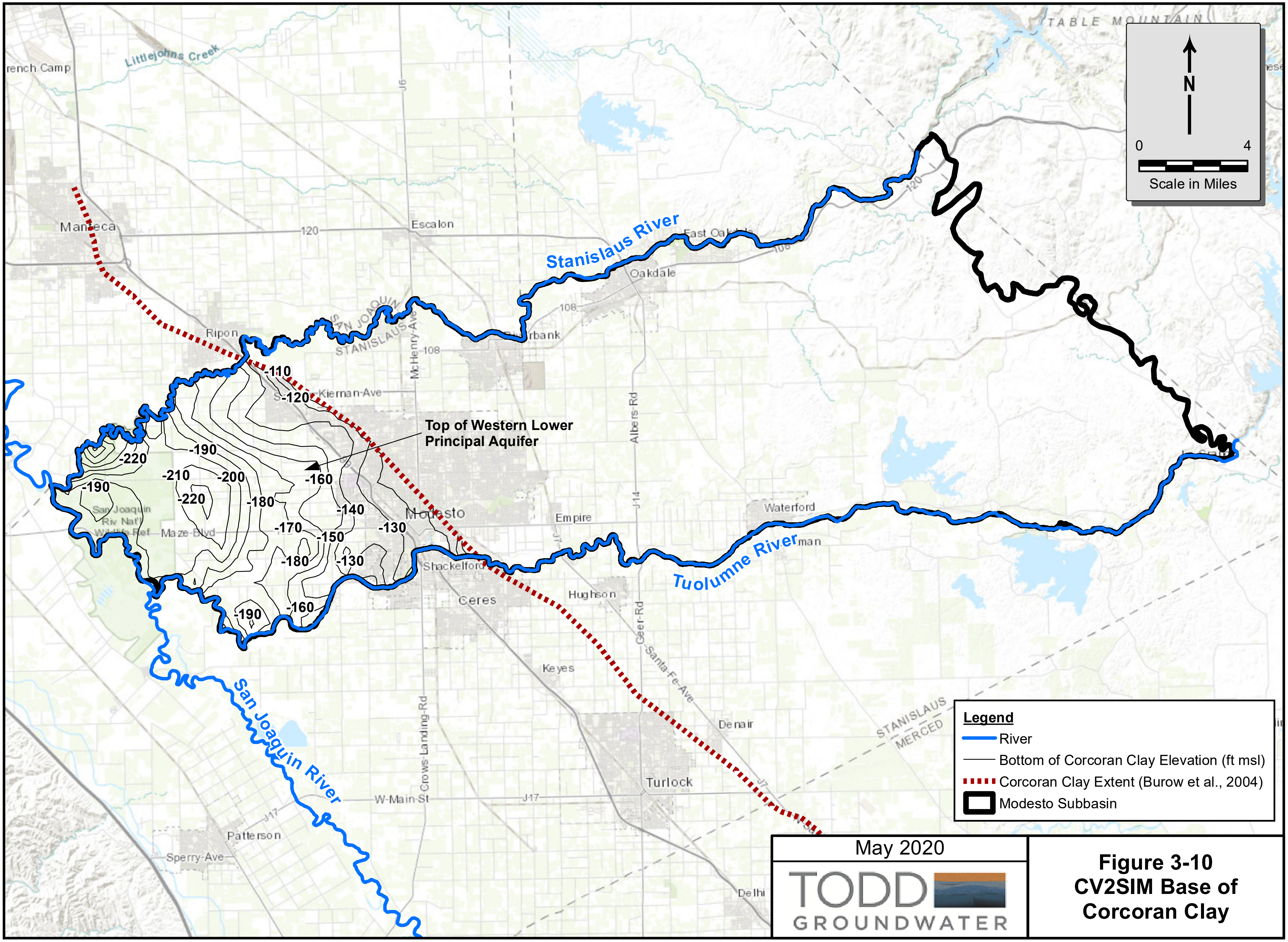

May 2020

TODD GROUNDWATER

Figure 3-10
CV2SIM Base of Corcoran Clay

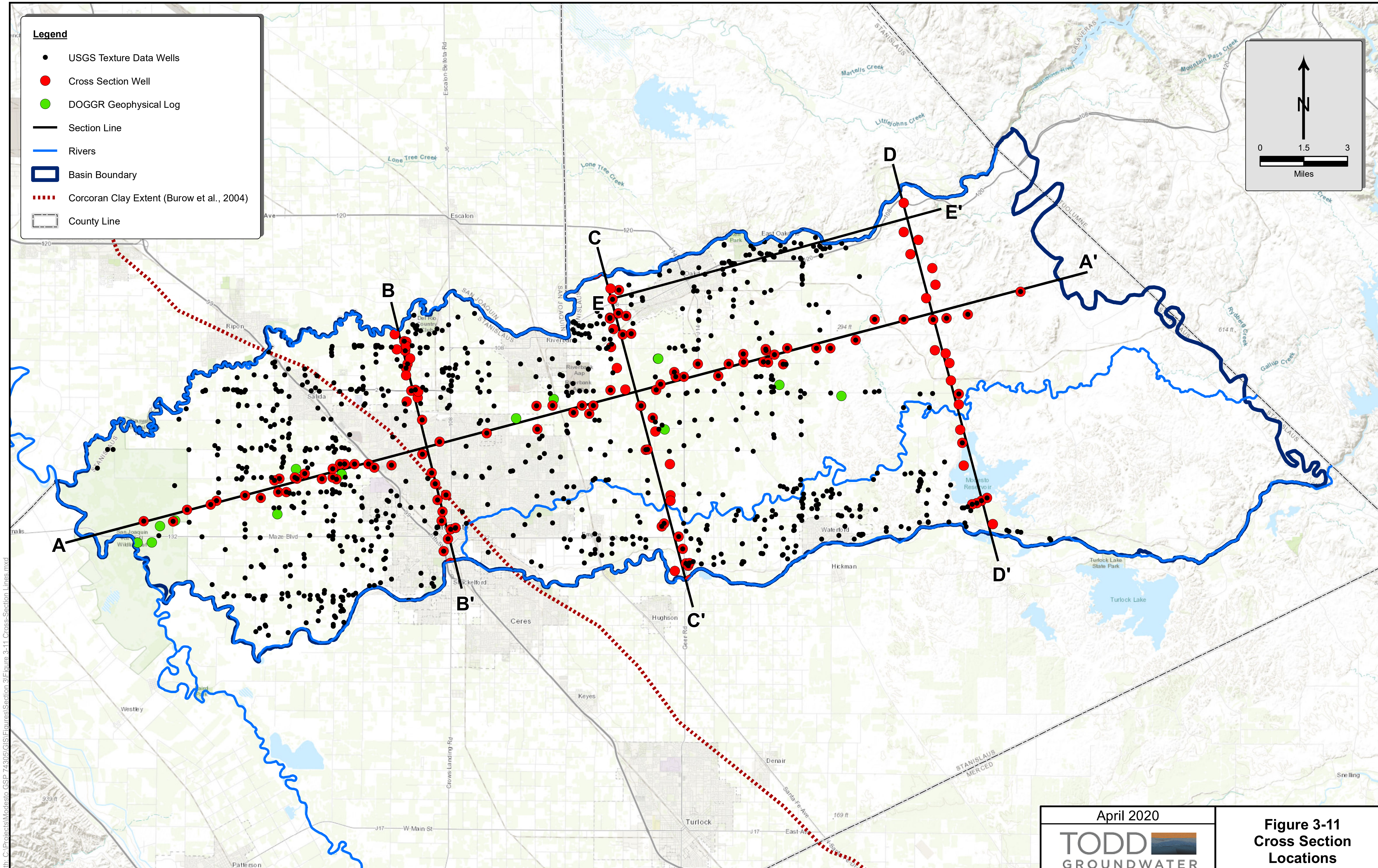

April 2020

TODD GROUNDWATER

Figure 3-11 Cross Section Locations

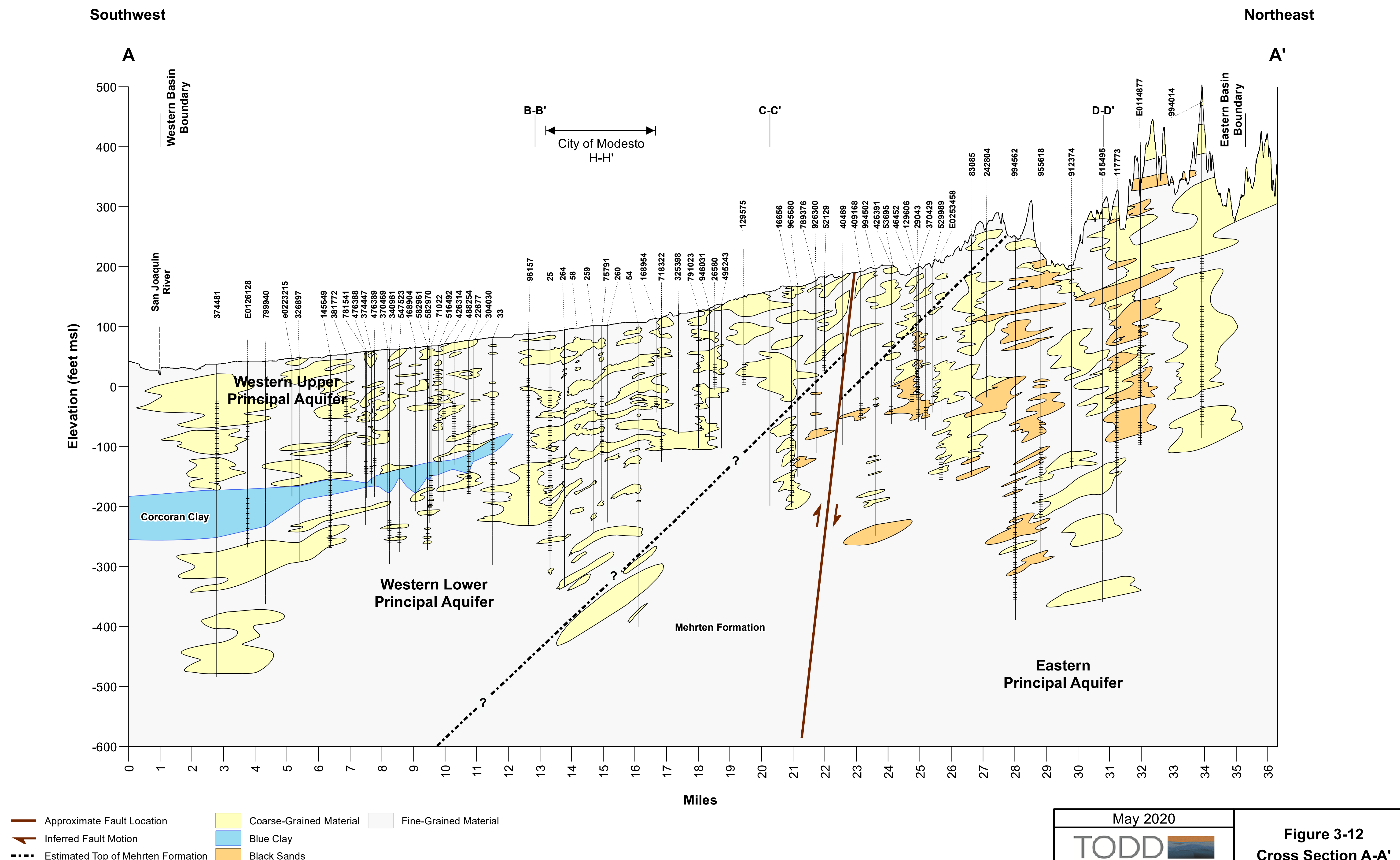

May 2020

TODD GROUNDWATER

Figure 3-12
Cross Section A-A'

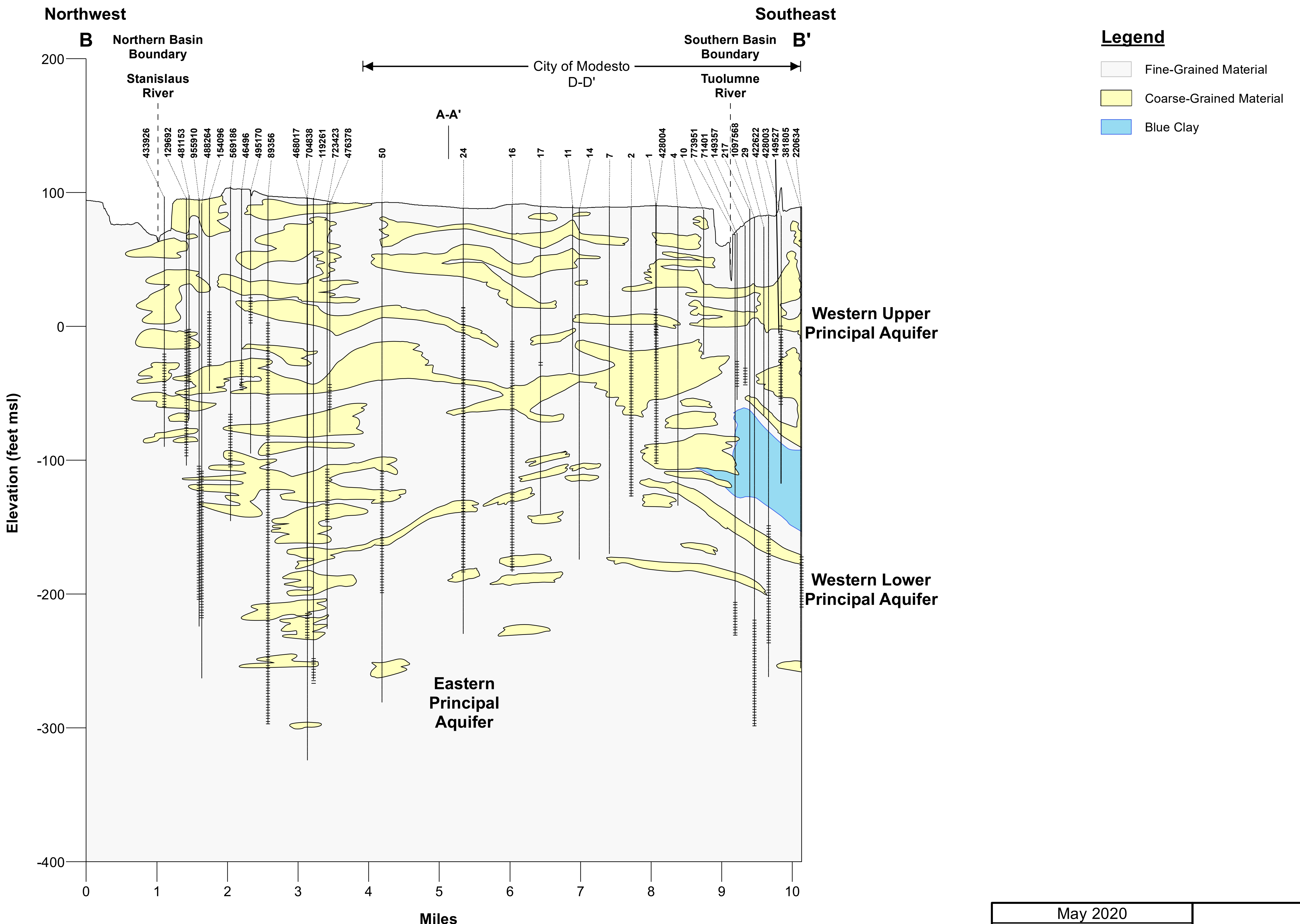

May 2020

TODD GROUNDWATER

Figure 3-13
Cross Section B-B'

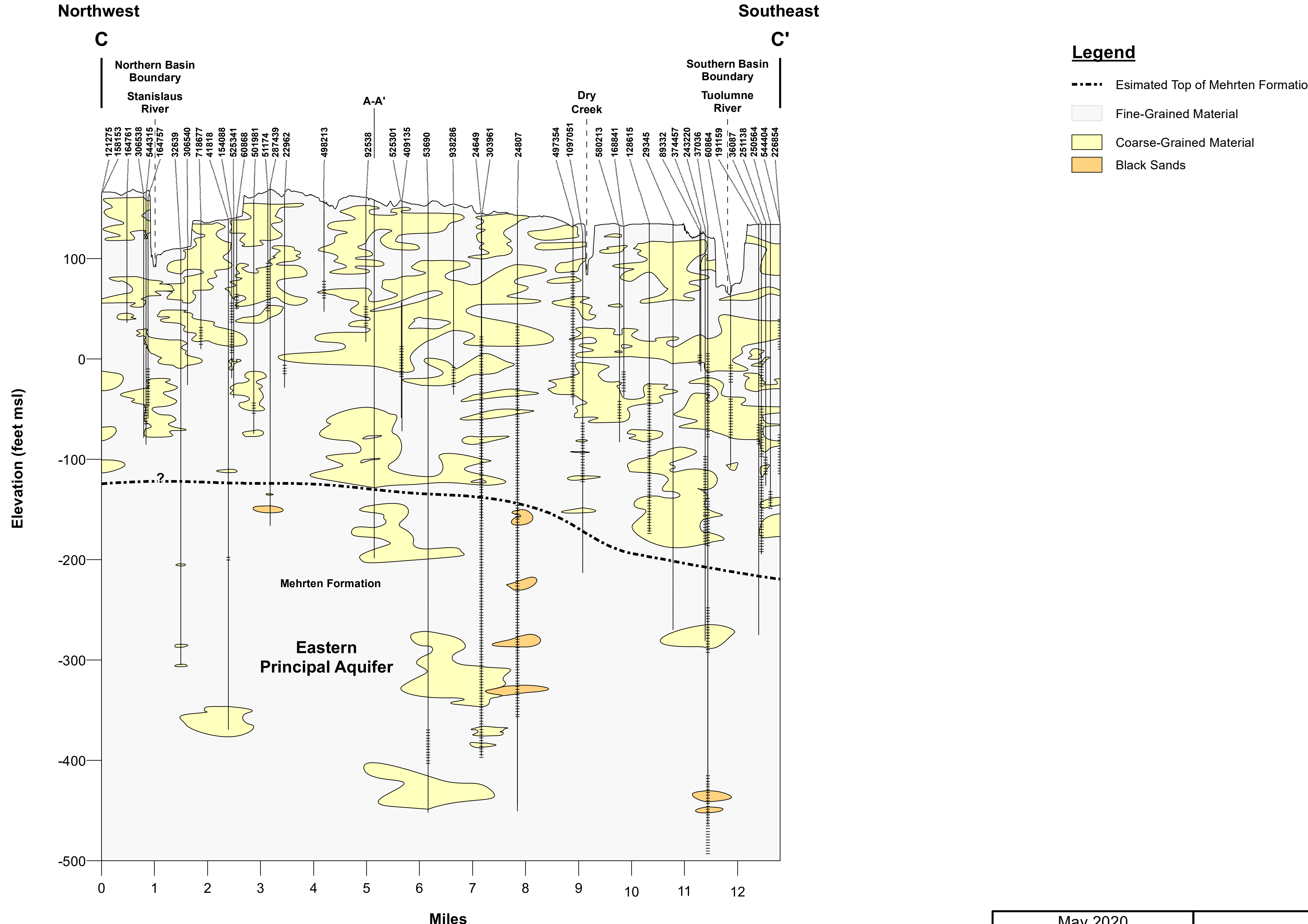

May 2020

TODD GROUNDWATER

Figure 3-14
Cross Section C-C'

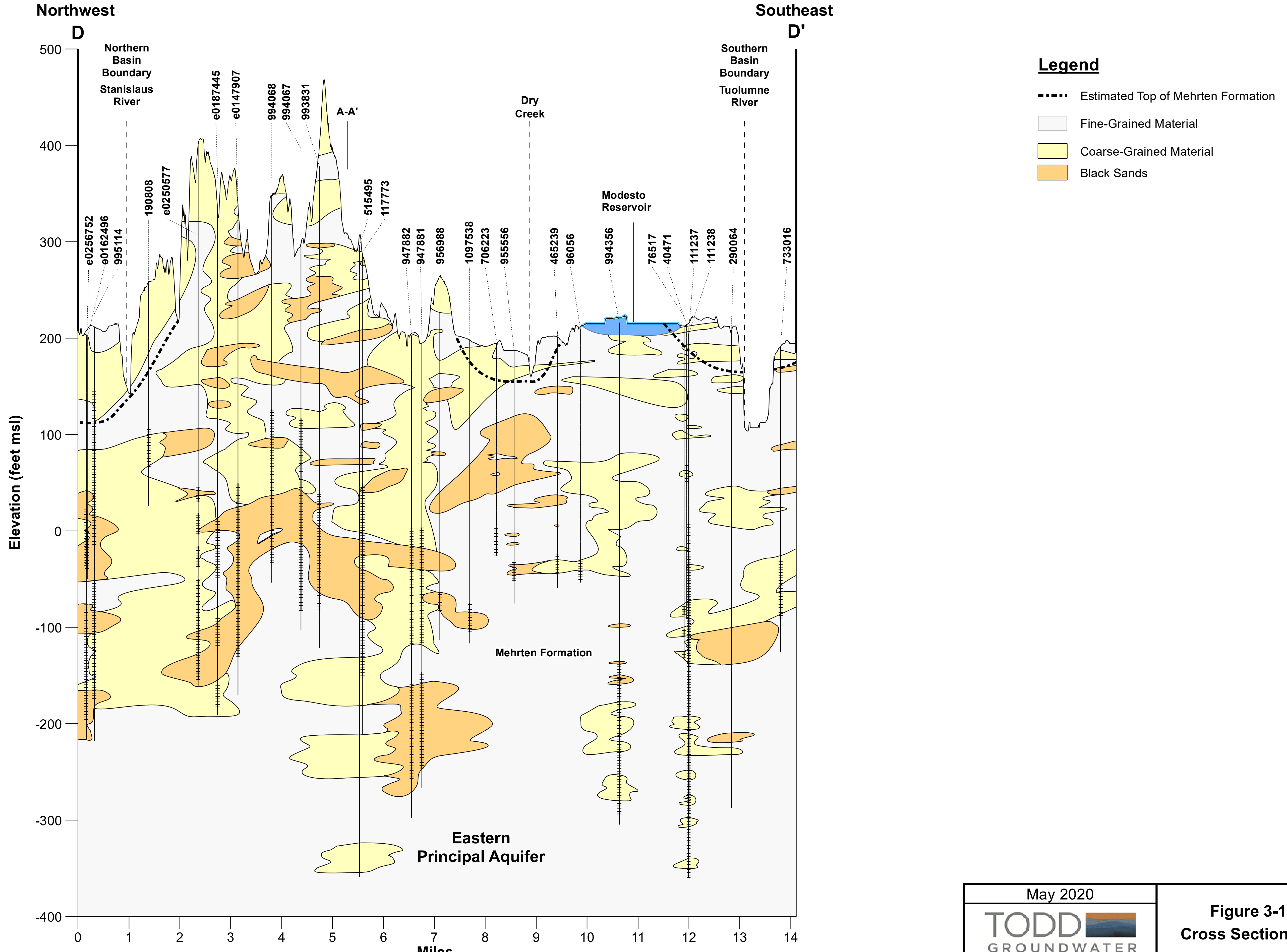

May 2020

TODD GROUNDWATER

Figure 3-15
Cross Section D-D'

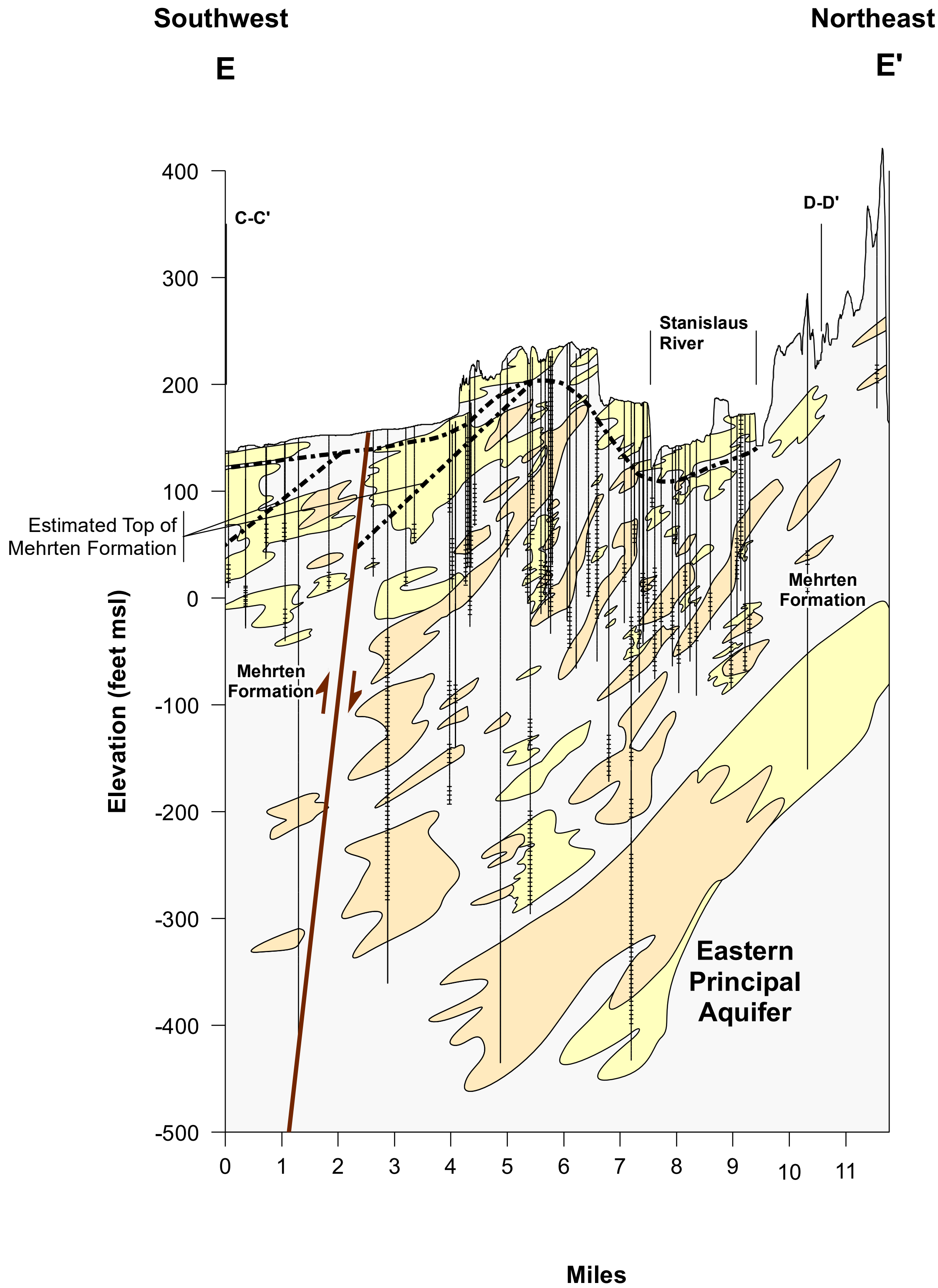

Legend

- Fine-Grained Material
- Coarse-Grained Material
- Black Sands
- Approximate Fault Location
- Inferred Fault Motion

Path: C:\Projects\Modesto GSP 74305\GIS\Figures\Section 3\Figure 3-16 Cross-Section E-E'.mxd

May 2020

TODD GROUNDWATER

Figure 3-16
Cross Section E-E'

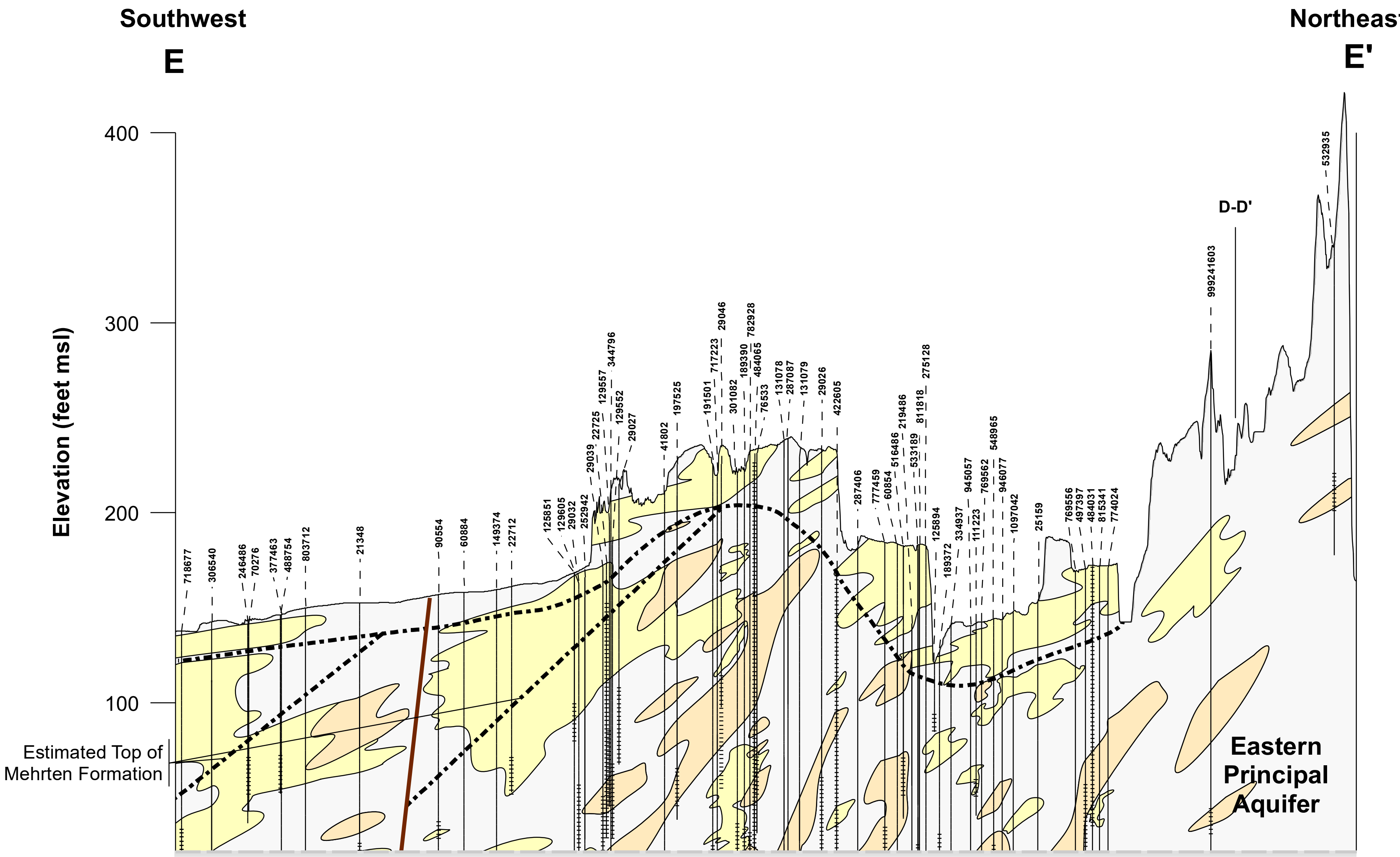

Legend

Fine-Grained Material

Coarse-Grained Material

Black Sands

Approximate Fault Location

Inferred Fault Motion

May 2020

TODD GROUNDWATER

Figure 3-17
Cross Section E-E'
Alternative Scale

Path: C:\Projects\Modesto GSP 74305\GIS\Figures\Section 3\Figure 3-17 Cross Section E-E' well labels.mxd

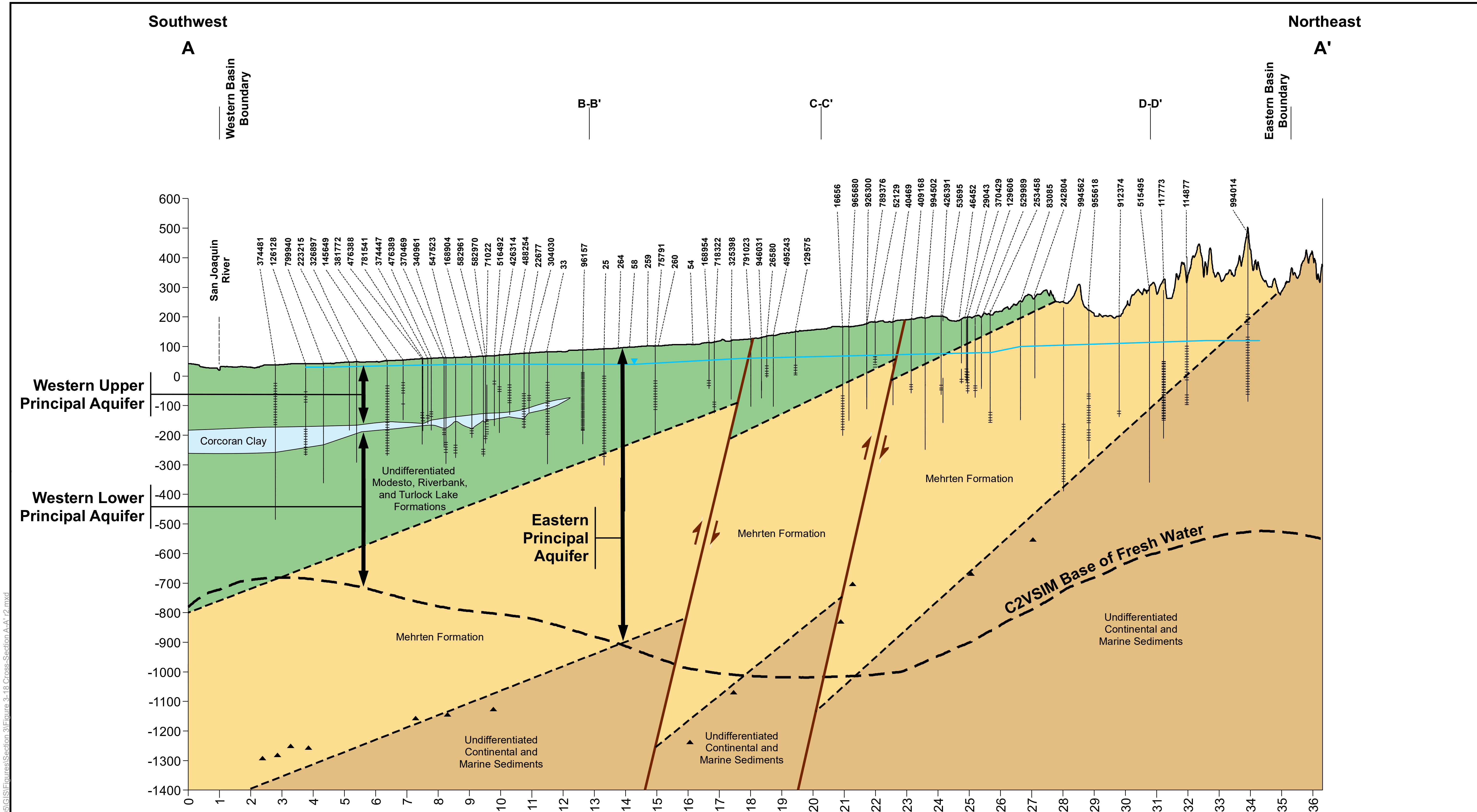

- Approximate Fault Location
- Inferred Fault Motion
- Approximate Formation Boundary
- Approximate Base of Mehrten Formation Inferred from DOGGR Geophysical Log
- Groundwater Elevation October 2015

May 2020

TODD GROUNDWATER

Figure 3-18
Hydrogeologic Framework
Cross Section A-A'

Path: C:\Projects\Modesto GSP 74305\GIS\Figures\Section 3\Figure 3-18 Cross-Section A-A' r2.mxd

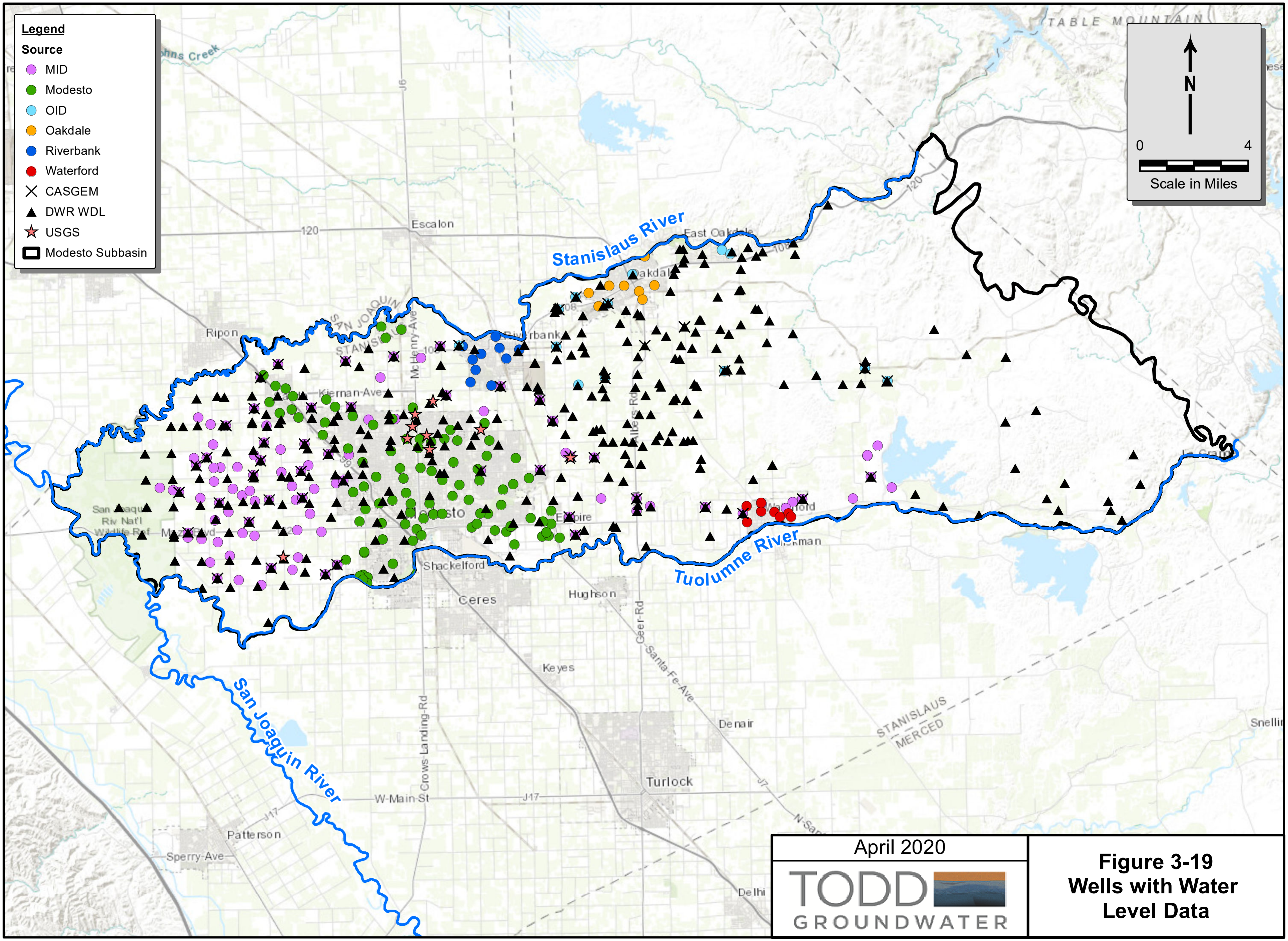

April 2020

TODD GROUNDWATER

Figure 3-19
Wells with Water Level Data

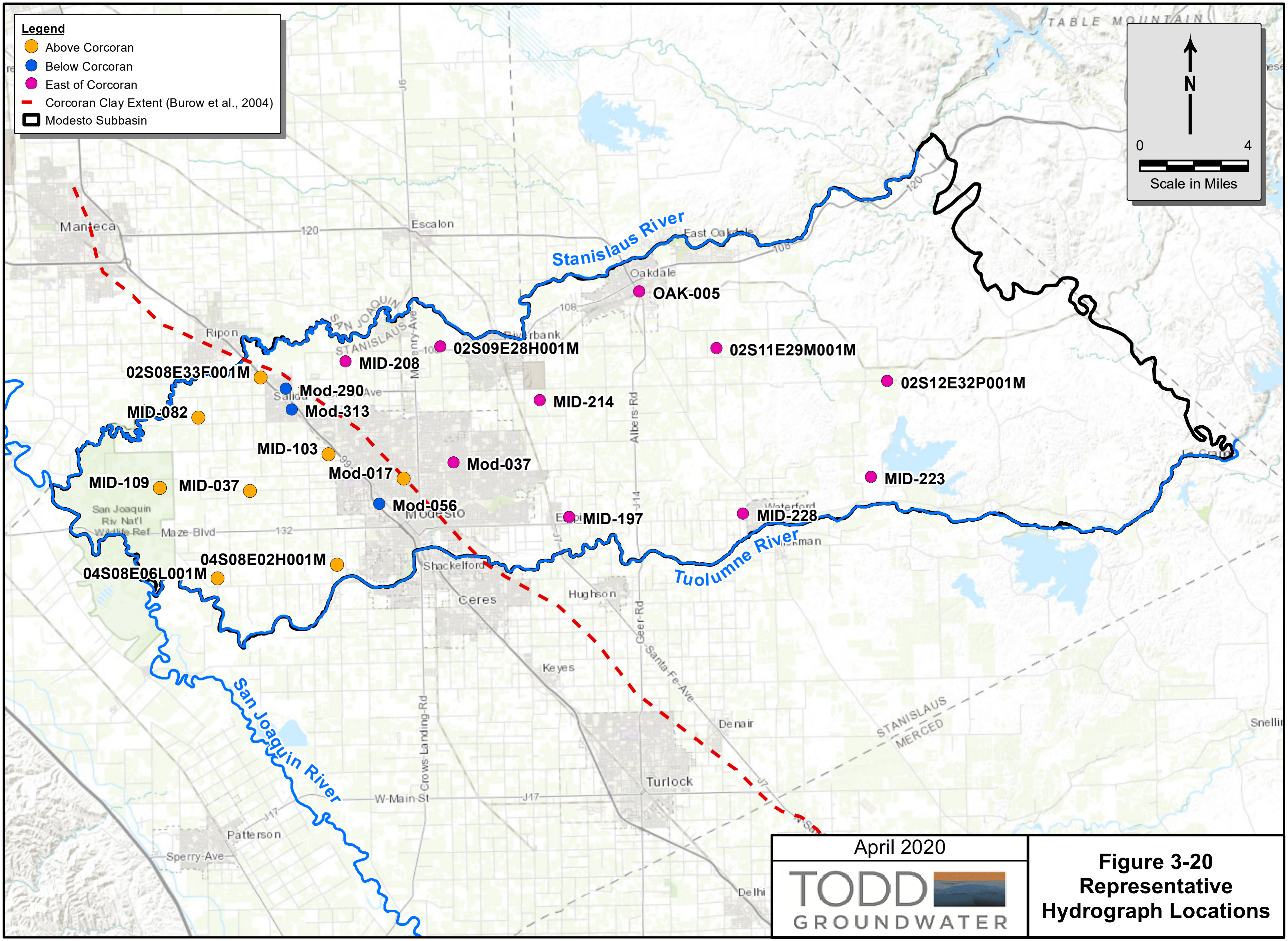

April 2020

TODD GROUNDWATER

Figure 3-20
Representative Hydrograph Locations

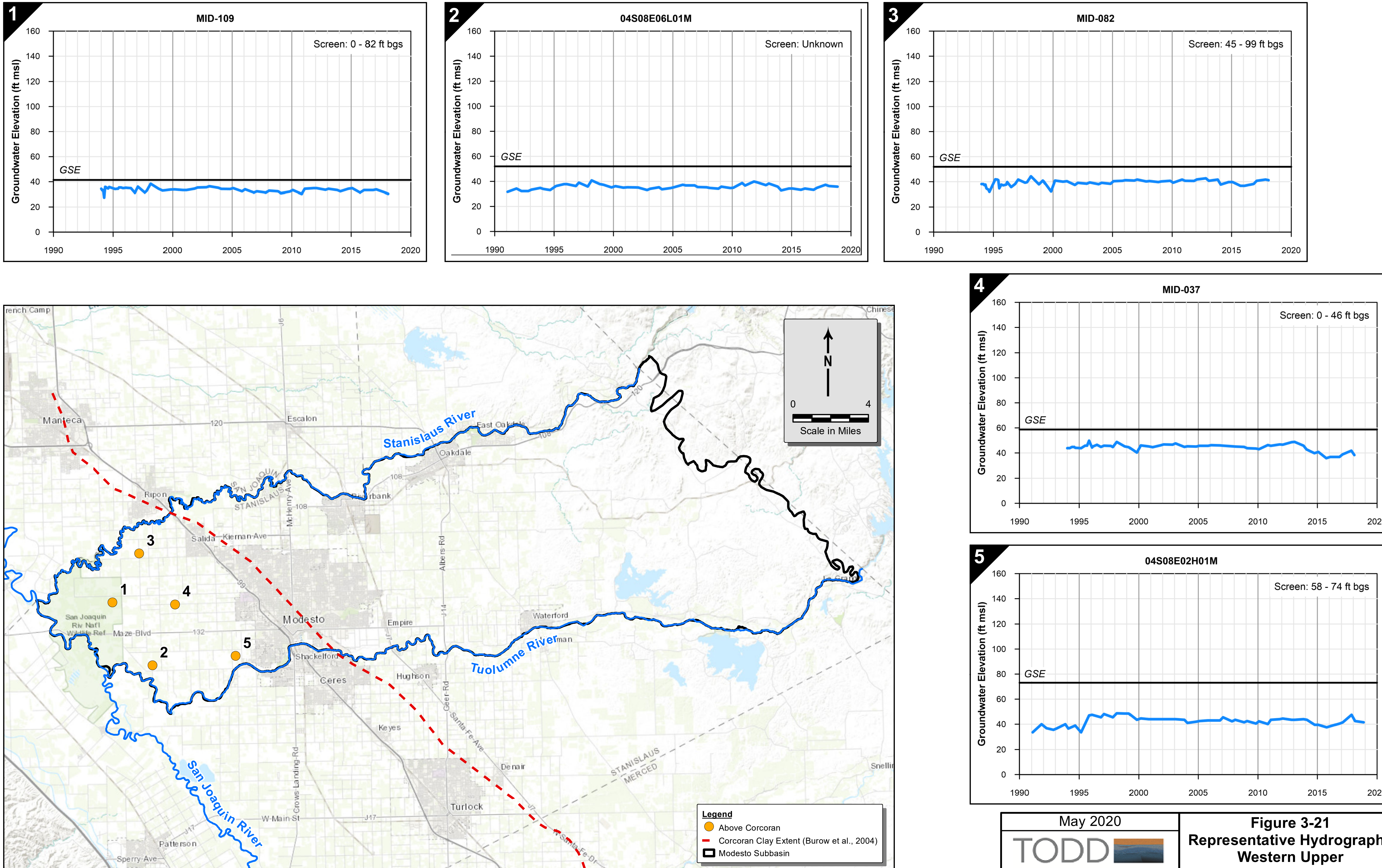

May 2020

TODD GROUNDWATER

Figure 3-21
Representative Hydrographs
Western Upper
Principal Aquifer (1 of 2)

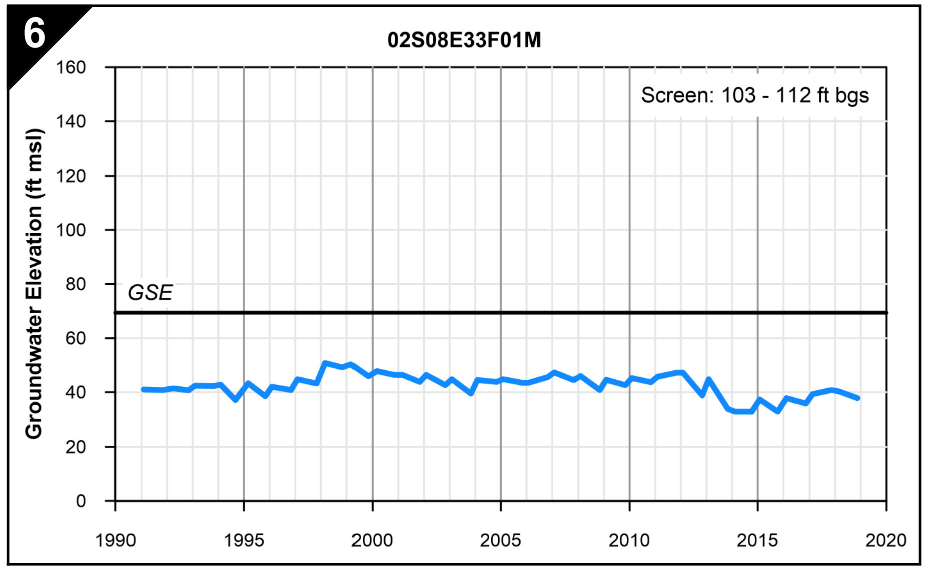

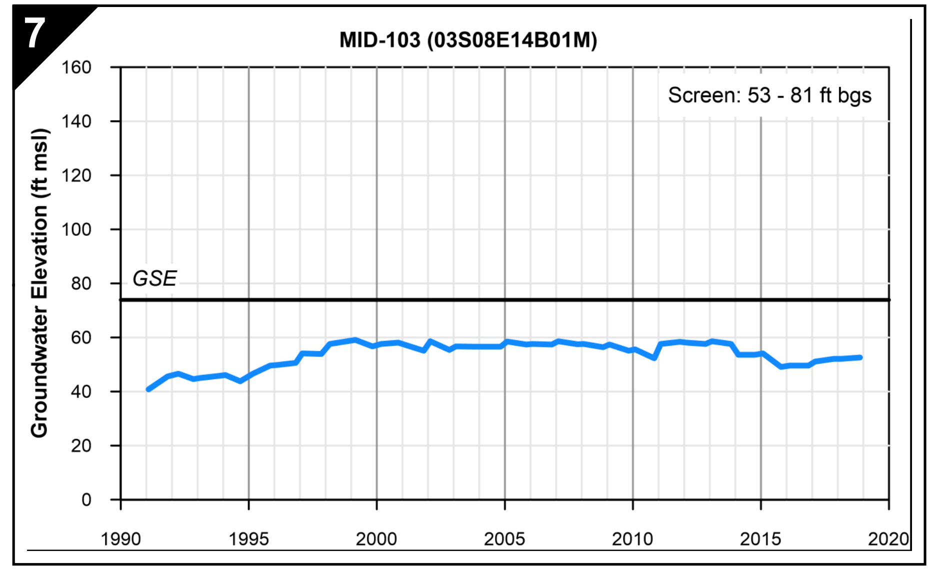

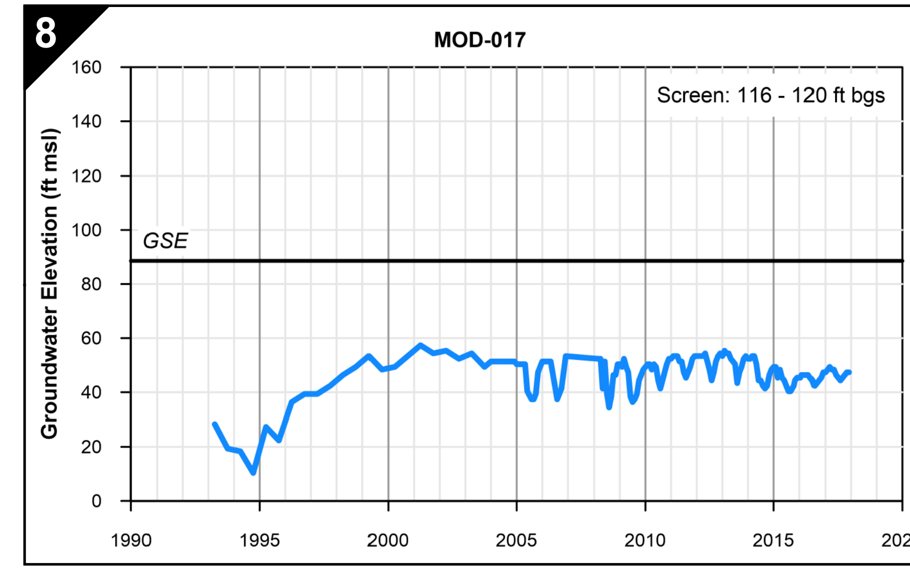

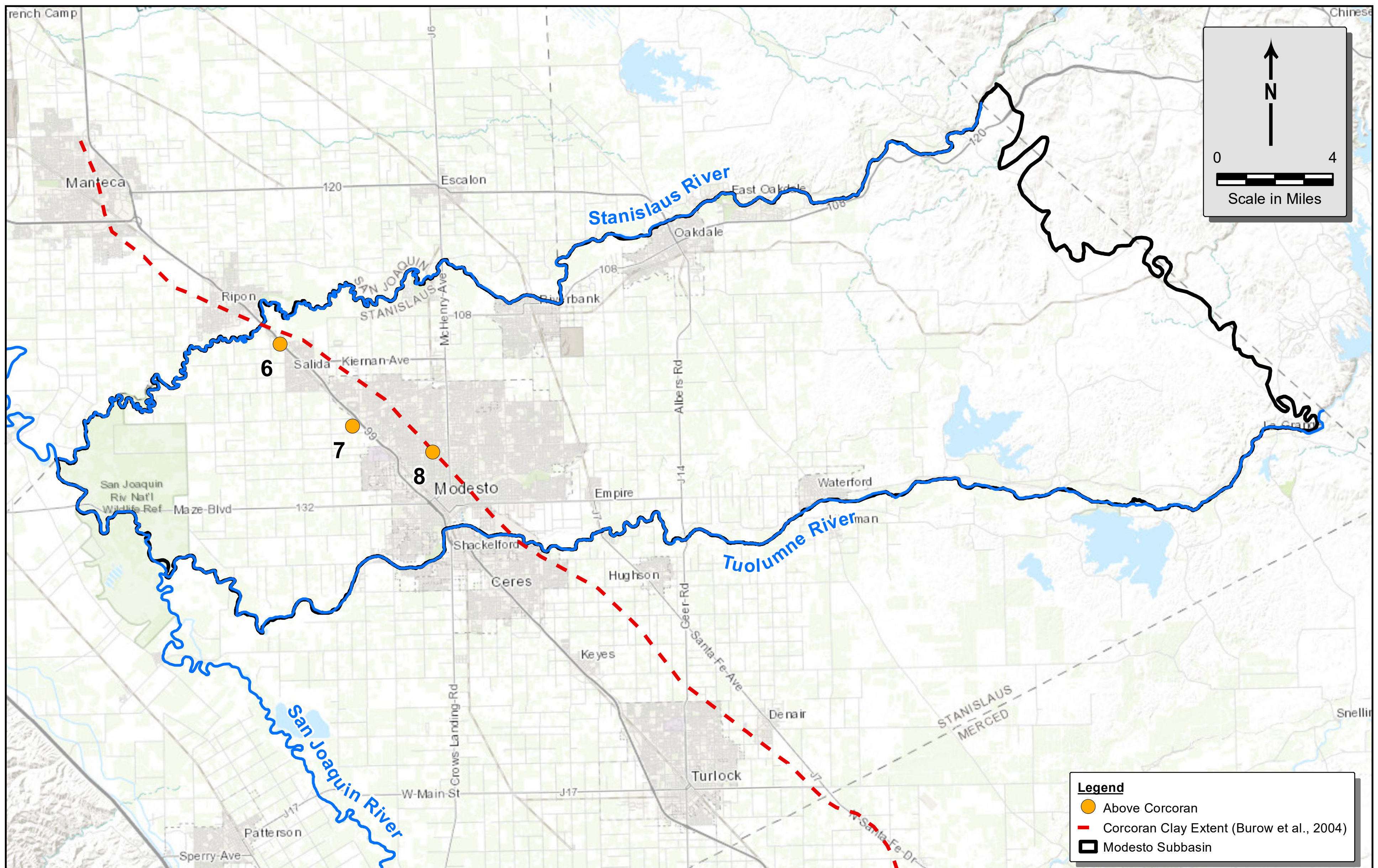

May 2020

TODD GROUNDWATER

Figure 3-22
Representative Hydrographs
Western Upper
Principal Aquifer (2 of 2)

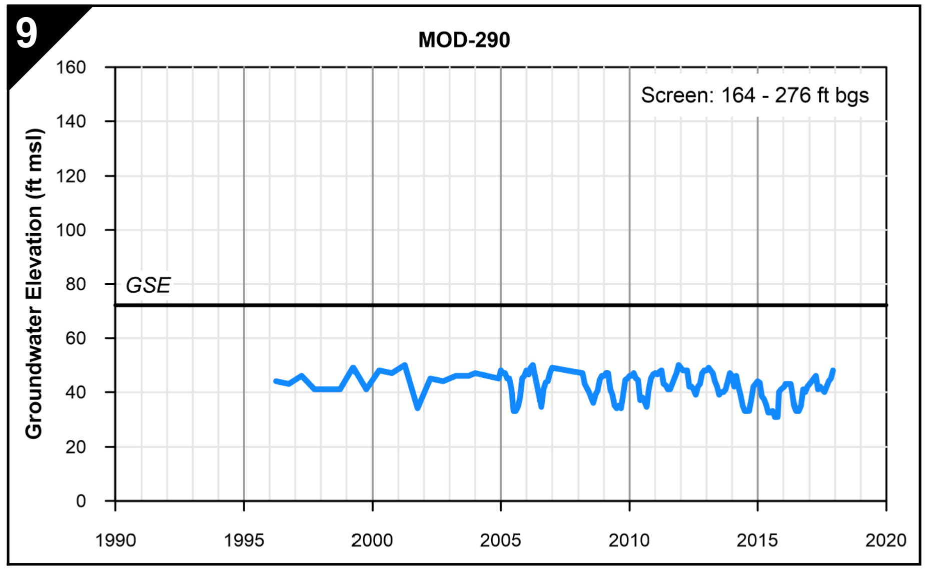

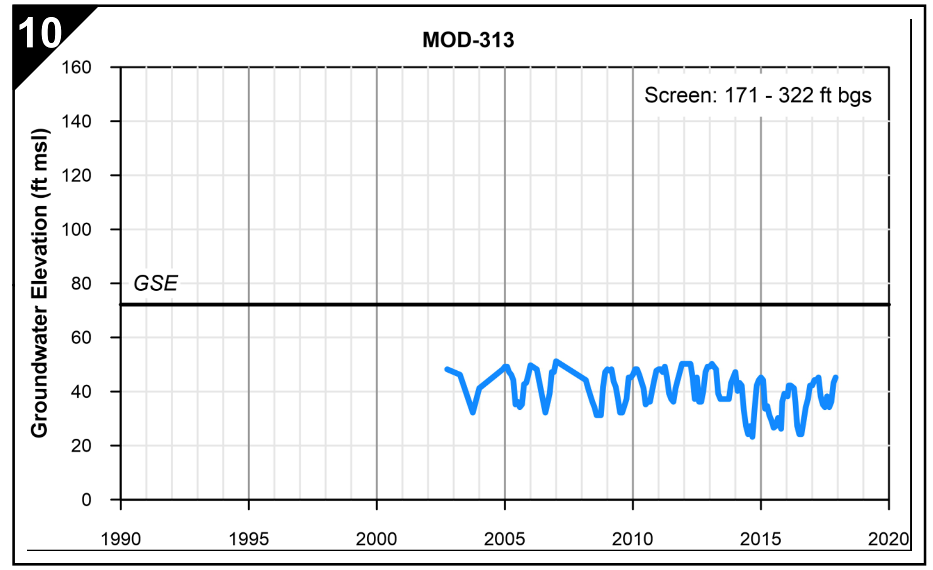

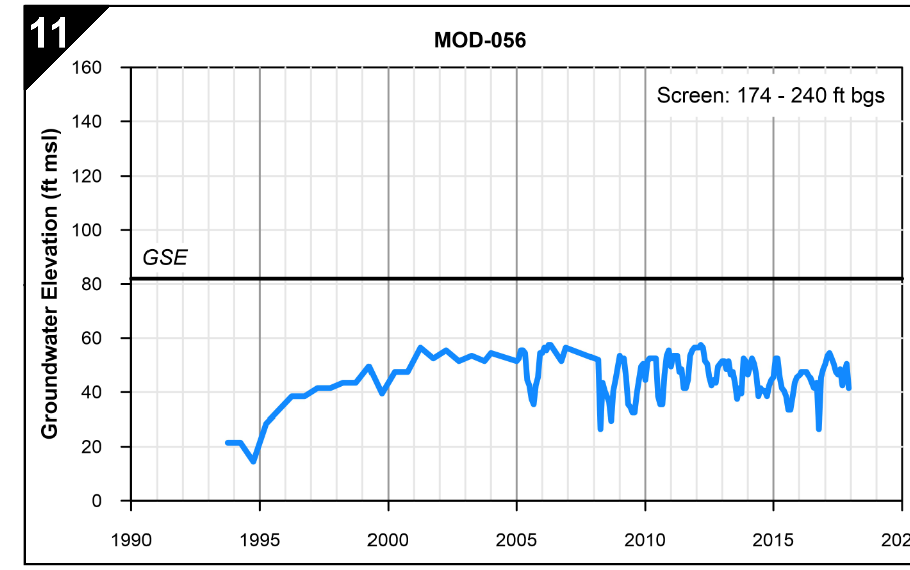

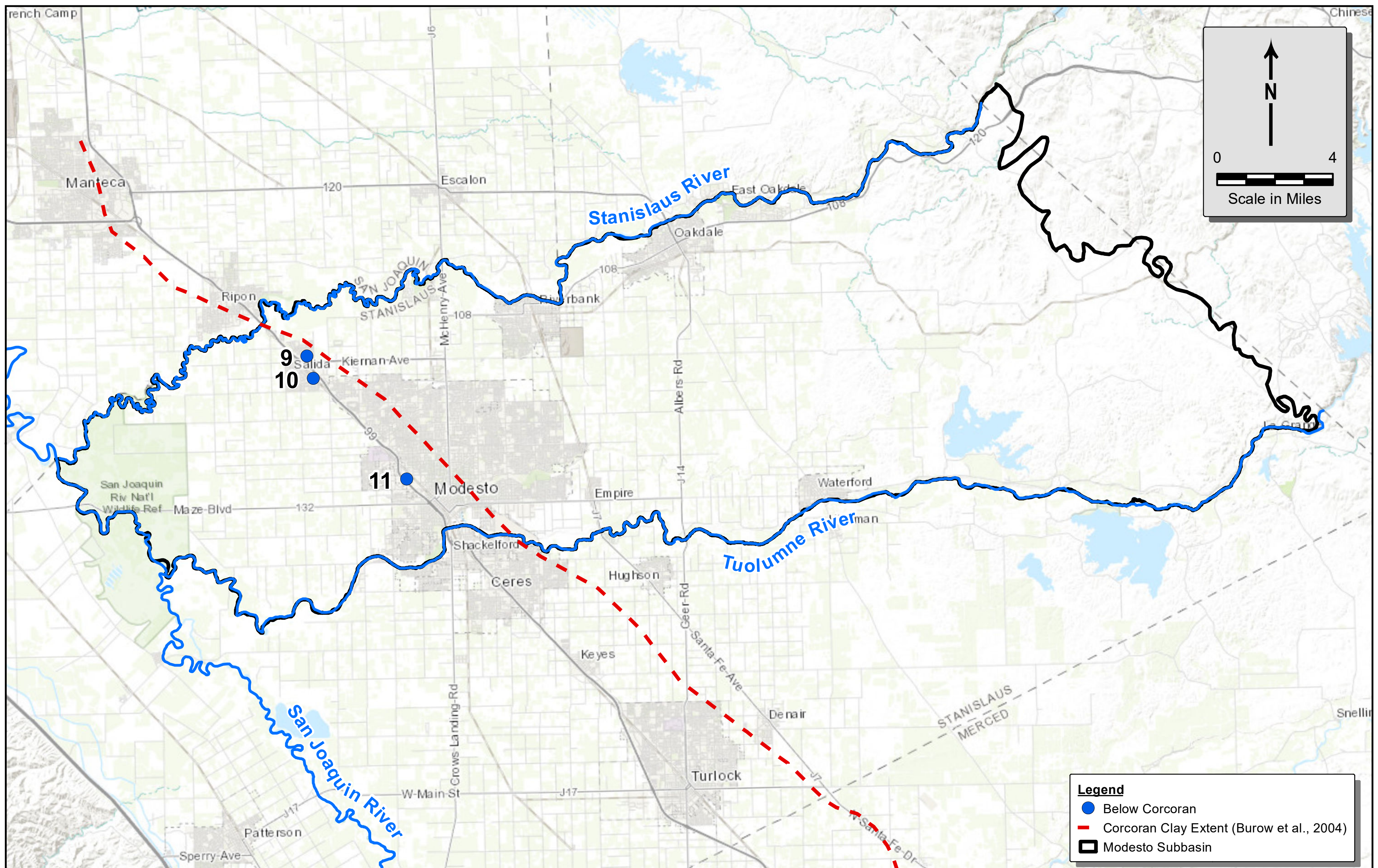

May 2020

TODD GROUNDWATER

Figure 3-23
Representative Hydrographs
Western Lower
Principal Aquifer

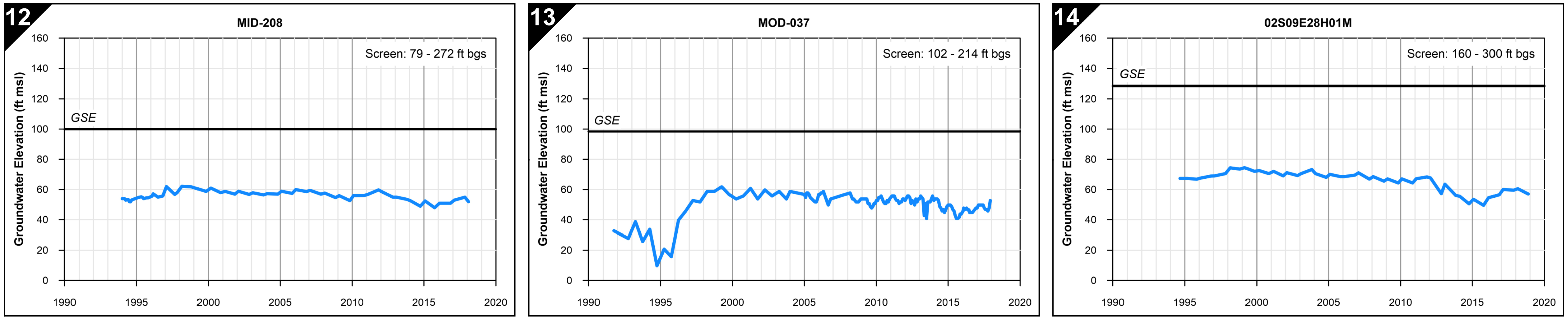

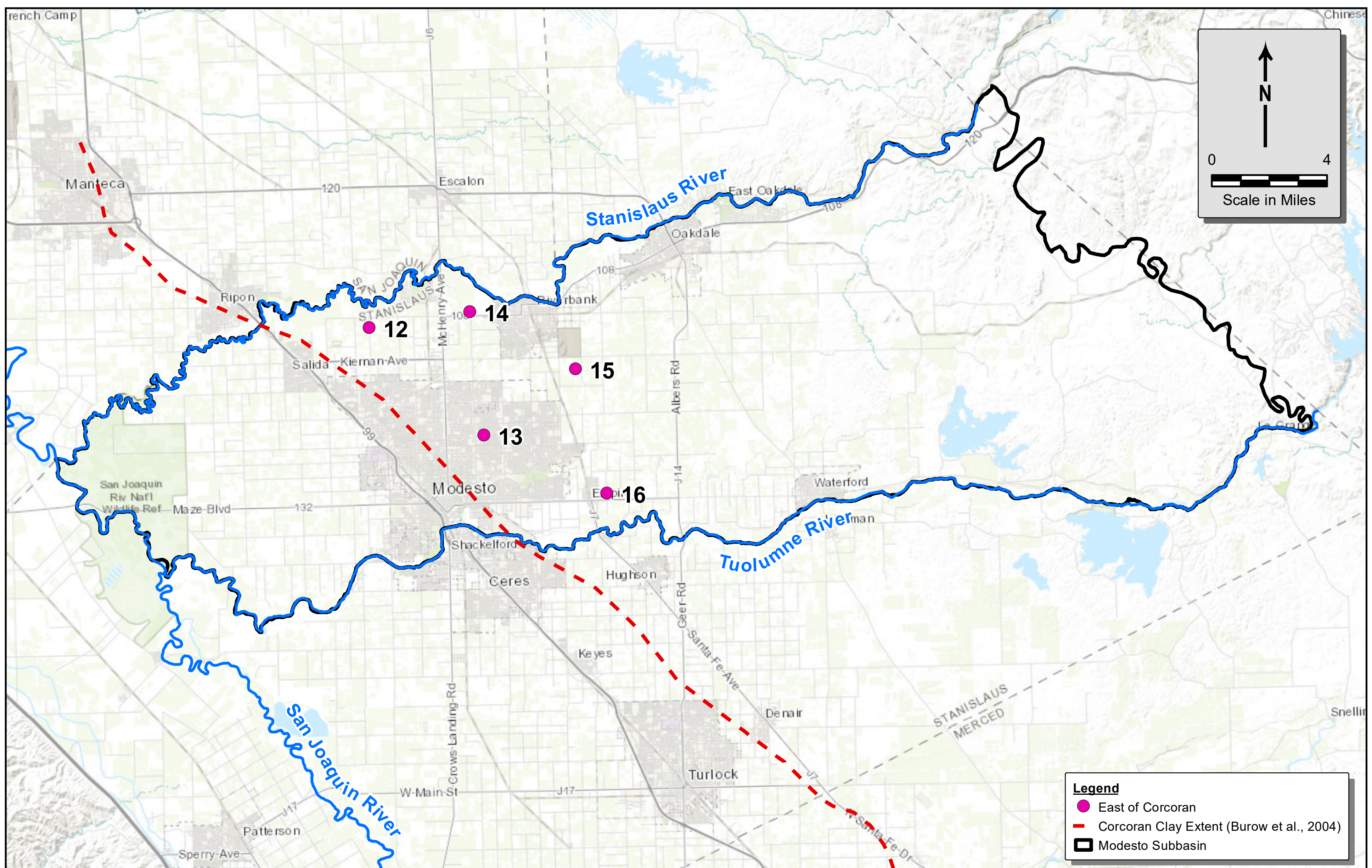

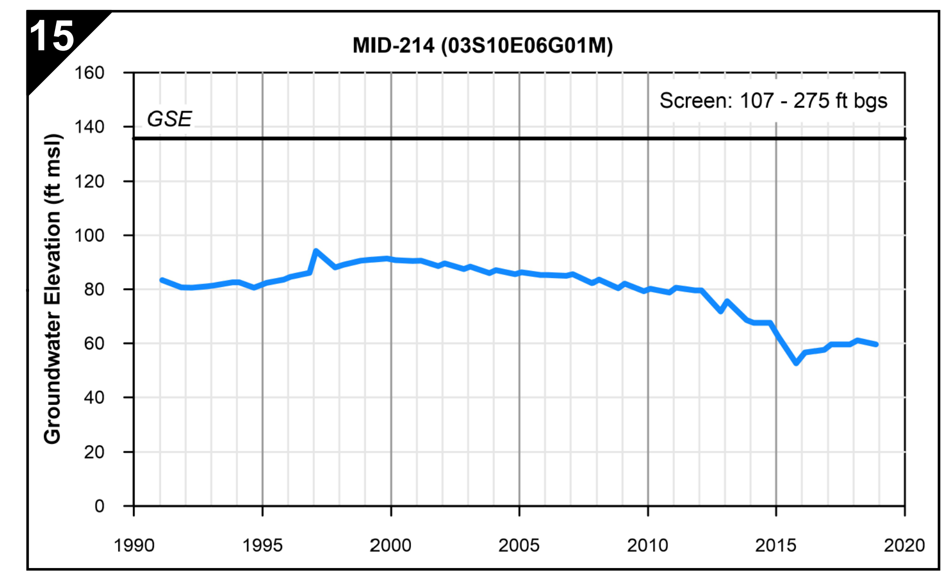

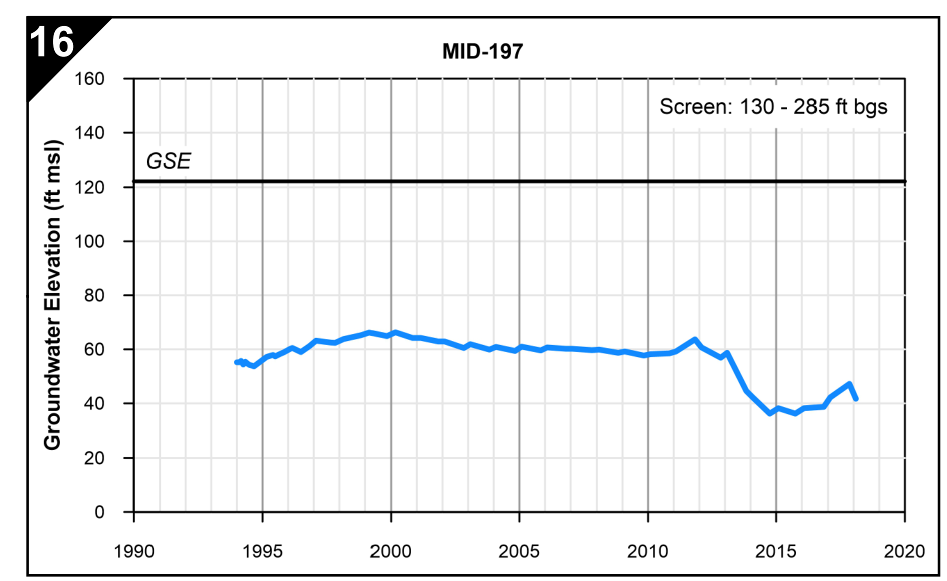

May 2020

TODD GROUNDWATER

Figure 3-24
Representative Hydrographs
Eastern Principal Aquifer (1 of 2)

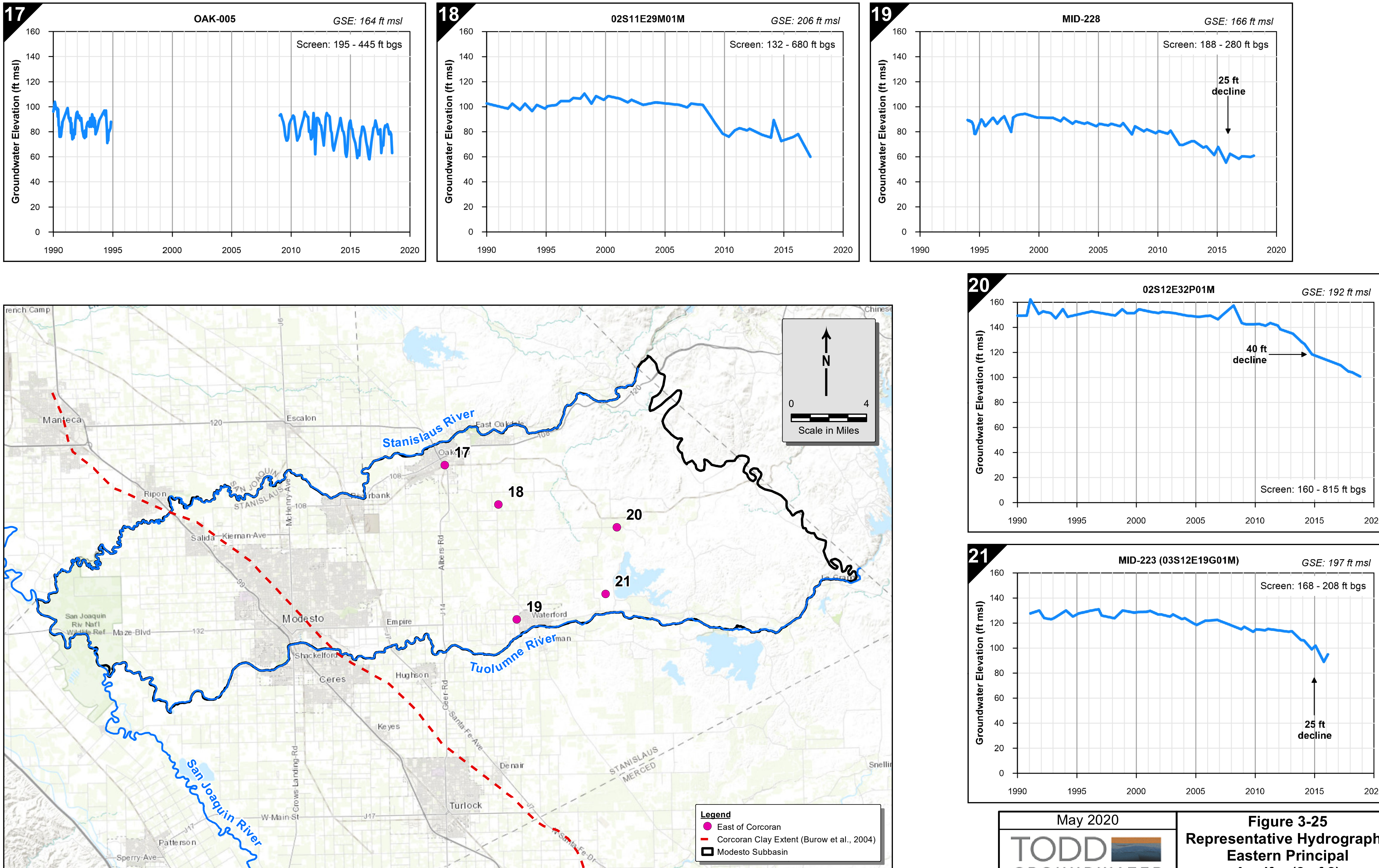

May 2020

TODD GROUNDWATER

Figure 3-25
Representative Hydrographs
Eastern Principal Aquifer (2 of 2)

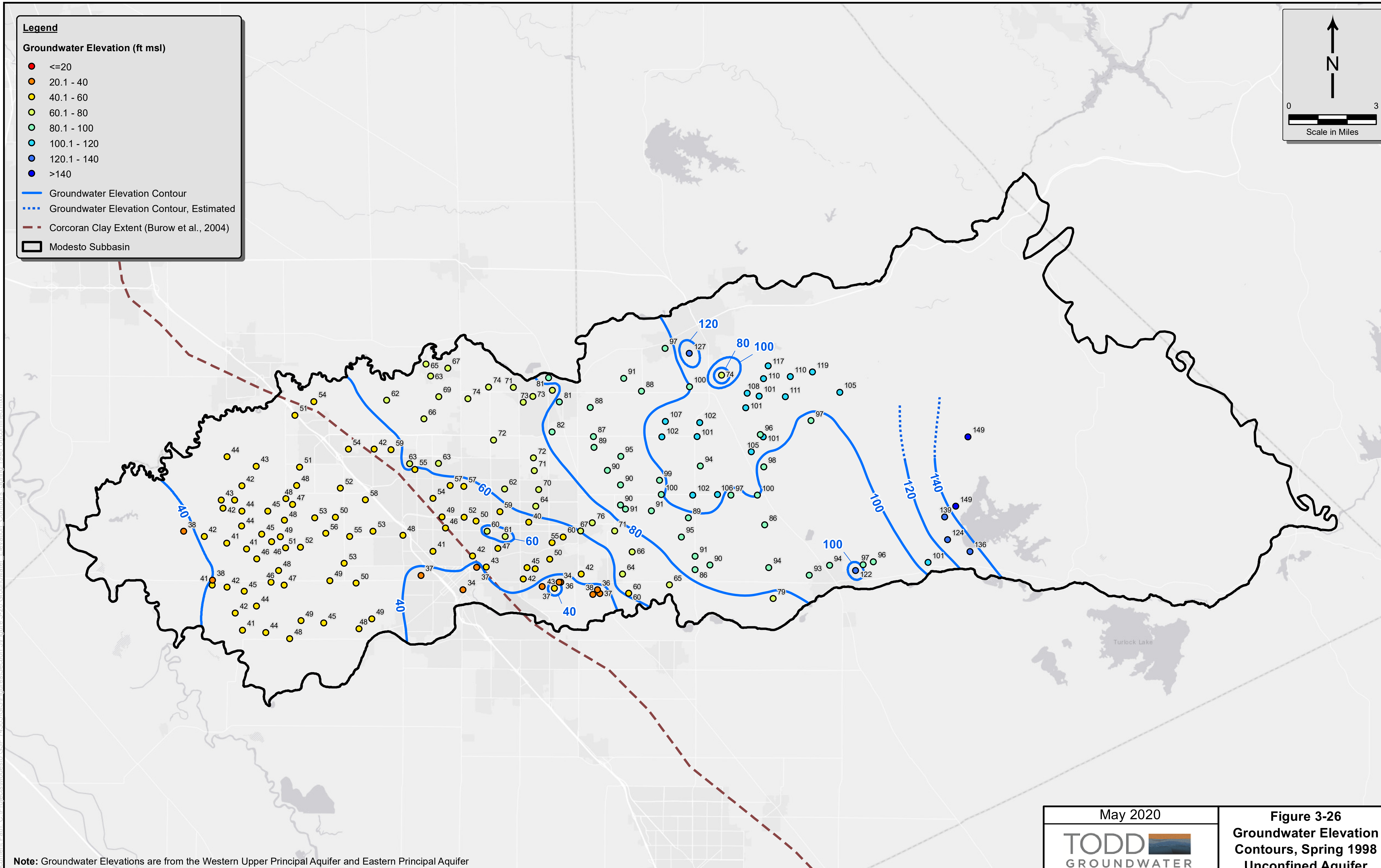

May 2020

TODD GROUNDWATER

Figure 3-26
Groundwater Elevation Contours, Spring 1998
Unconfined Aquifer

Note: Groundwater Elevations are from the Western Upper Principal Aquifer and Eastern Principal Aquifer

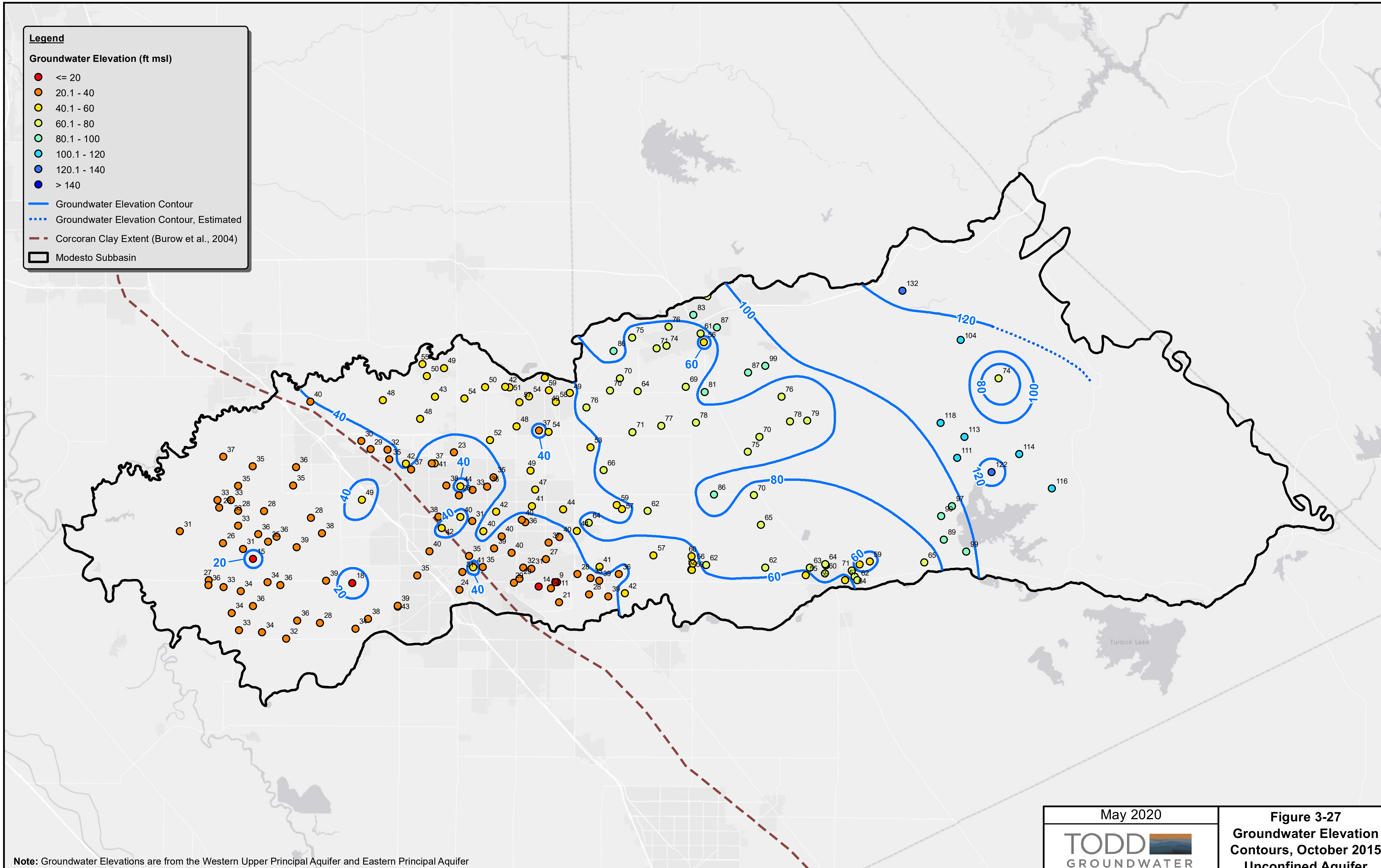

Figure 3-27
Groundwater Elevation Contours, October 2015 Unconfined Aquifer

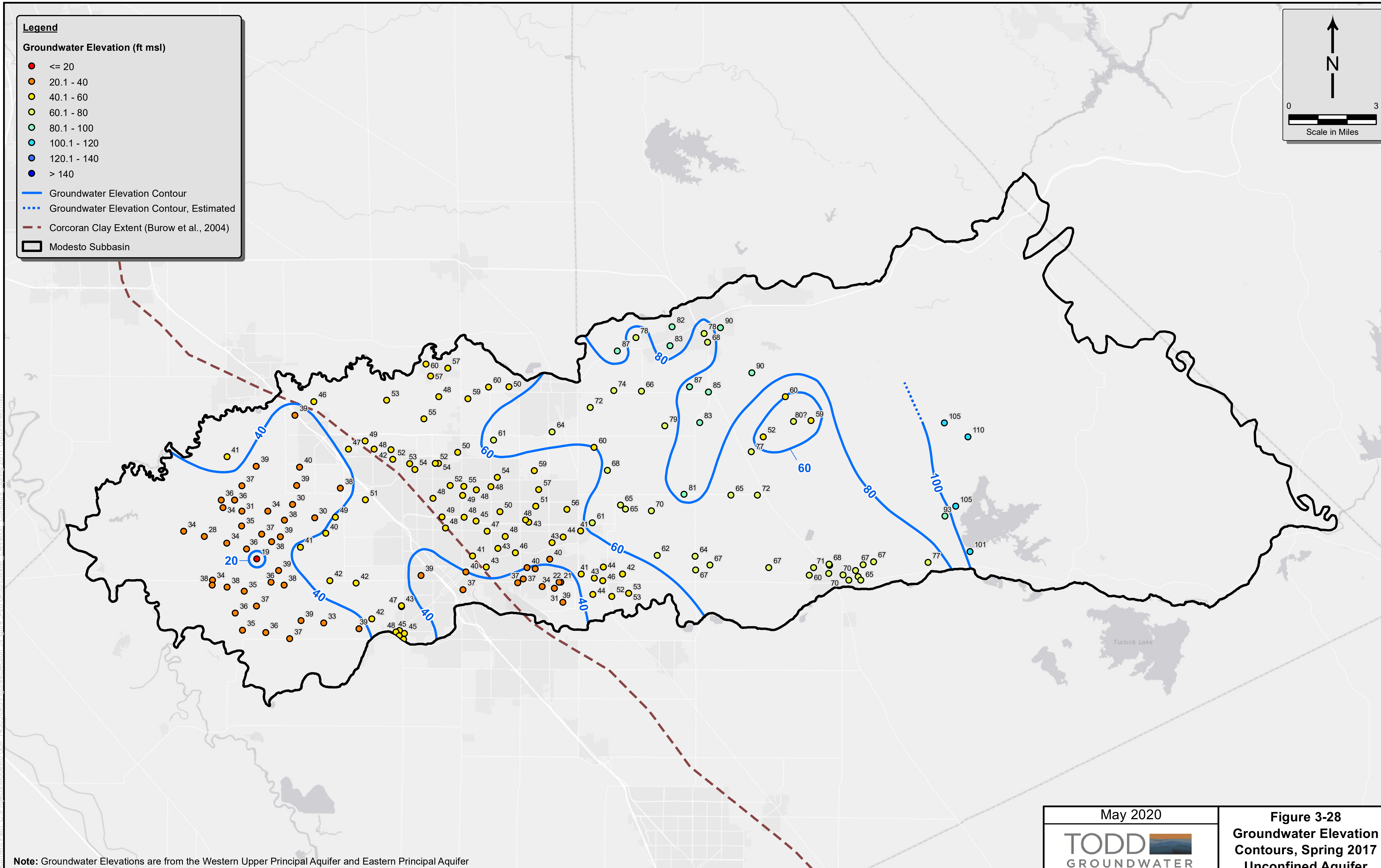

Note: Groundwater Elevations are from the Western Upper Principal Aquifer and Eastern Principal Aquifer

May 2020

TODD GROUNDWATER

Figure 3-28
Groundwater Elevation Contours, Spring 2017
Unconfined Aquifer

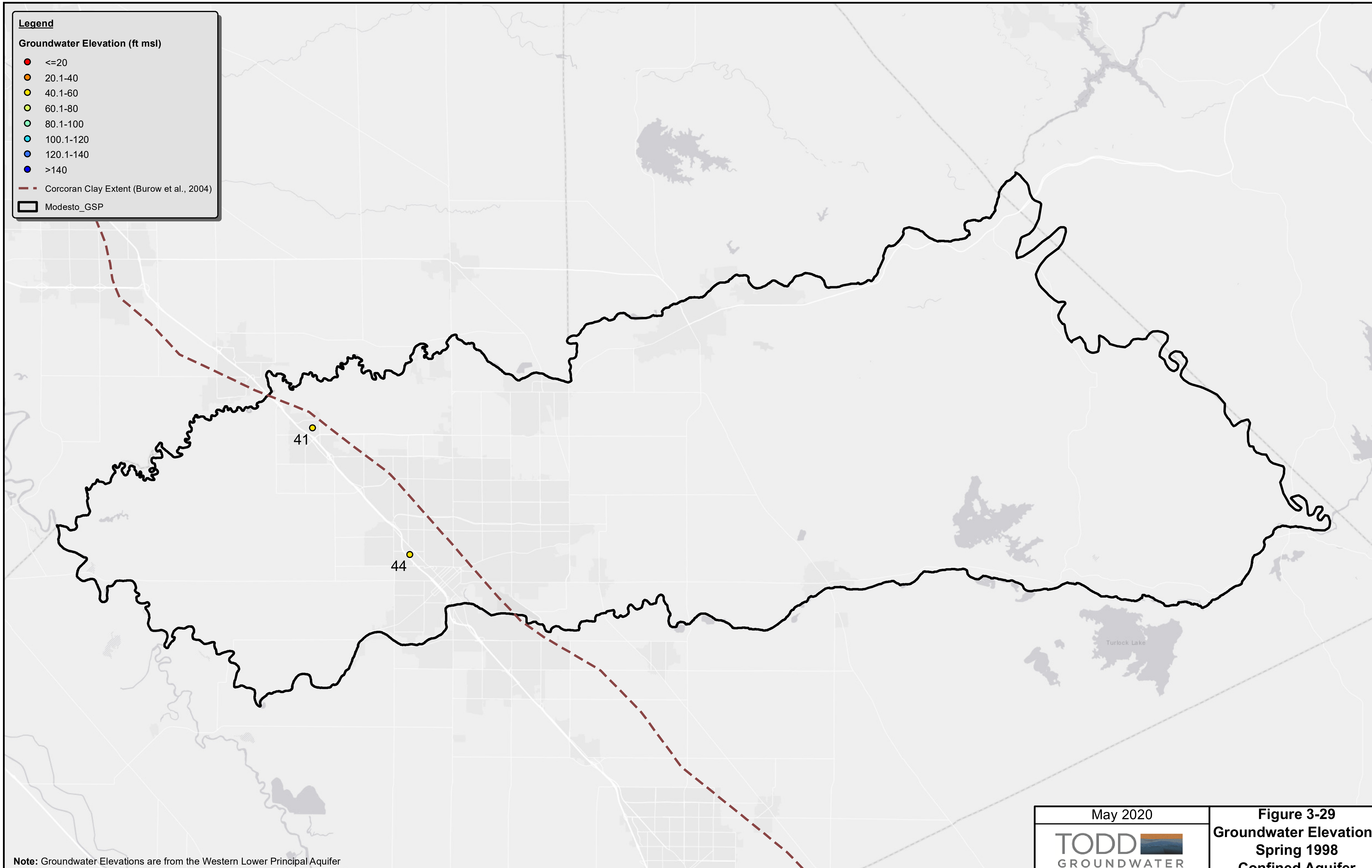

Note: Groundwater Elevations are from the Western Lower Principal Aquifer

May 2020

TODD GROUNDWATER

Figure 3-29
Groundwater Elevations
Spring 1998
Confined Aquifer

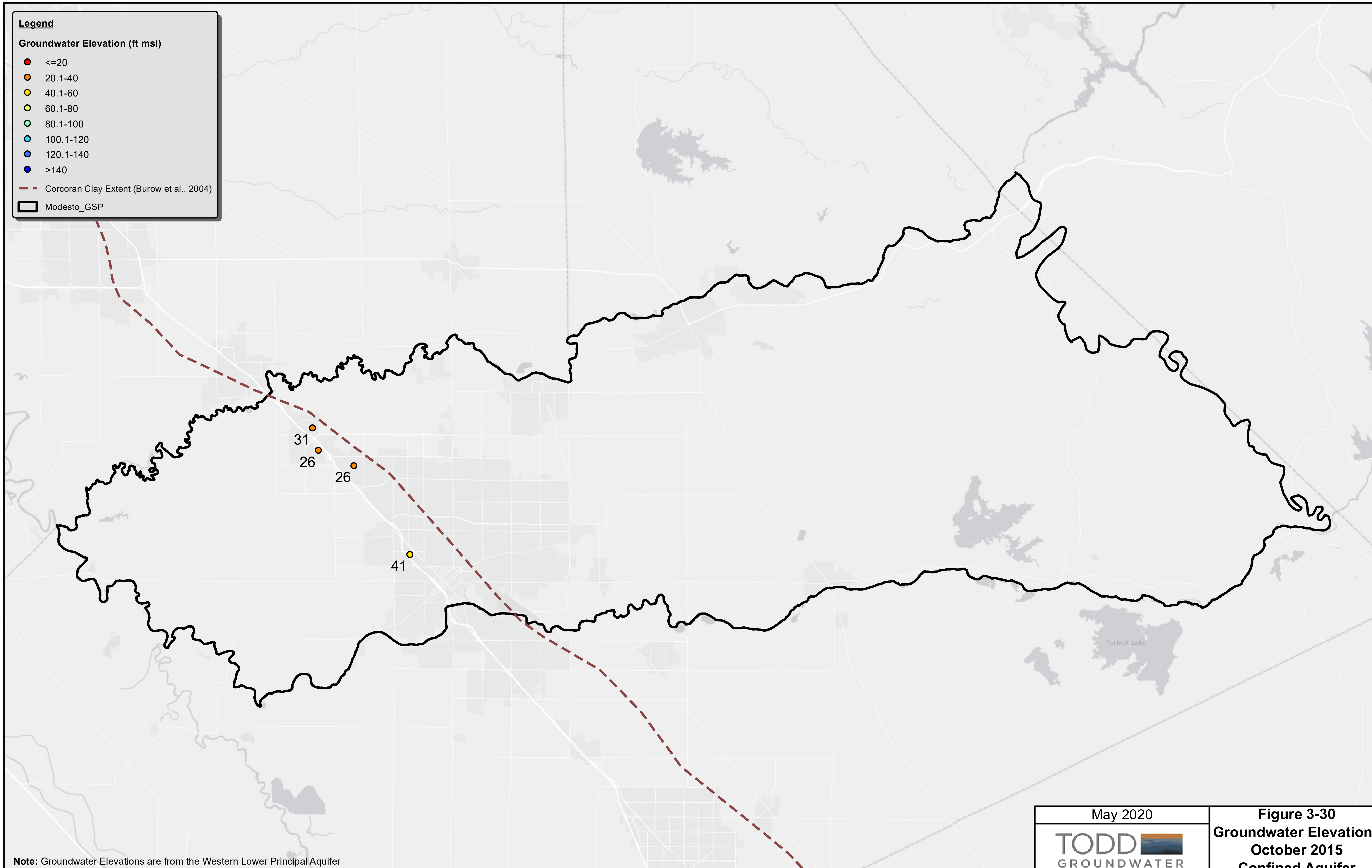

Figure 3-30
Groundwater Elevations
October 2015
Confined Aquifer

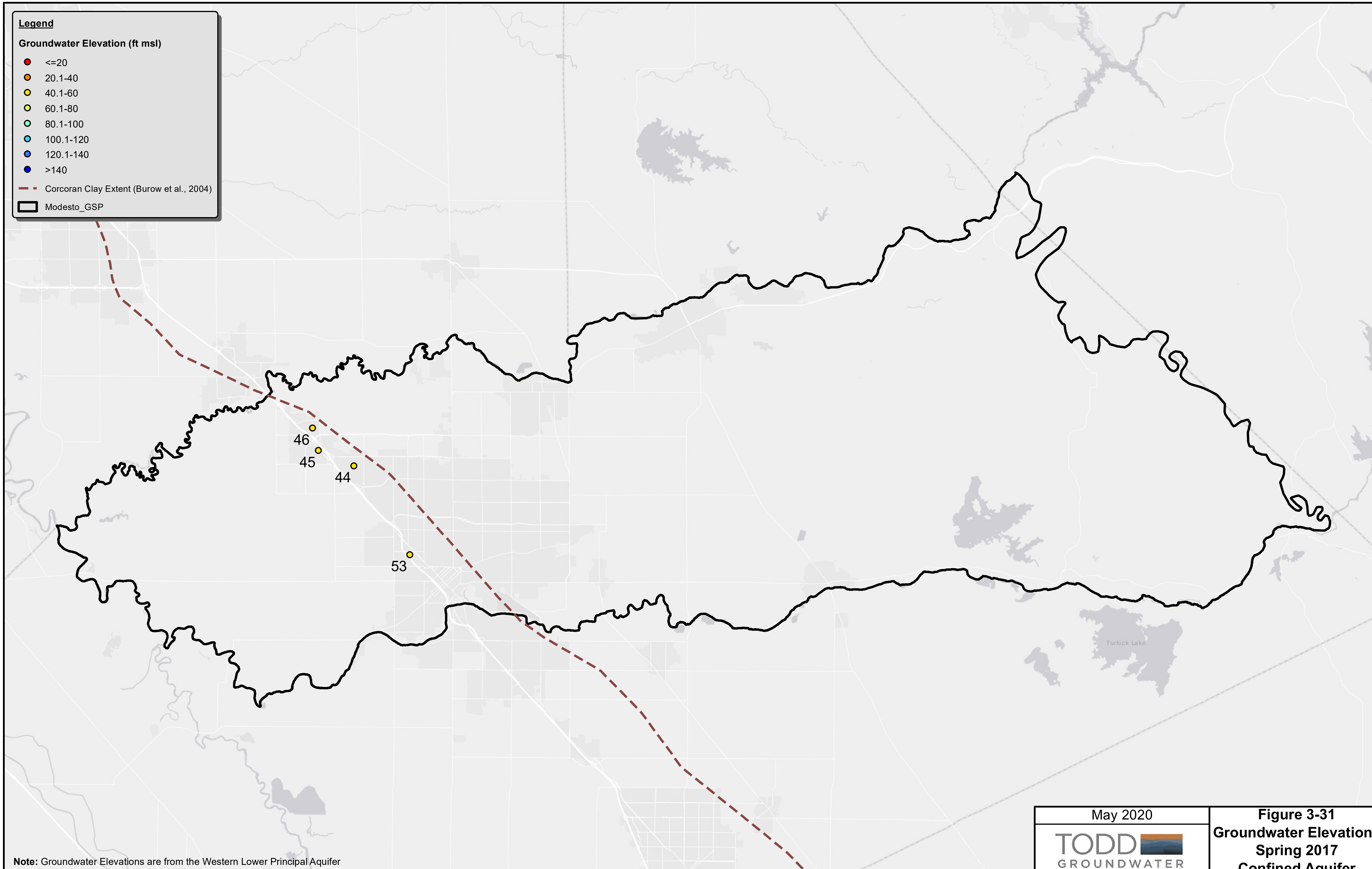

Figure 3-31
Groundwater Elevations Spring 2017 Confined Aquifer

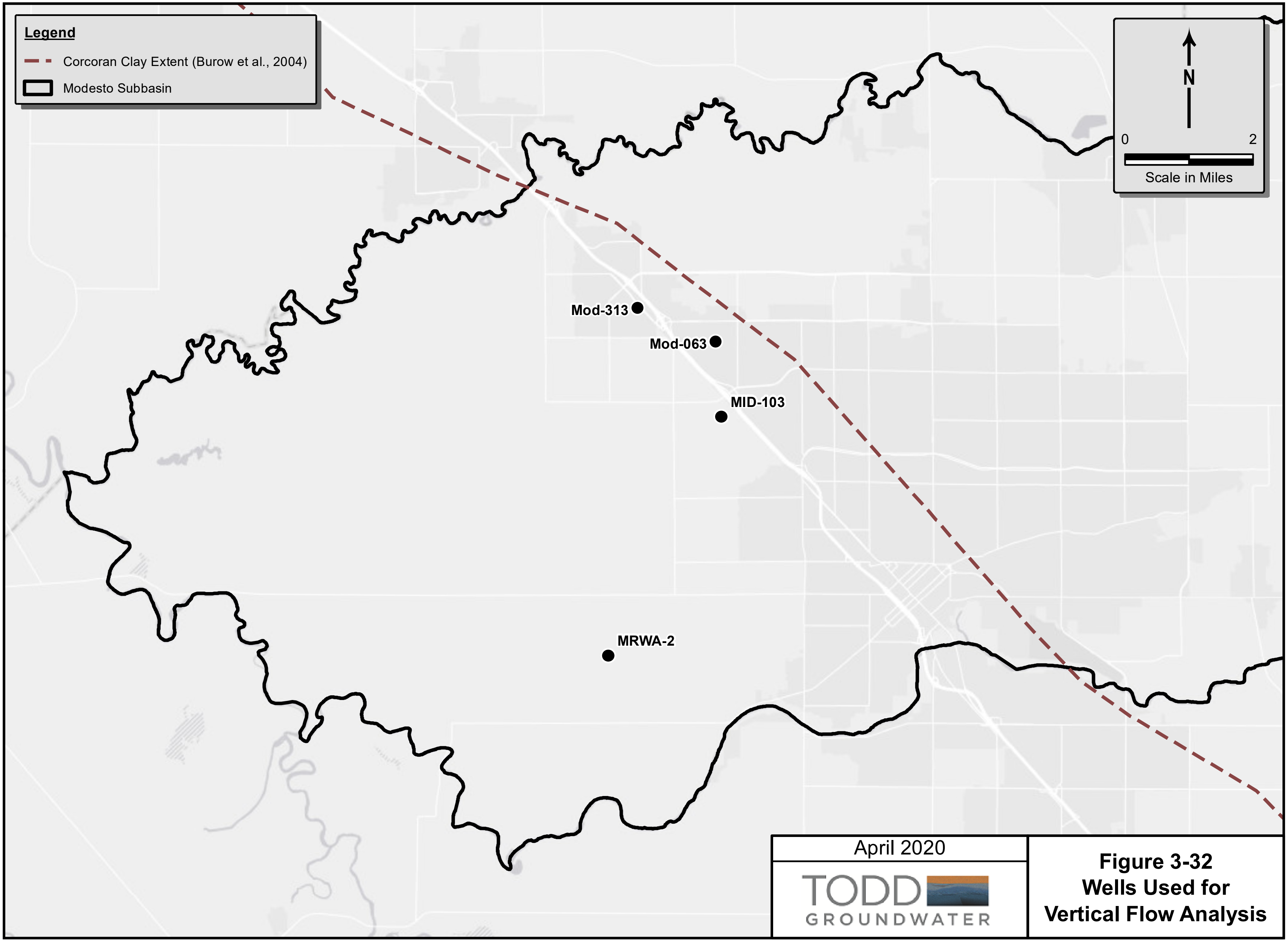

April 2020

TODD GROUNDWATER

Figure 3-32
Wells Used for Vertical Flow Analysis

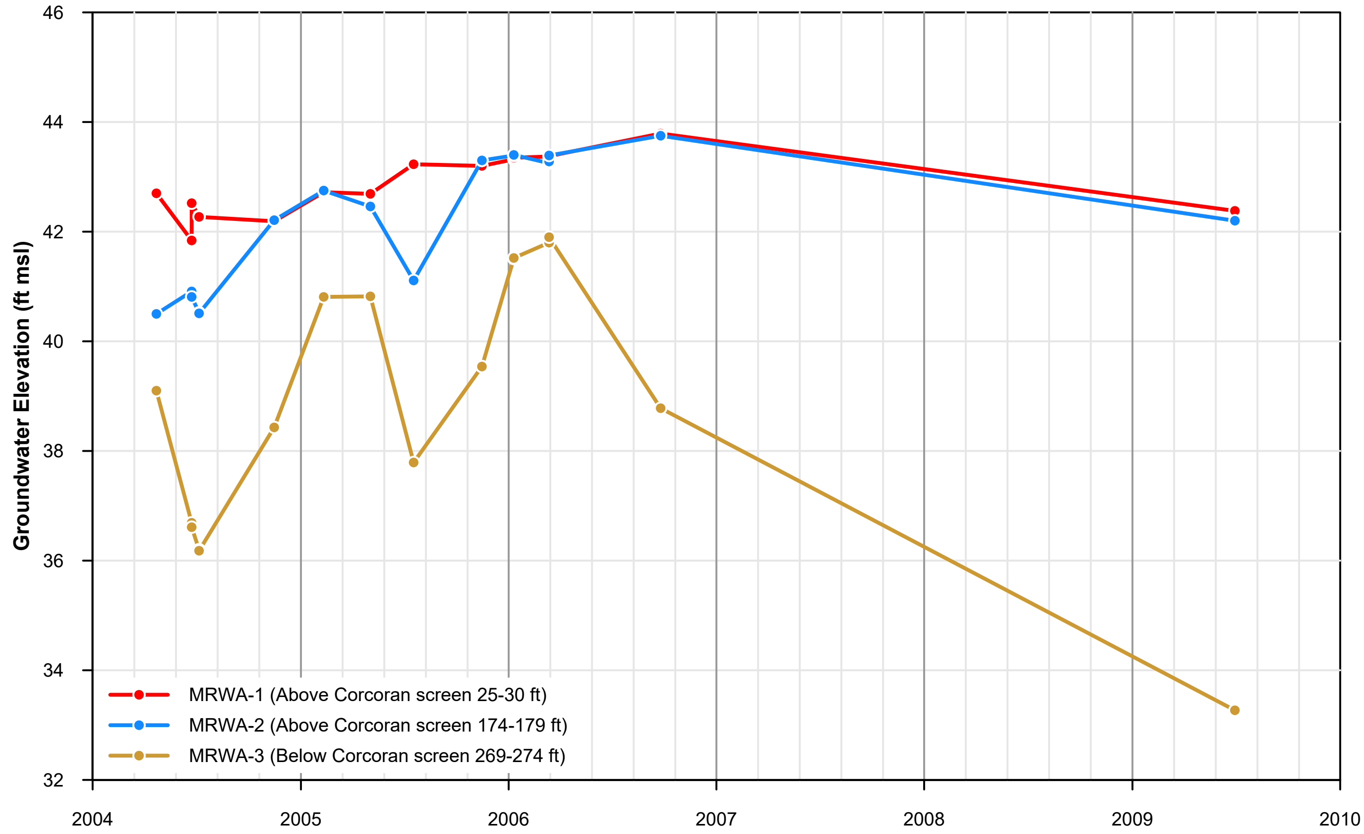

April 2020

TODD GROUNDWATER

Figure 3-33
Vertical Flow Hydrographs, USGS Well Cluster

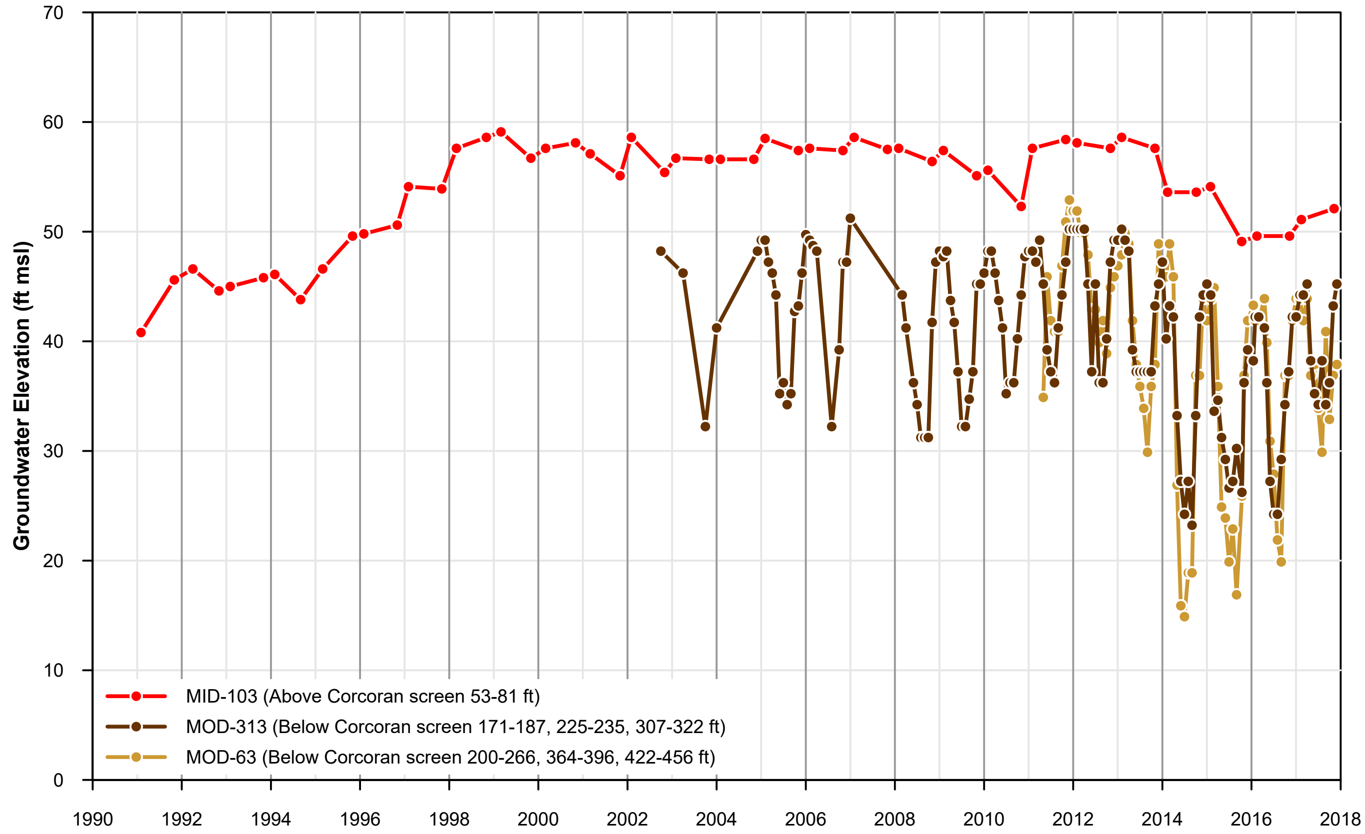

April 2020

TODD GROUNDWATER

Figure 3-34
Vertical Flow Hydrographs, MID and City of Modesto Wells

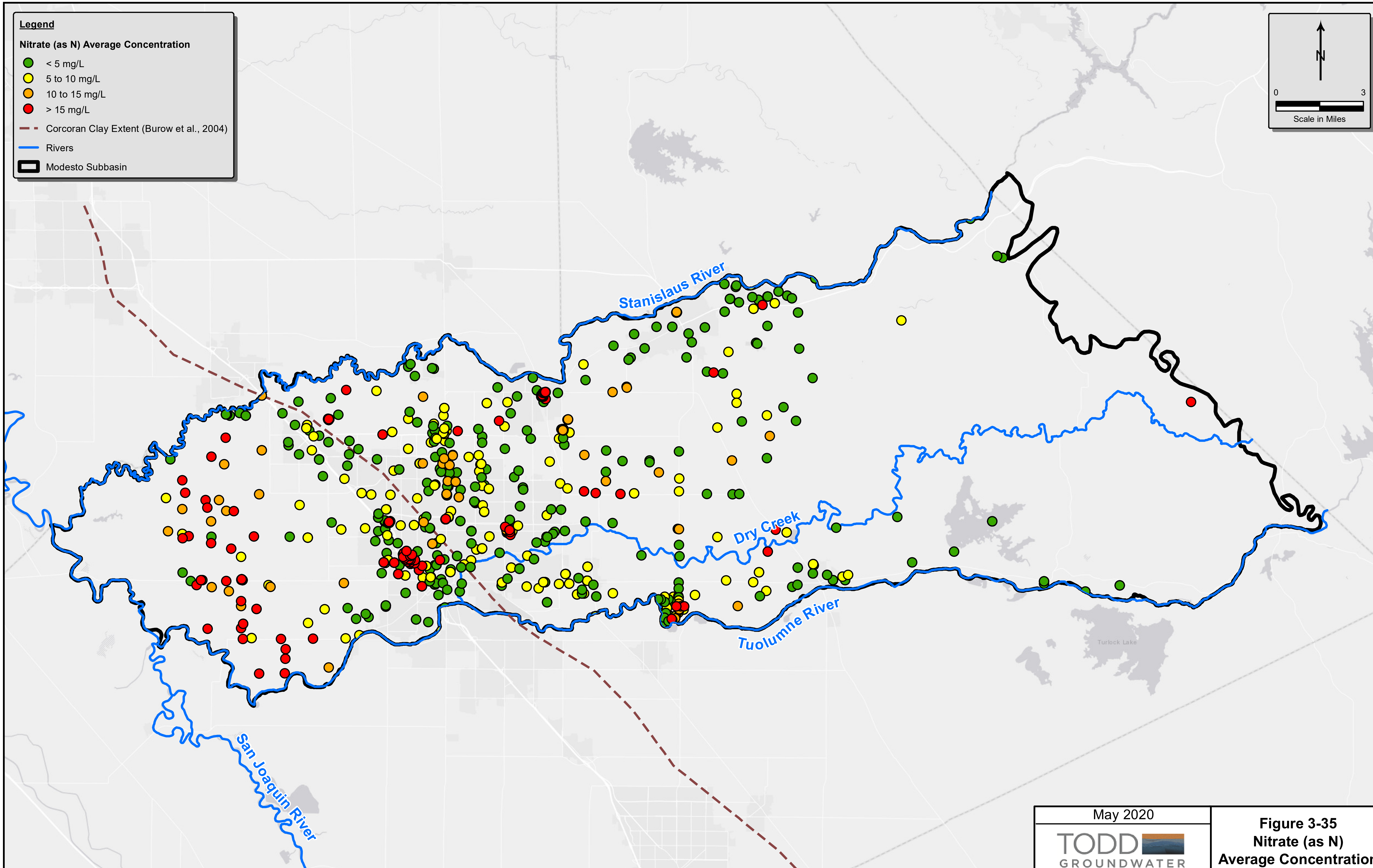

May 2020

Figure 3-35
Nitrate (as N)
Average Concentration

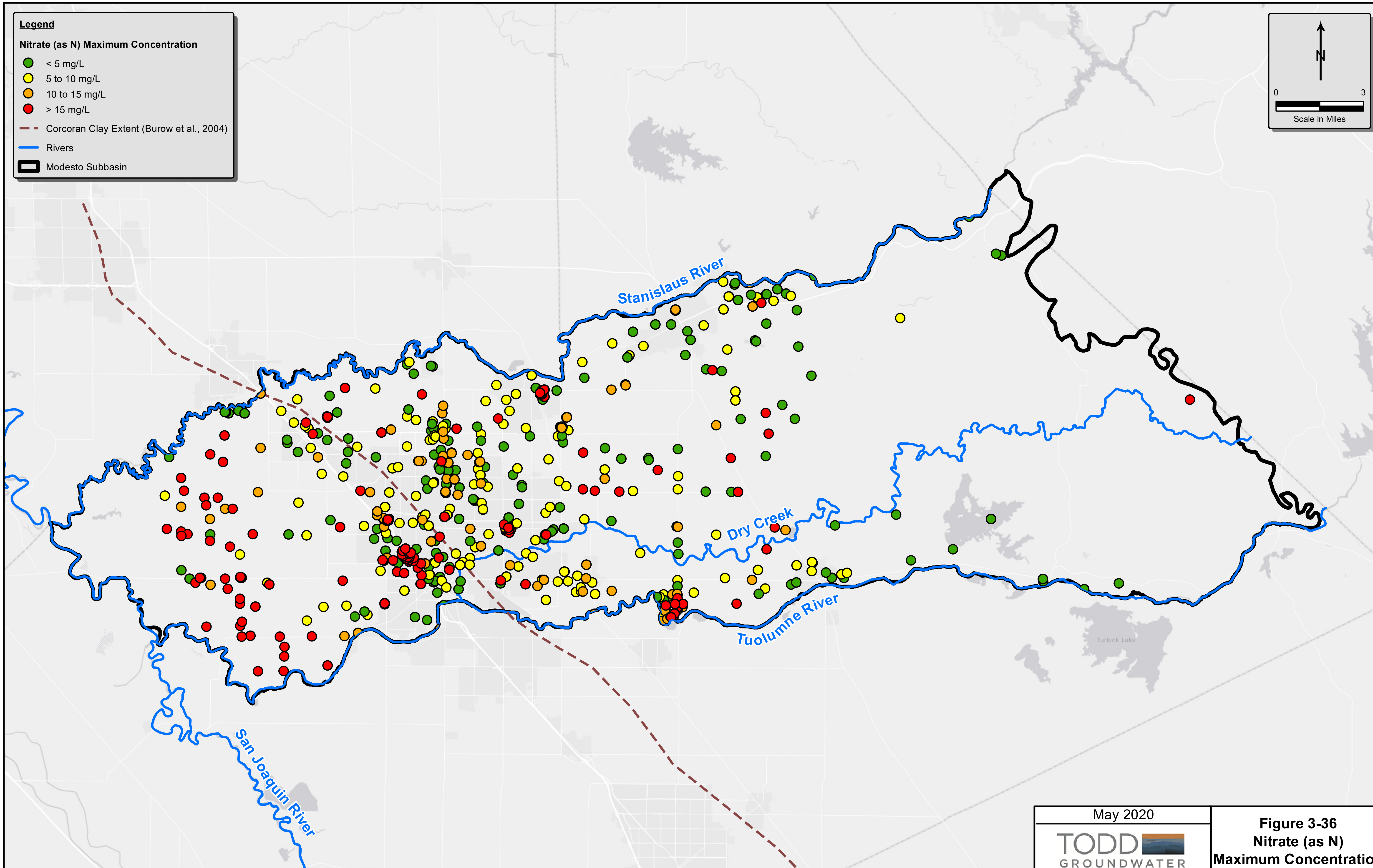

Figure 3-36
Nitrate (as N)
Maximum Concentration

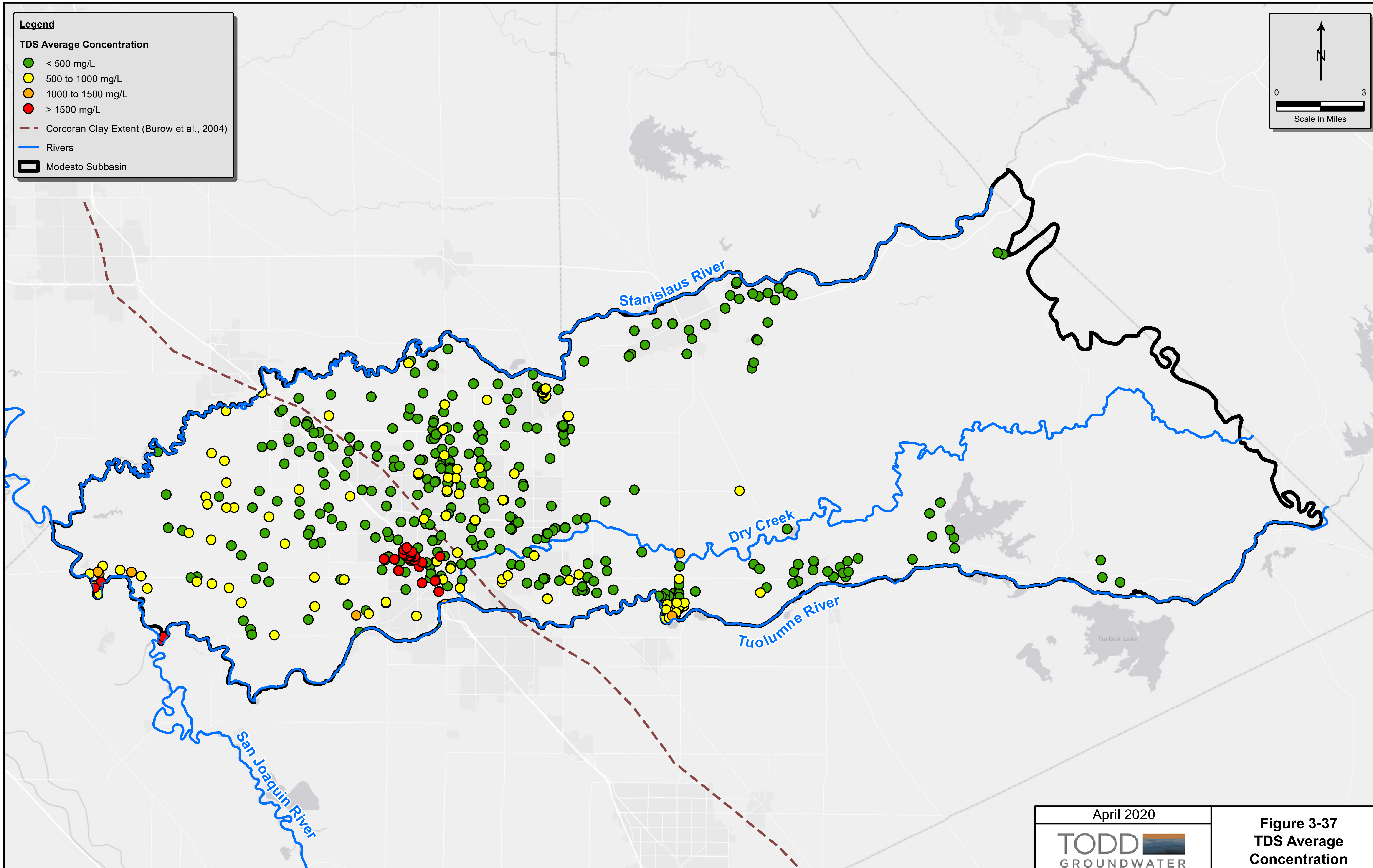

April 2020

TODD GROUNDWATER

Figure 3-37 TDS Average Concentration

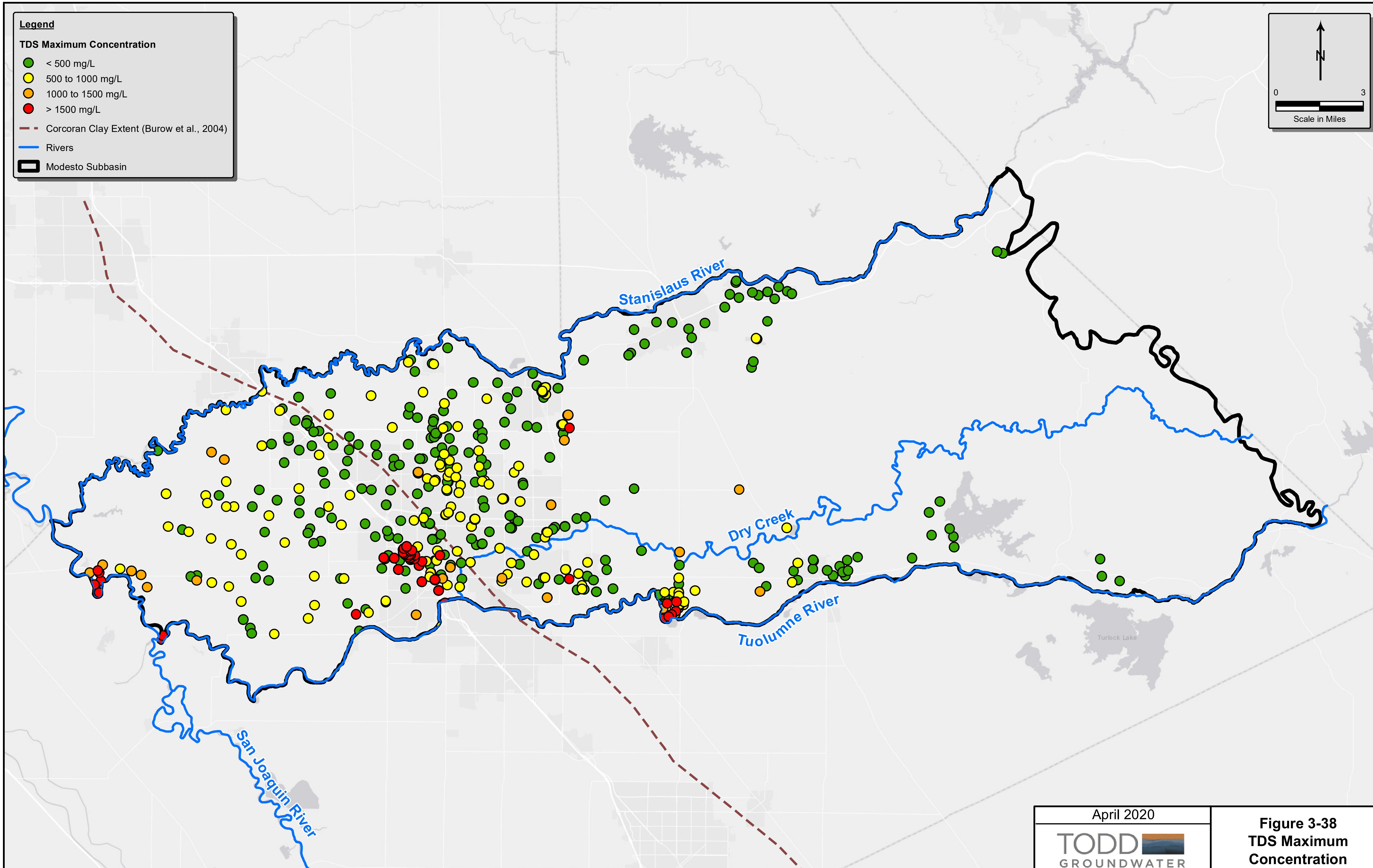

Figure 3-38
TDS Maximum Concentration

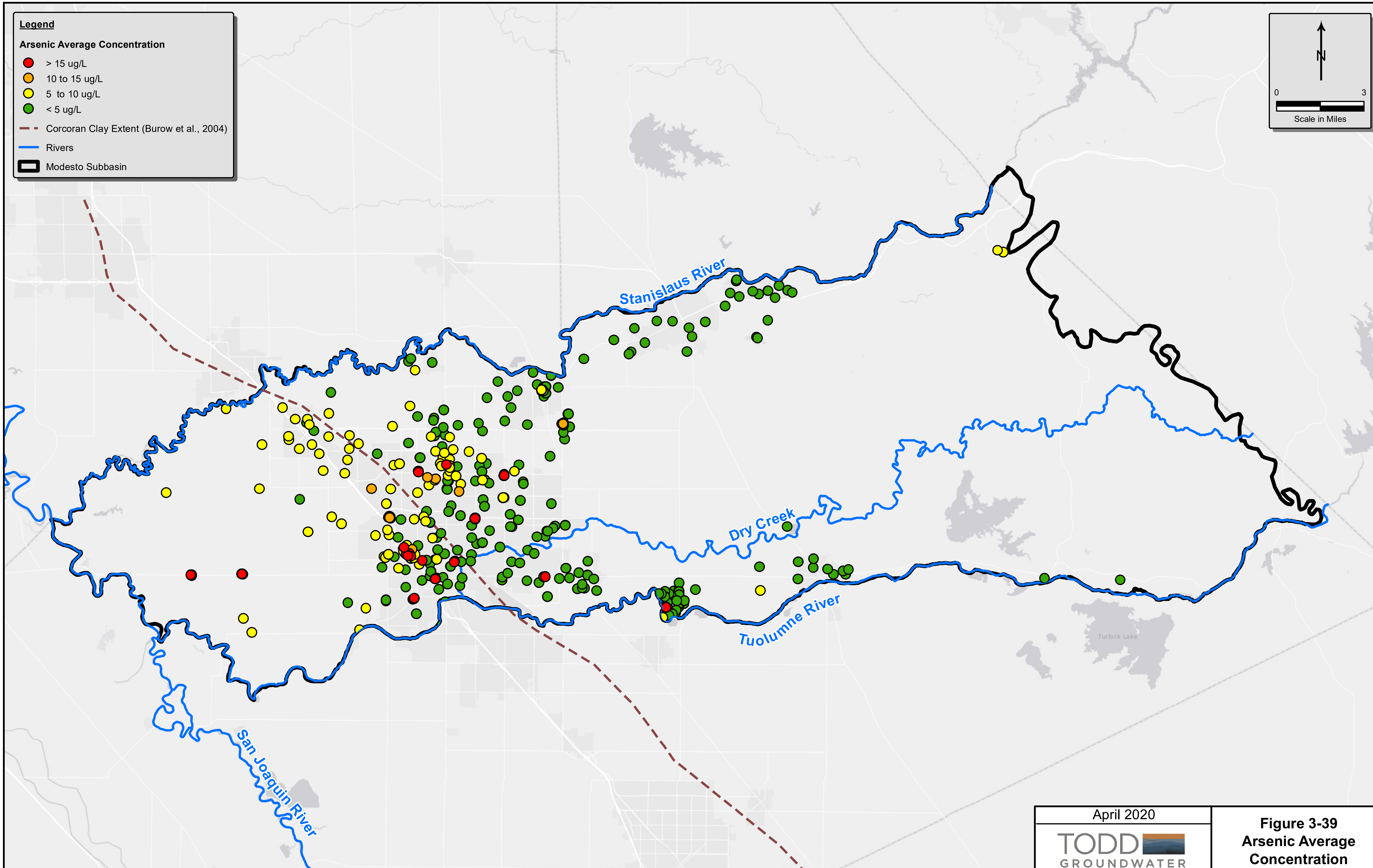

April 2020

TODD GROUNDWATER

Figure 3-39 Arsenic Average Concentration

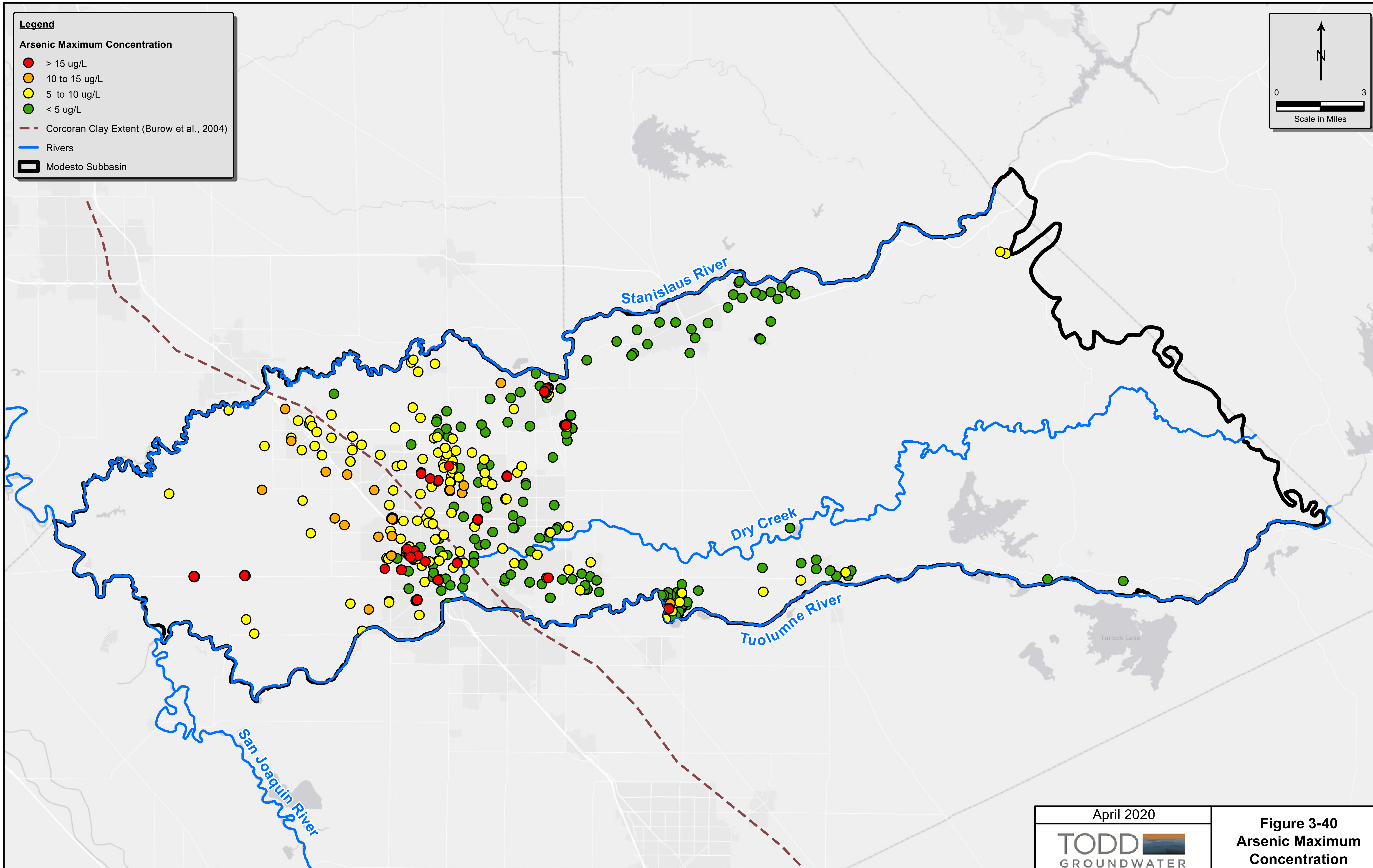

April 2020

TODD GROUNDWATER

Figure 3-40
Arsenic Maximum Concentration

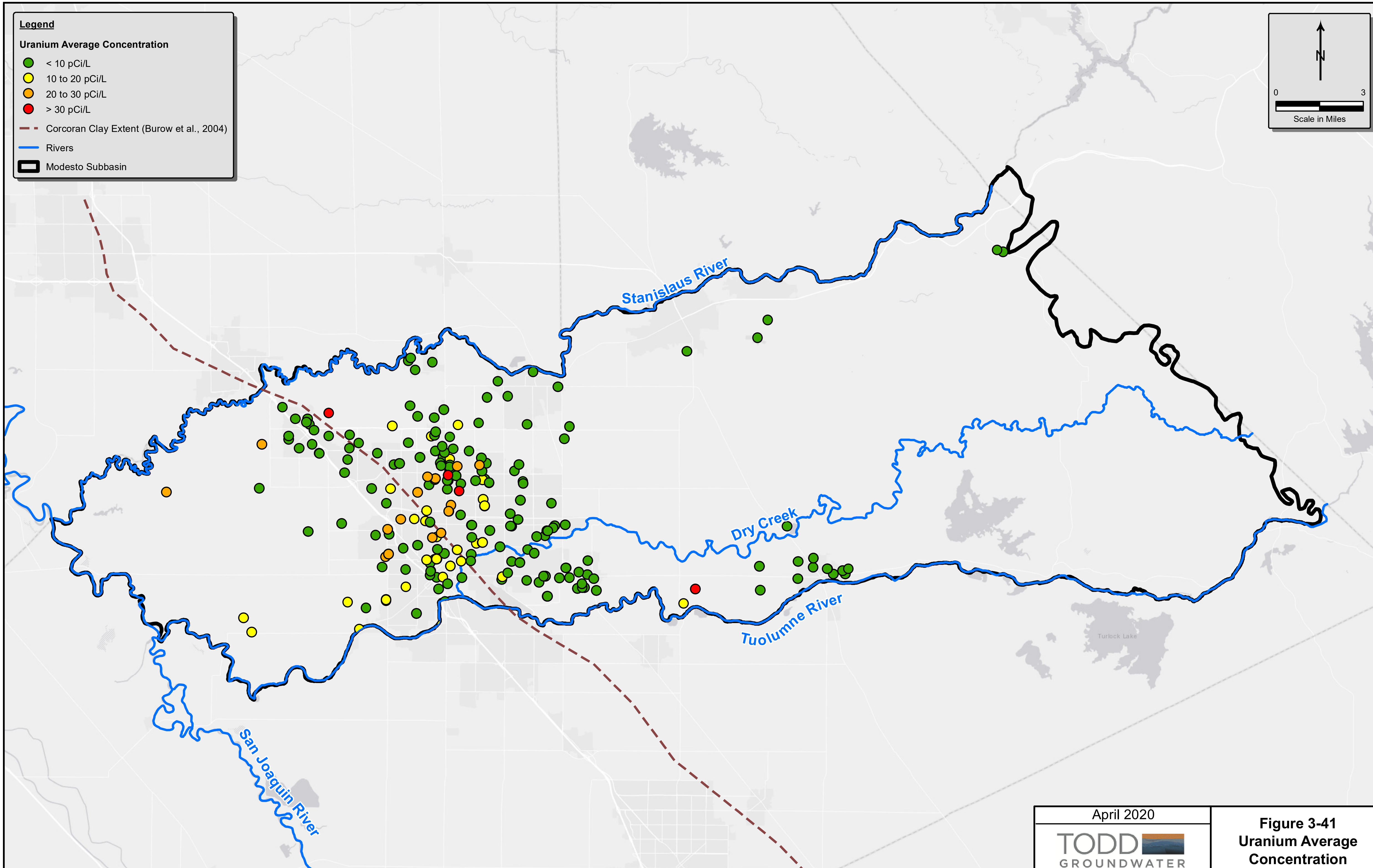

Figure 3-41
Uranium Average Concentration

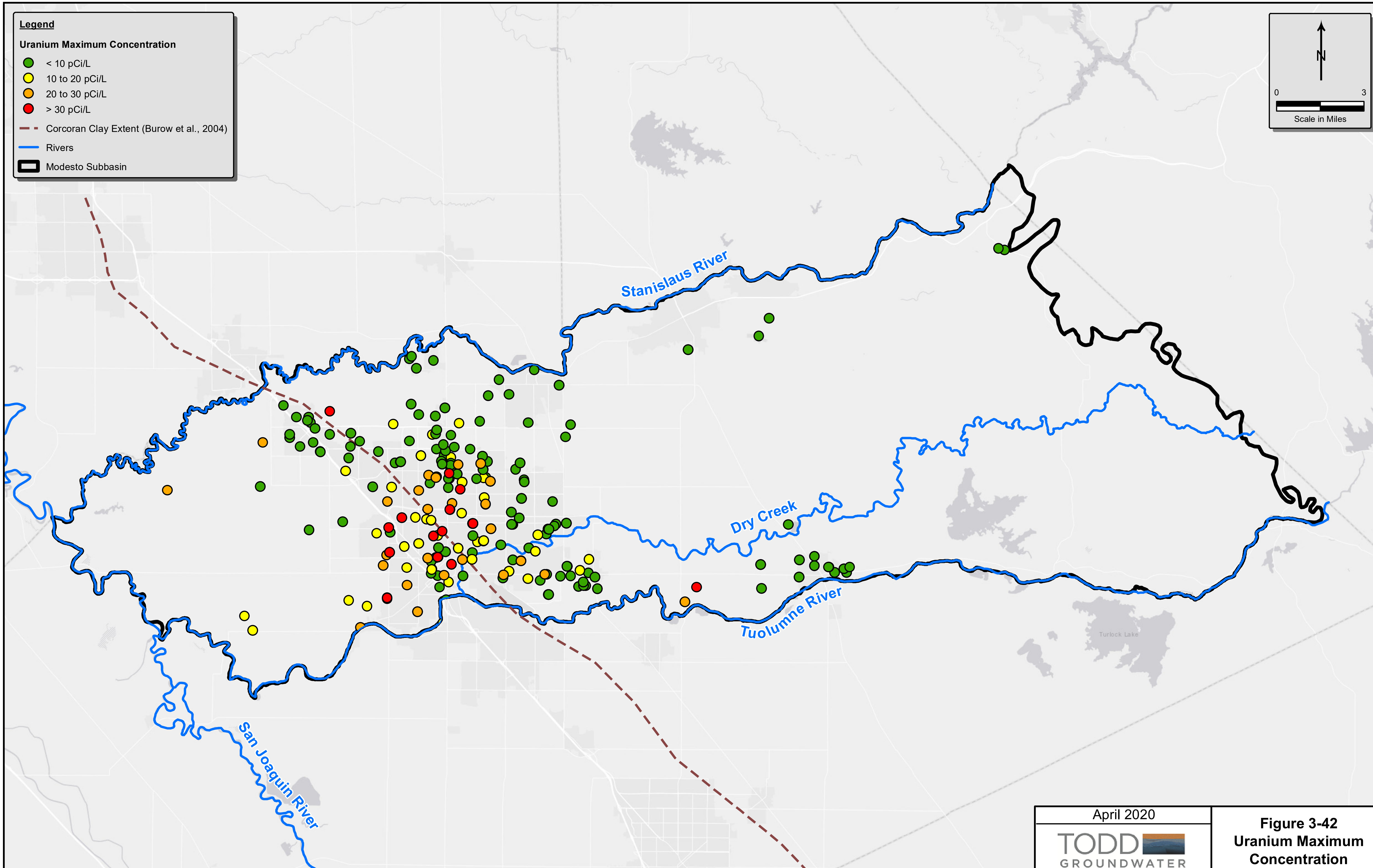

April 2020

TODD GROUNDWATER

Figure 3-42
Uranium Maximum Concentration

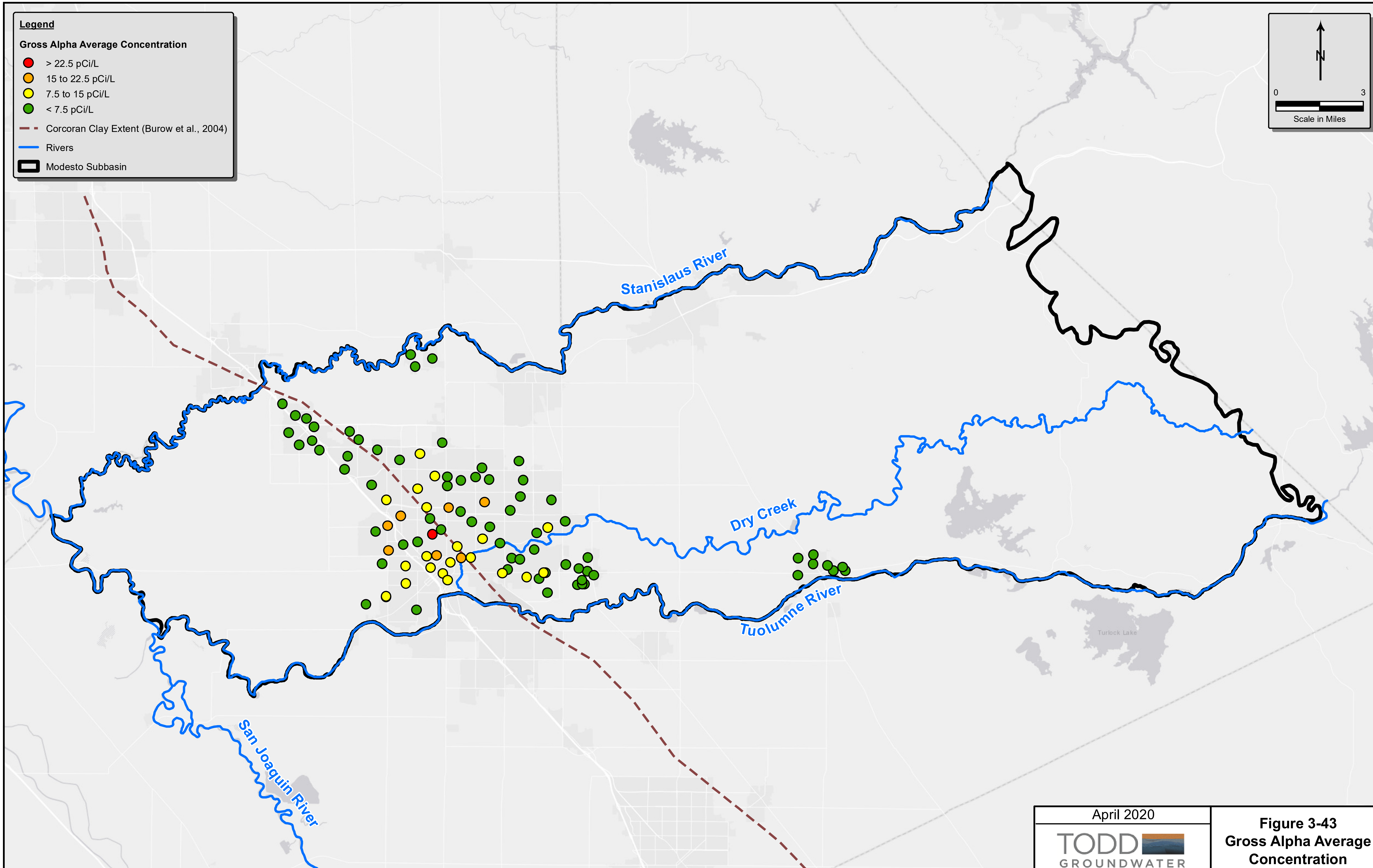

Figure 3-43
Gross Alpha Average Concentration

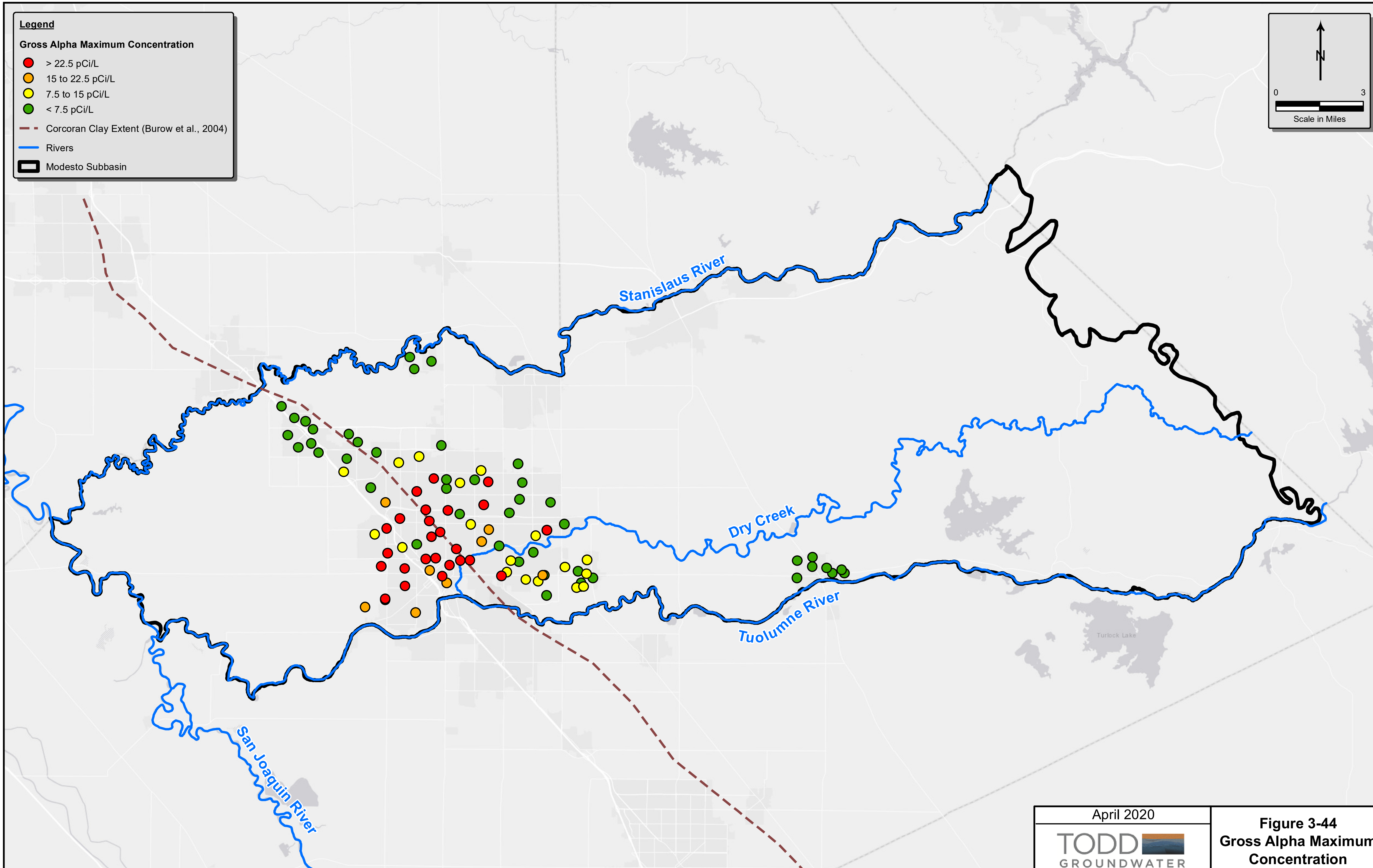

Figure 3-44
Gross Alpha Maximum Concentration

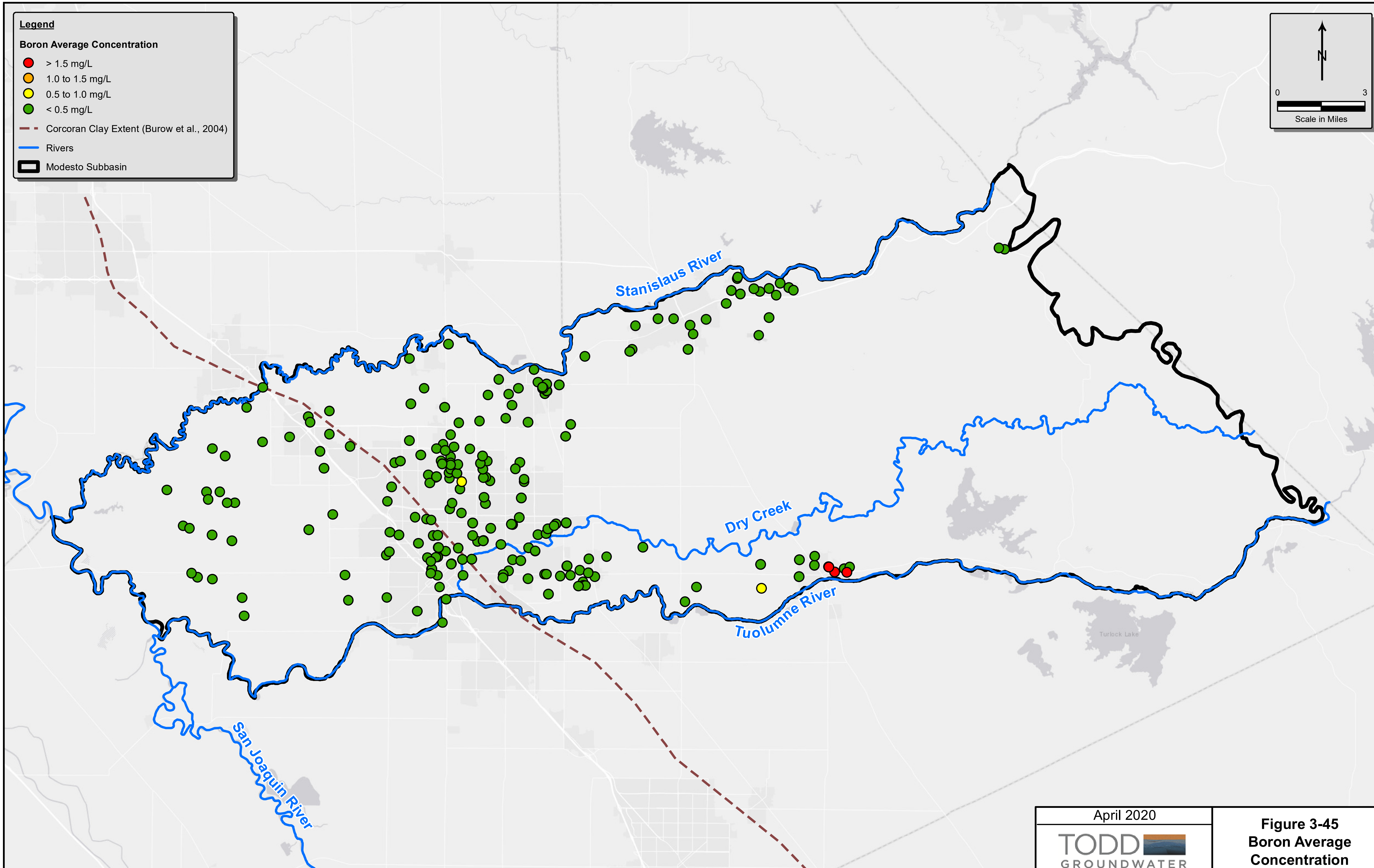

Figure 3-45
Boron Average Concentration

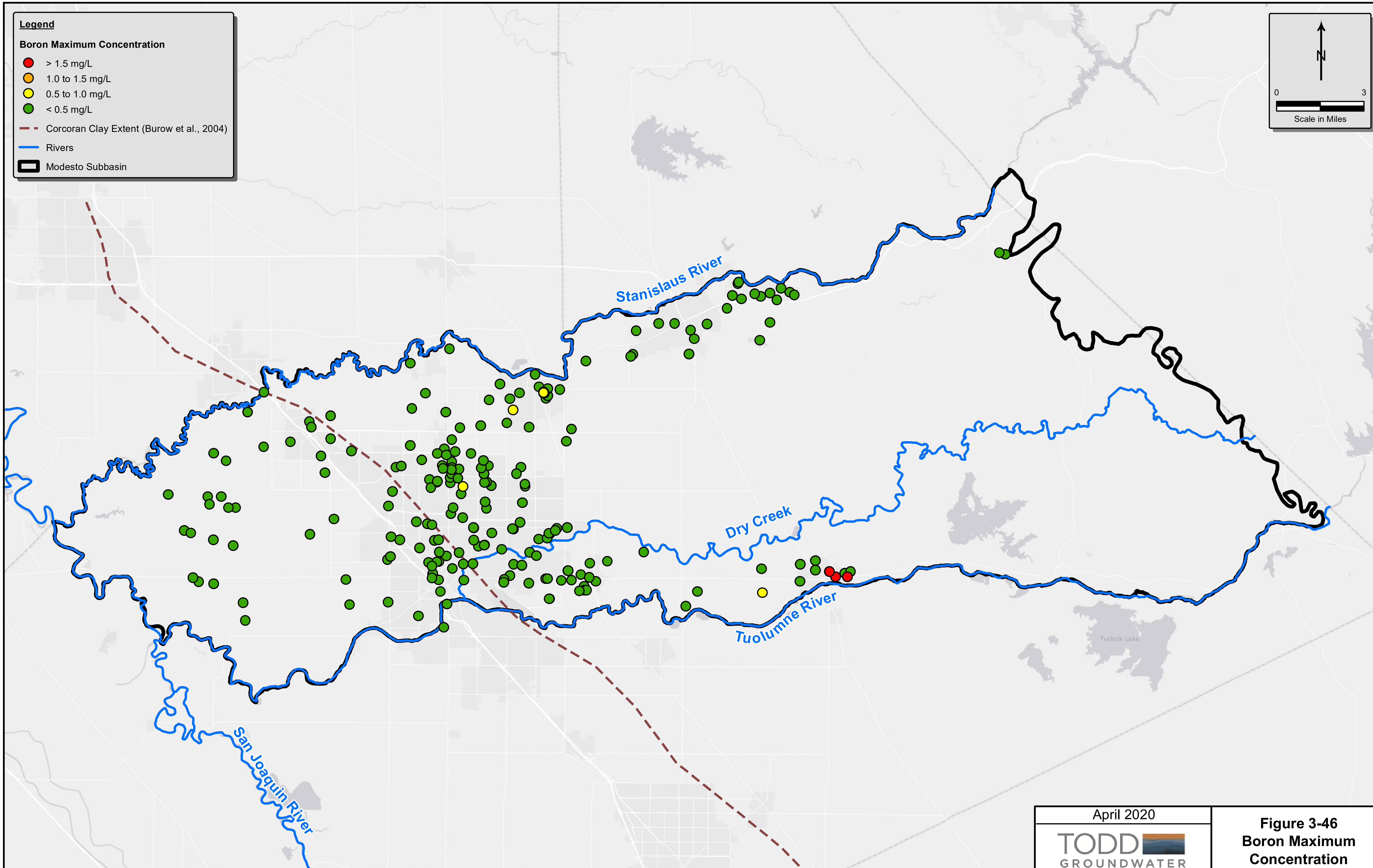

Figure 3-46
Boron Maximum Concentration

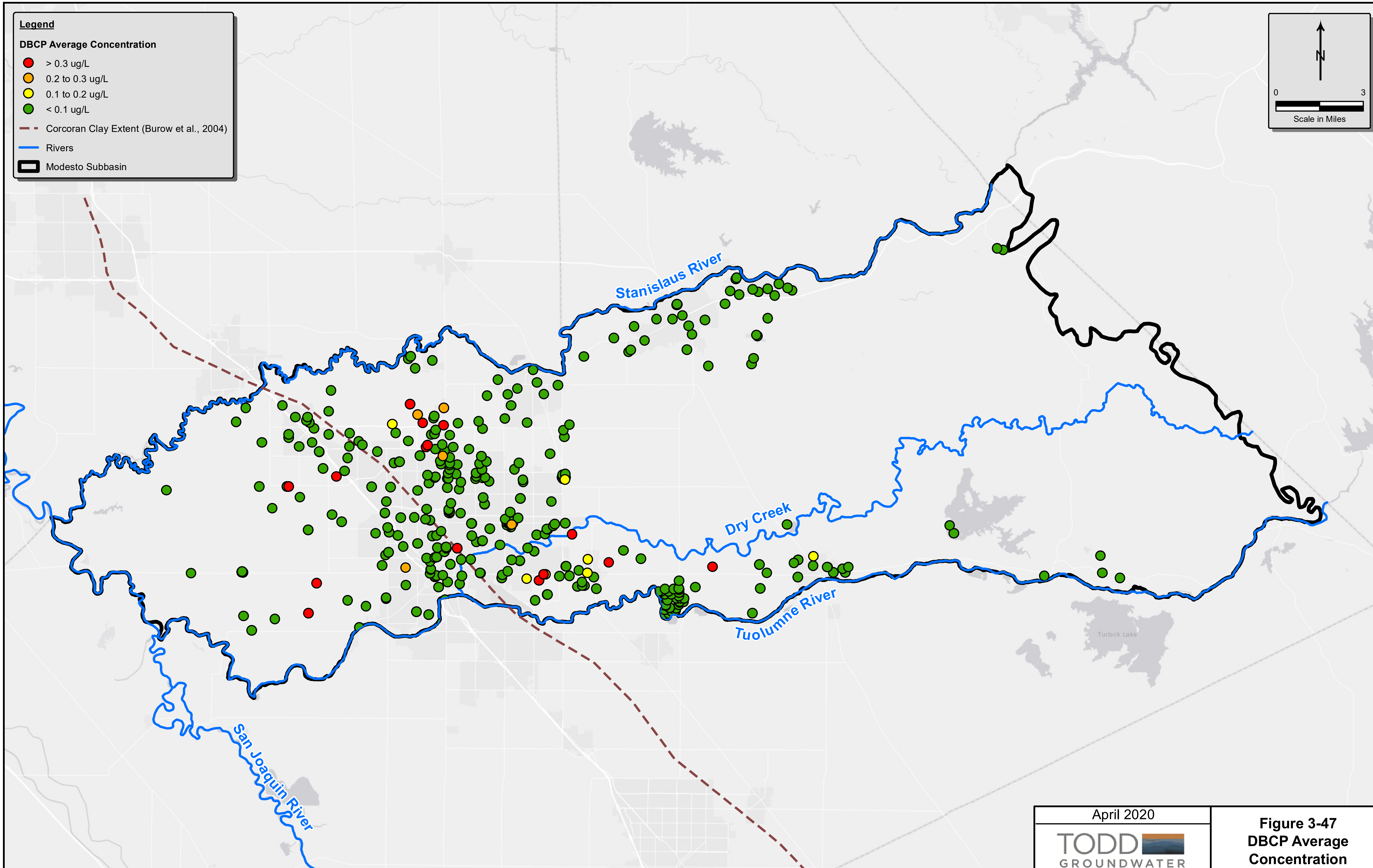

April 2020

TODD GROUNDWATER

Figure 3-47
DBCP Average Concentration

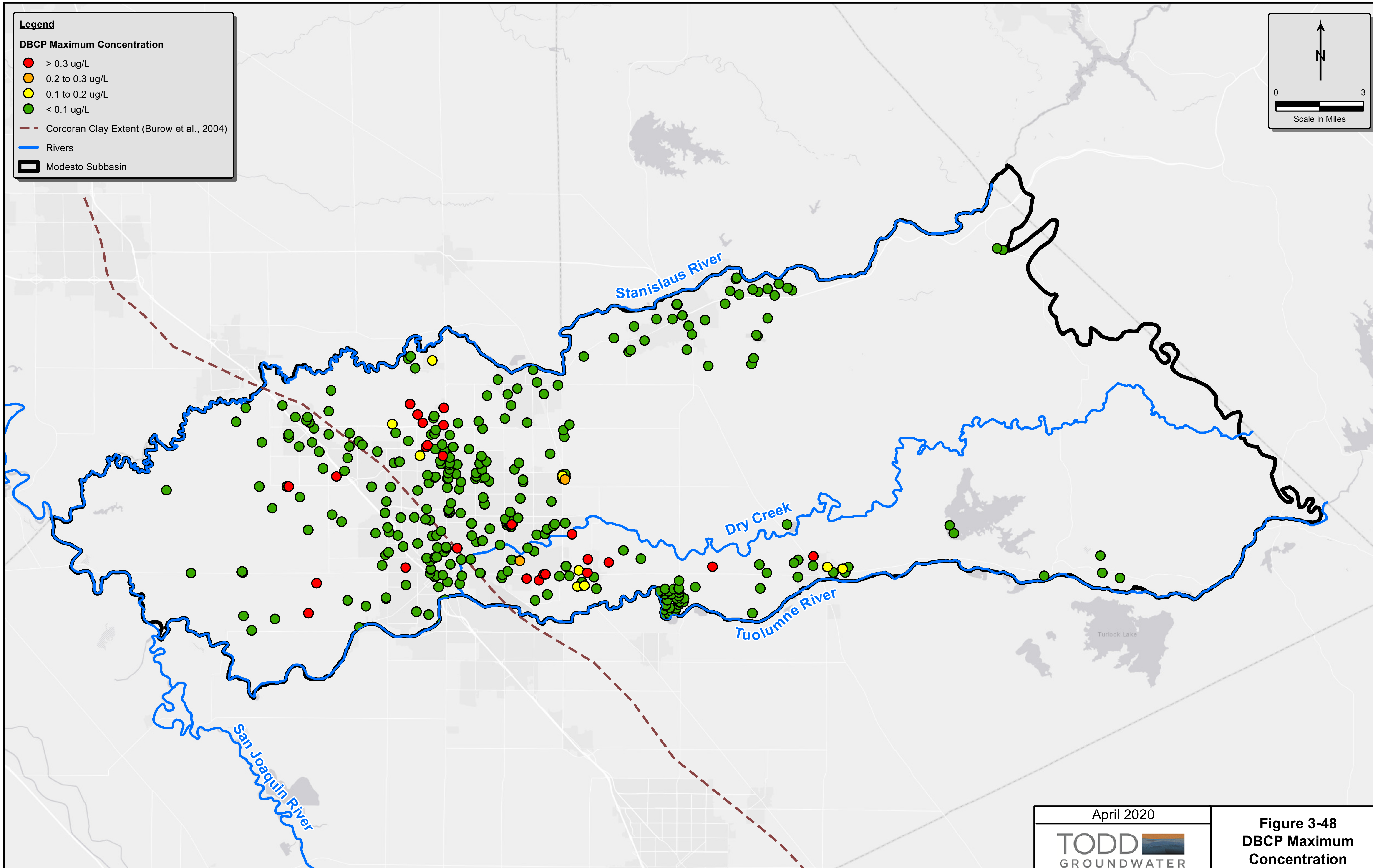

Figure 3-48
DBCP Maximum Concentration

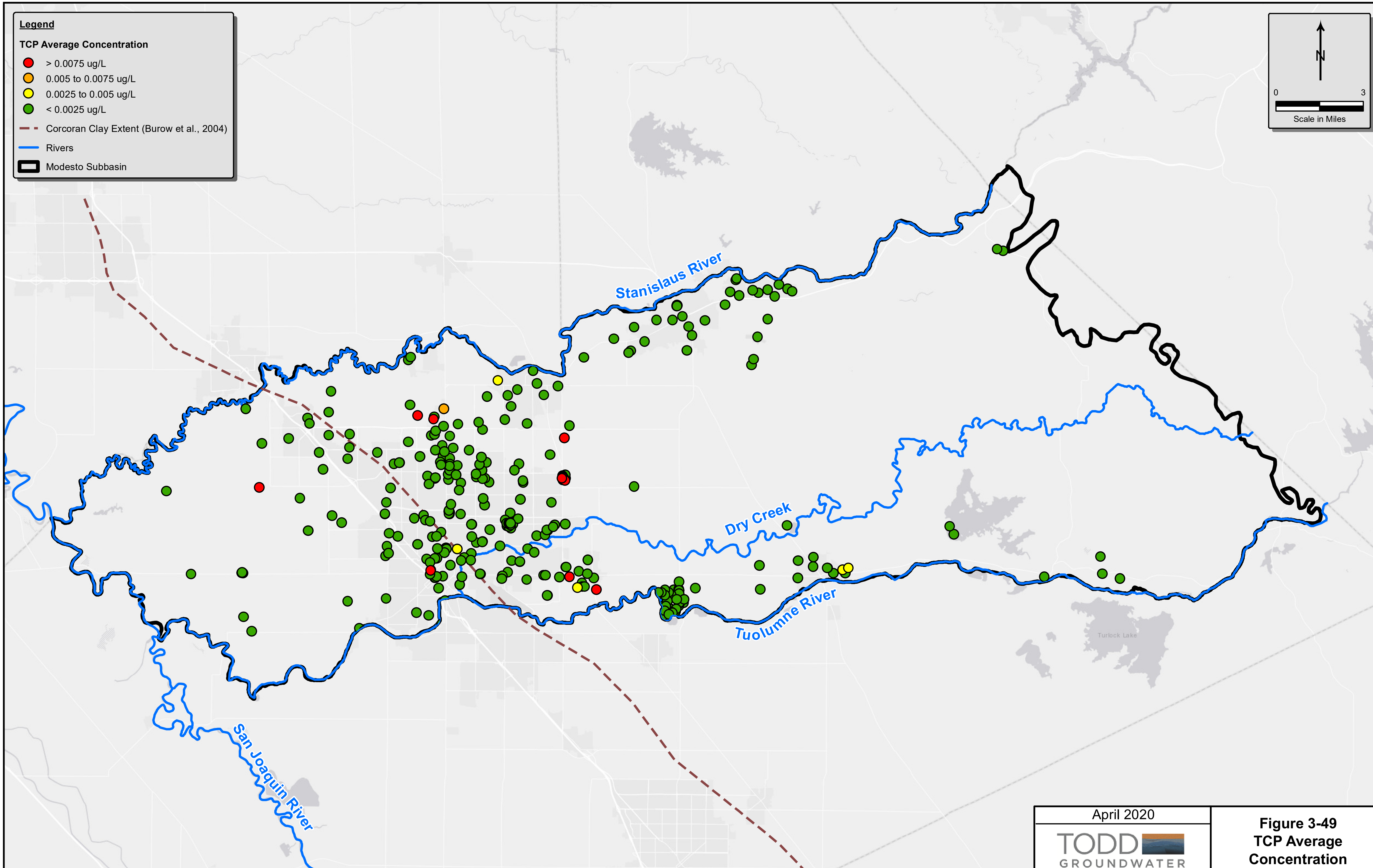

Figure 3-49
TCP Average Concentration

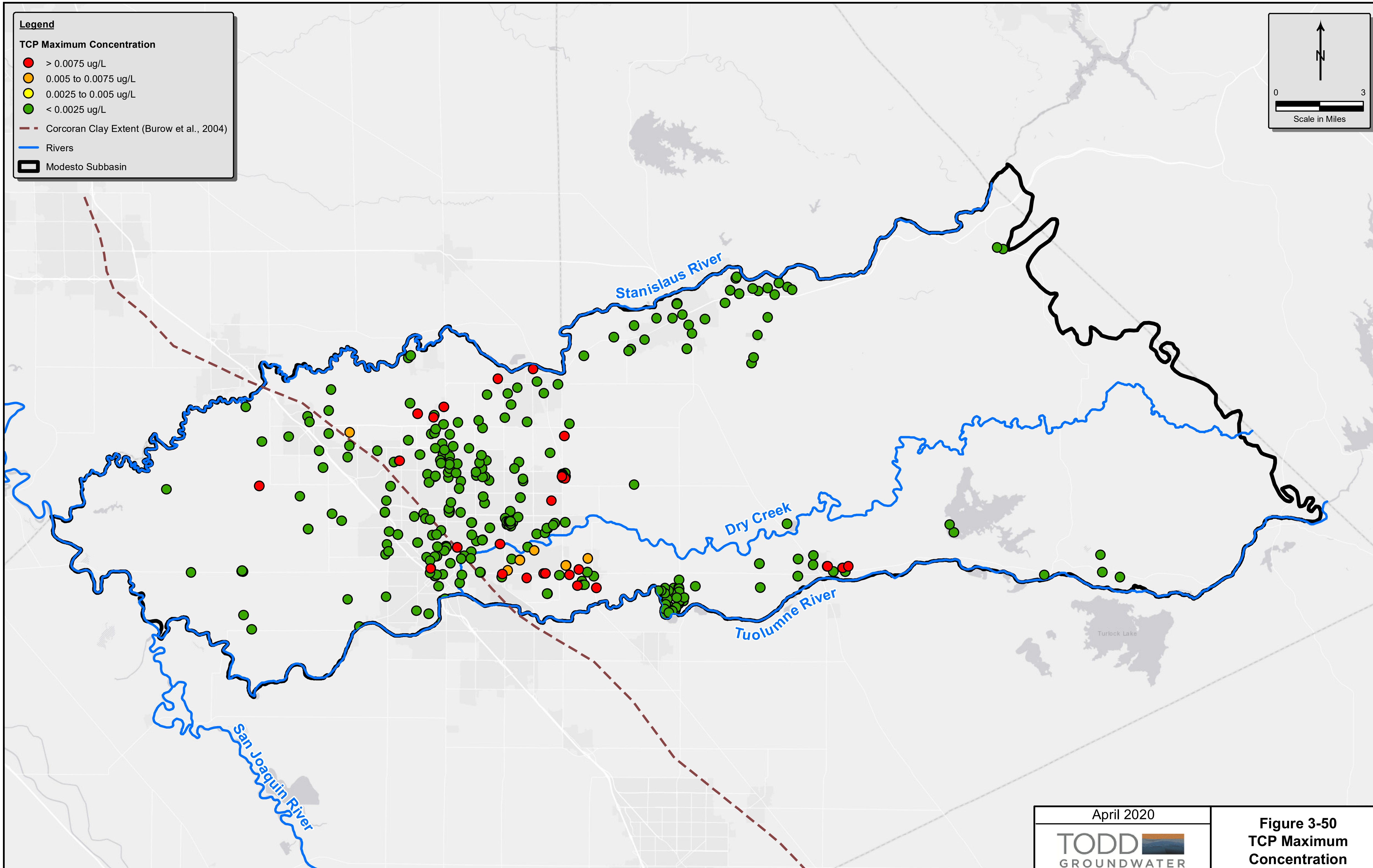

Figure 3-50
TCP Maximum Concentration

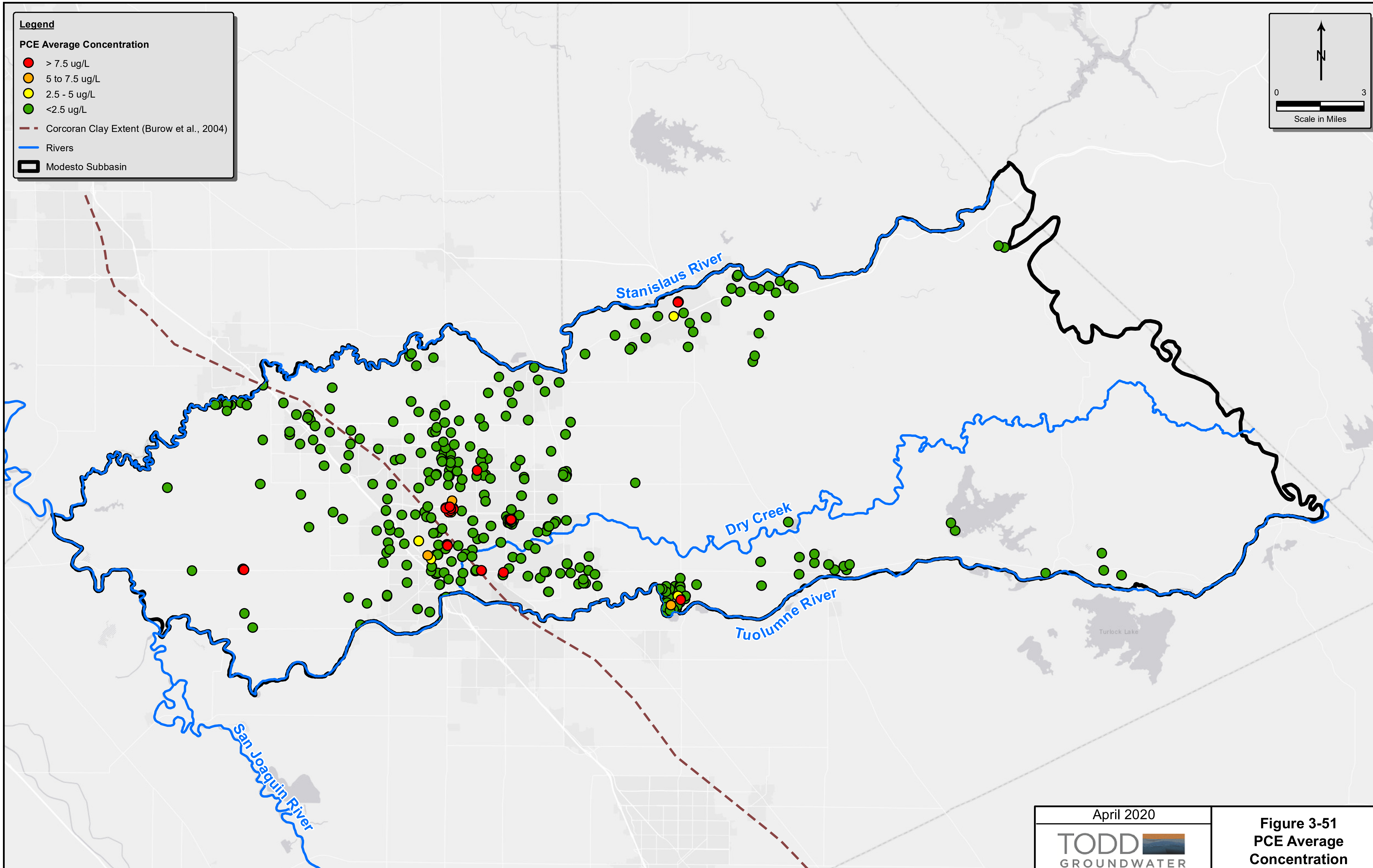

April 2020

TODD GROUNDWATER

Figure 3-51
PCE Average Concentration

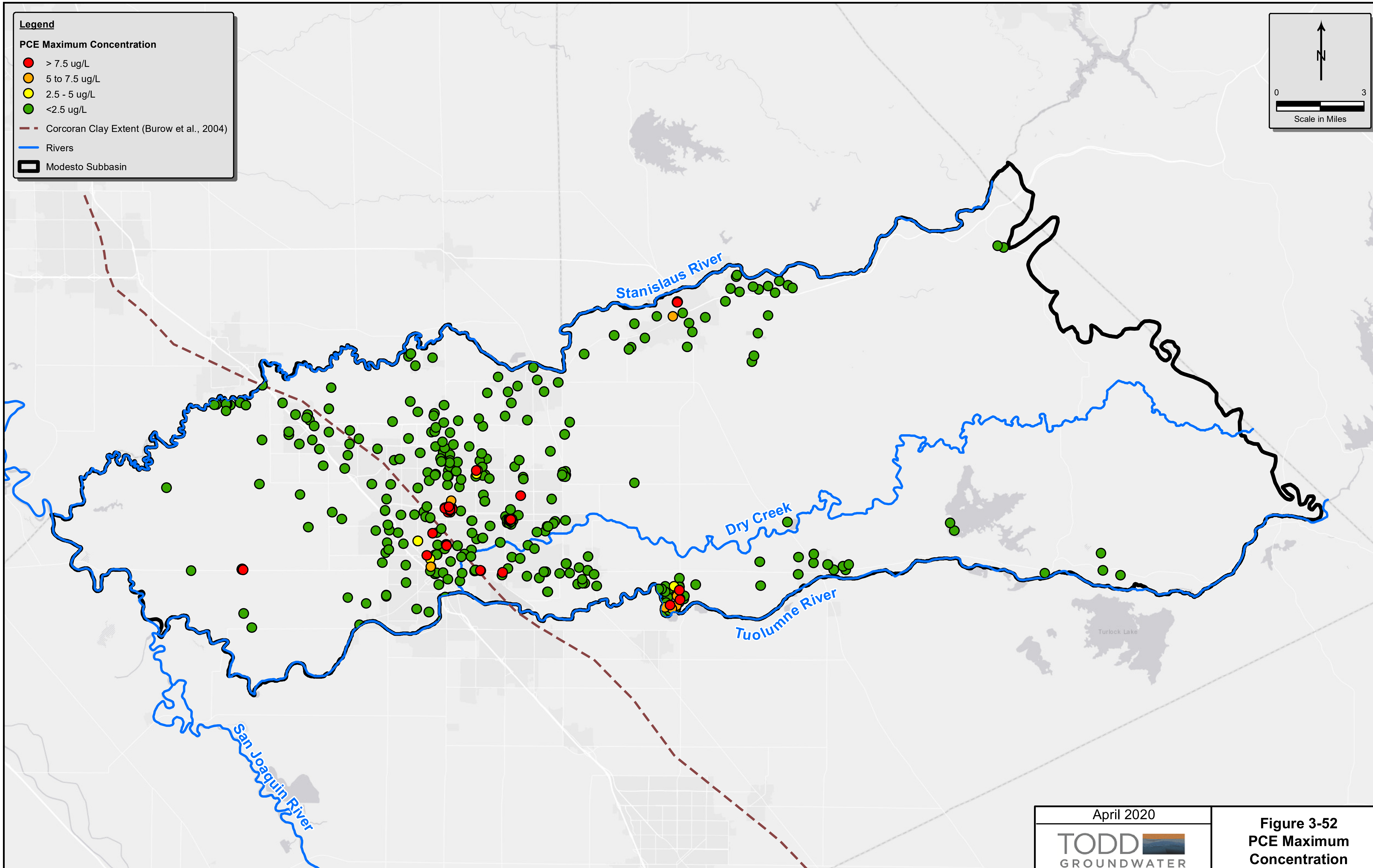

April 2020

TODD GROUNDWATER

Figure 3-52
PCE Maximum Concentration

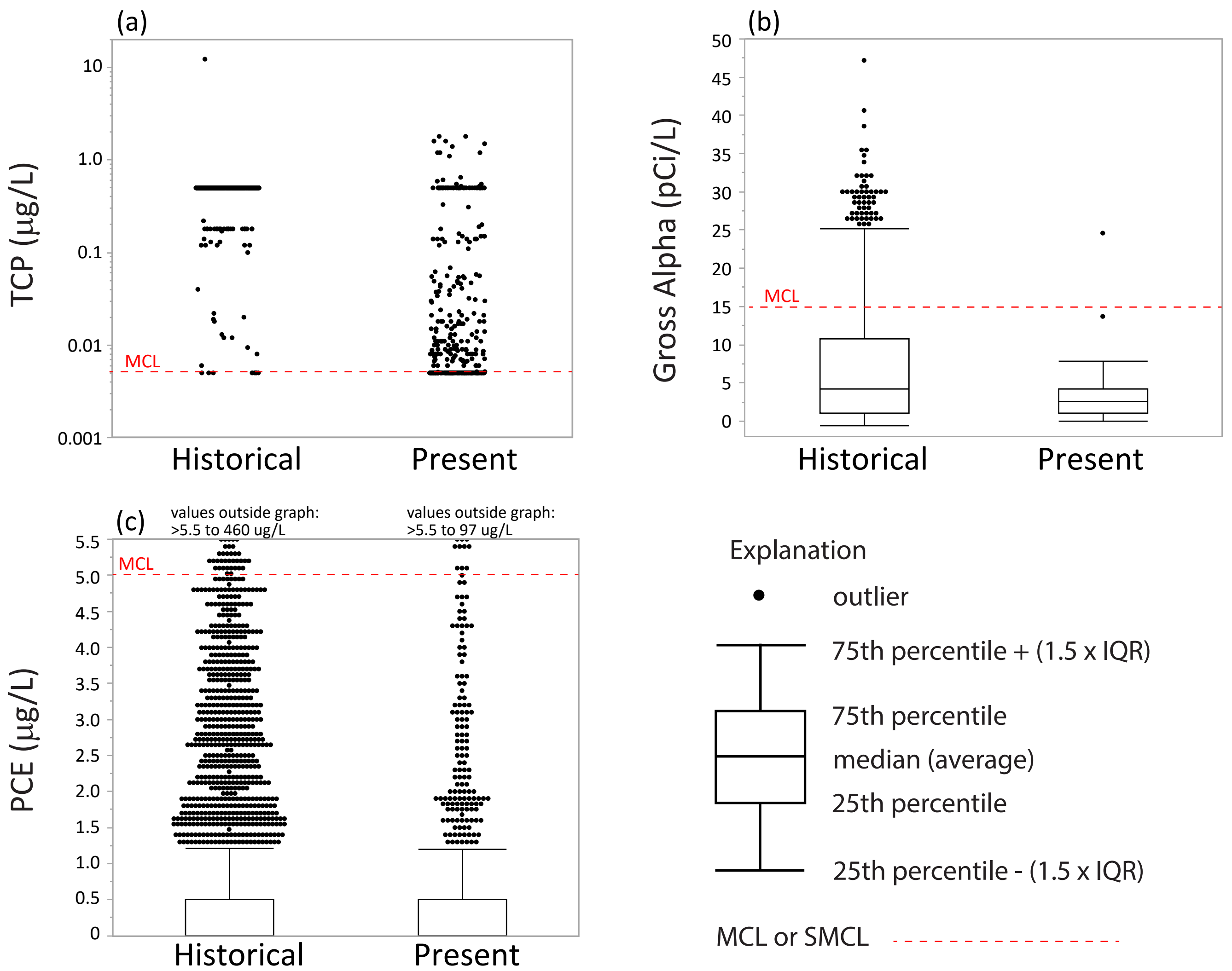

Note:
Concentrations of (a) TCP, (b) Gross Alpha, and (c) PCE under historical (water year 1995 to 2014) and present (2015 to 2019) periods, as compared to their respective Maximum Contaminant Level (MCL) or Secondary Maximum Contaminant Level (SMCL).

April 2020

TODD GROUNDWATER

Figure 3-53
Box Plots (1 of 2)

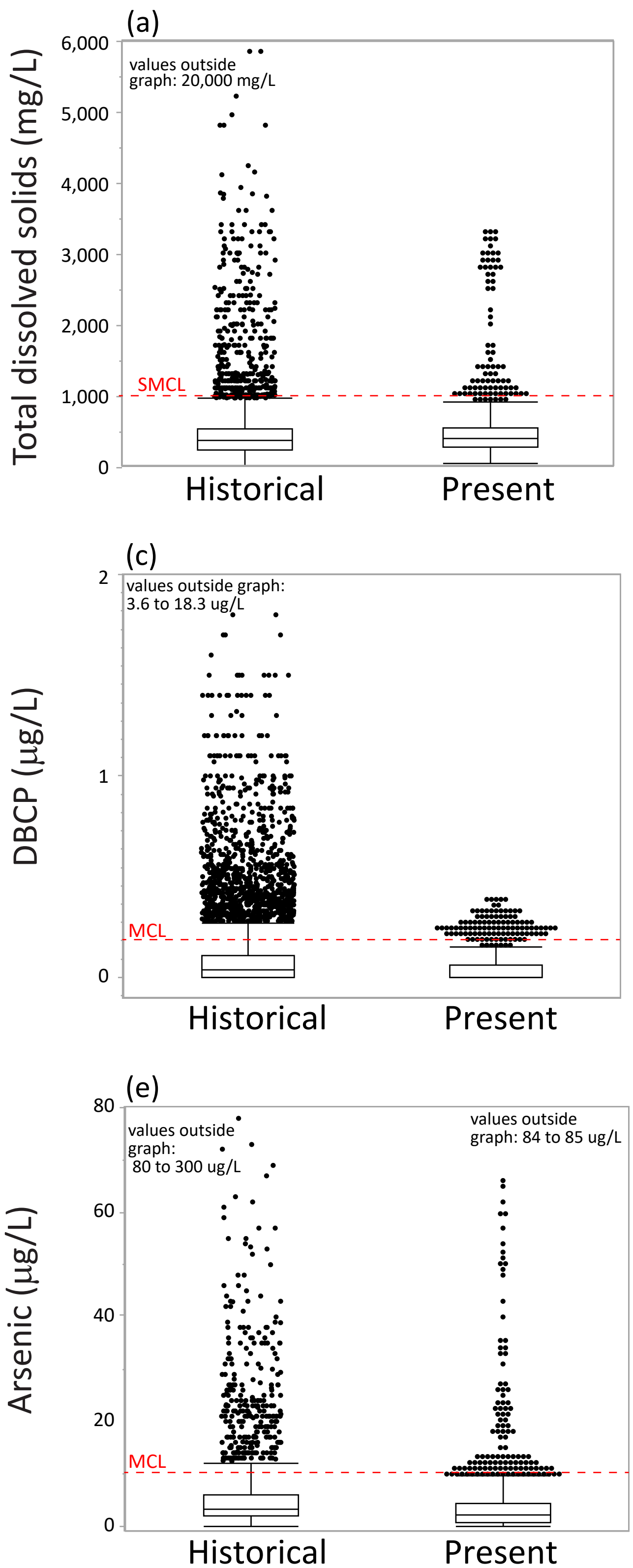

Note:
Concentrations of (a) total dissolved solids, (b) nitrate (as N), (c) DBCP, (d) uranium, (e) arsenic, and (f) boron under historical (water year 1995 to 2014) and present (2015 to 2019) periods, as compared to their respective Maximum Contaminant Level (MCL) or Secondary Maximum Contaminant Level (SMCL).

April 2020

TODD GROUNDWATER

Figure 3-54
Box Plots (2 of 2)

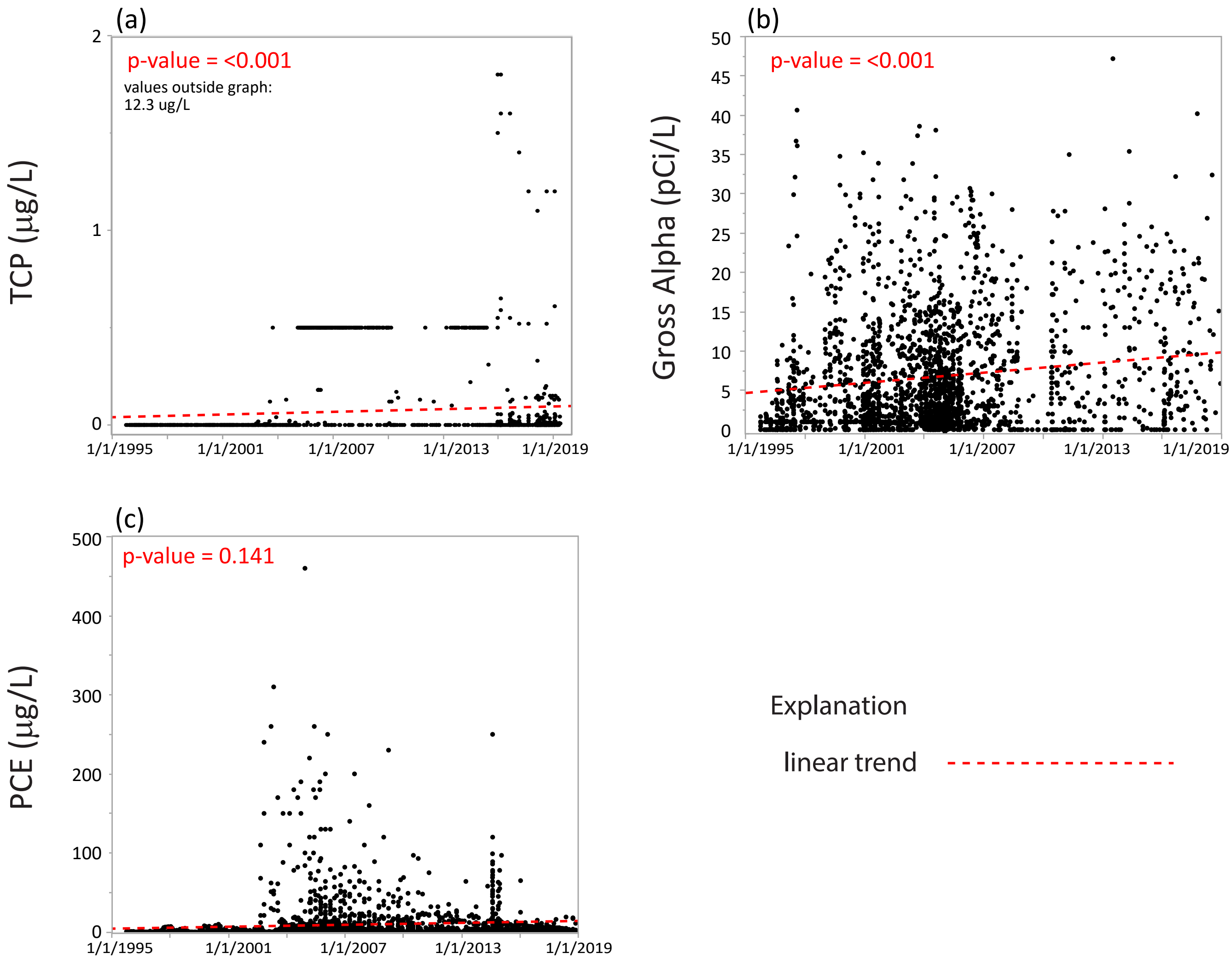

Note:
Linear temporal trends of (a) TCP, (b) Gross Alpha, and (c) PCE. The p-values less than the alpha-level of 0.05 are statistically significant trends.

April 2020

TODD GROUNDWATER

Figure 3-55
Linear Temporal Trends (1 of 2)

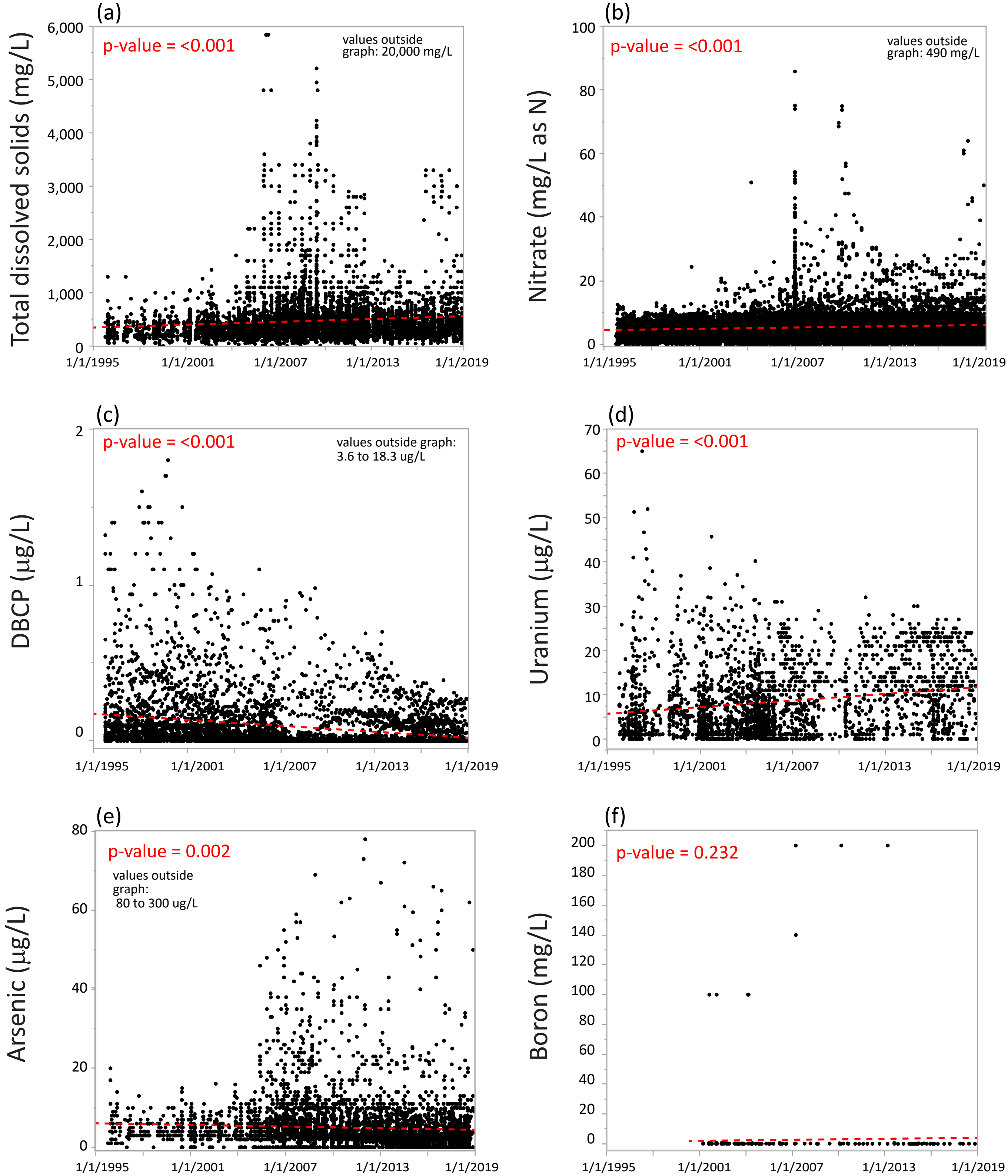

Note:
Linear temporal trends of (a) total dissolved solids, (b) nitrate (as N), (c) DBCP, (d) uranium, (e) arsenic, and (f) boron . The p-values less than the alpha-level of 0.05 are statistically significant trends.

April 2020

TODD GROUNDWATER

Figure 3-56
Linear Temporal Trends (2 of 2)

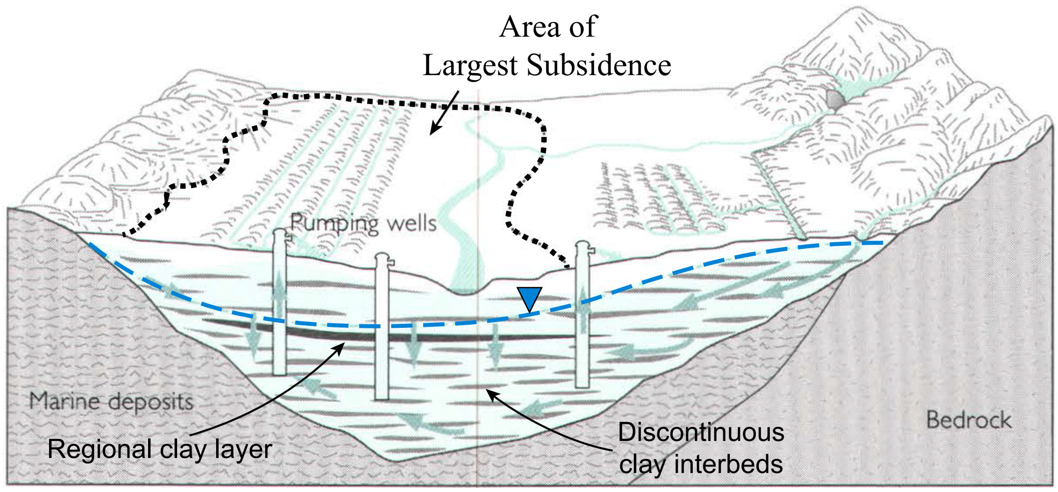

Source: Galloway et al., 1999.

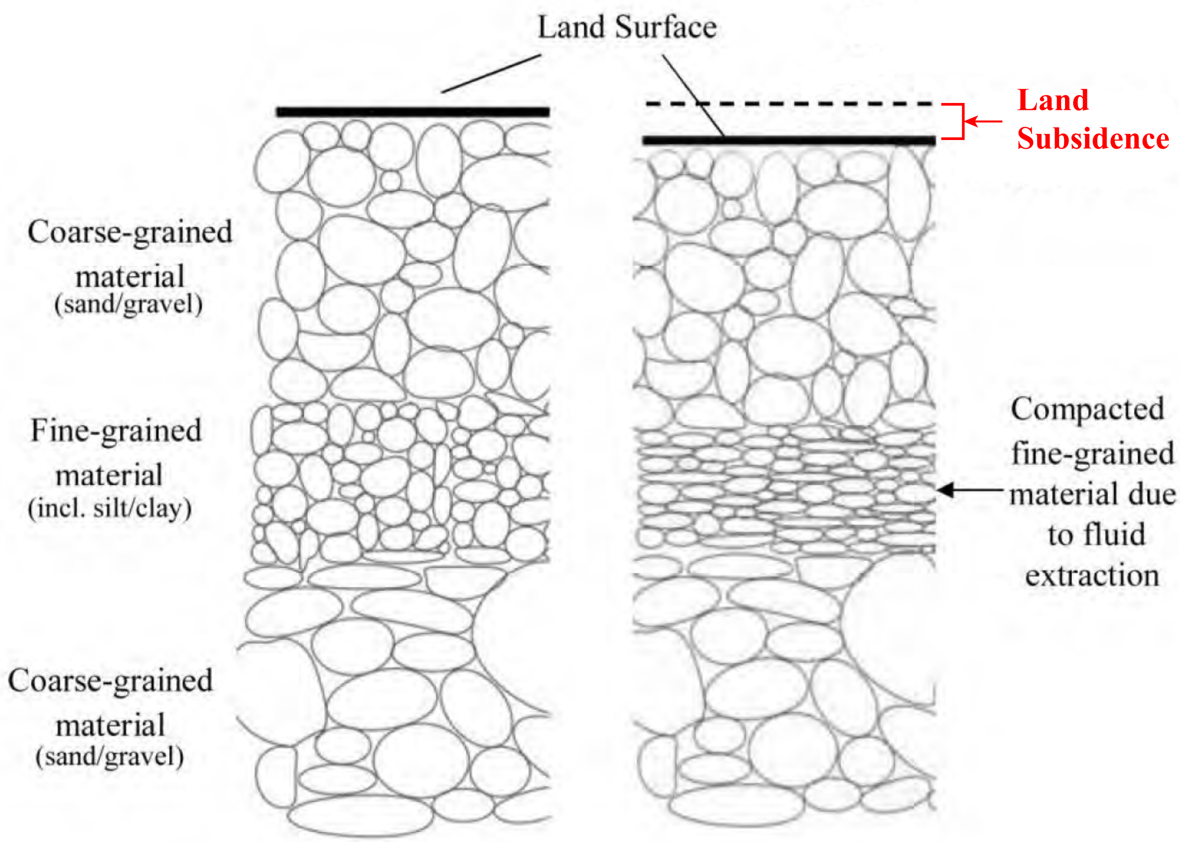

After LSCE et al., 2014.

April 2020

TODD GROUNDWATER

Figure 3-57
Concepts of
Land Subsidence

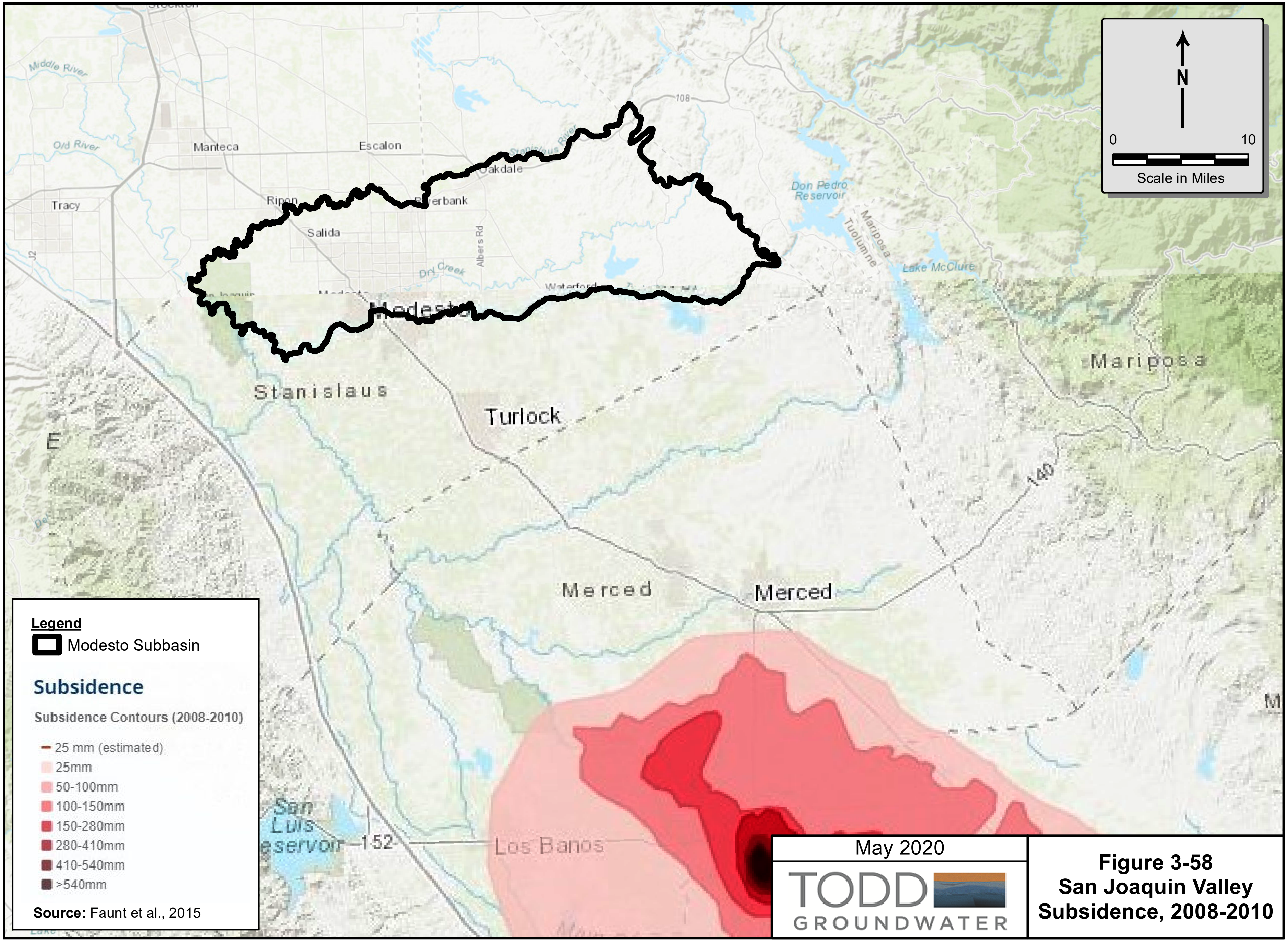

May 2020

TODD GROUNDWATER

Figure 3-58
San Joaquin Valley Subsidence, 2008-2010

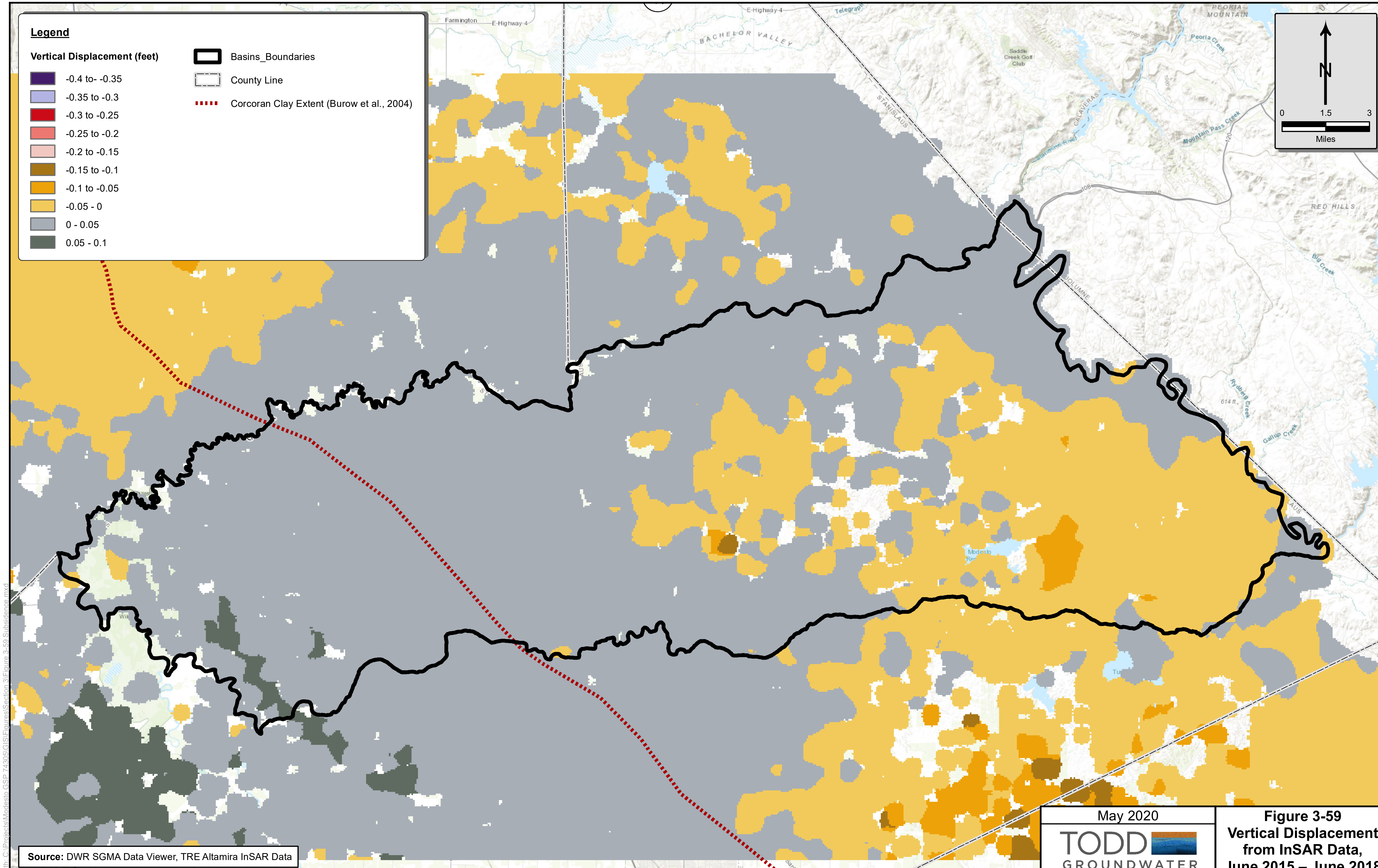

Figure 3-59
Vertical Displacement from InSAR Data, June 2015 – June 2018

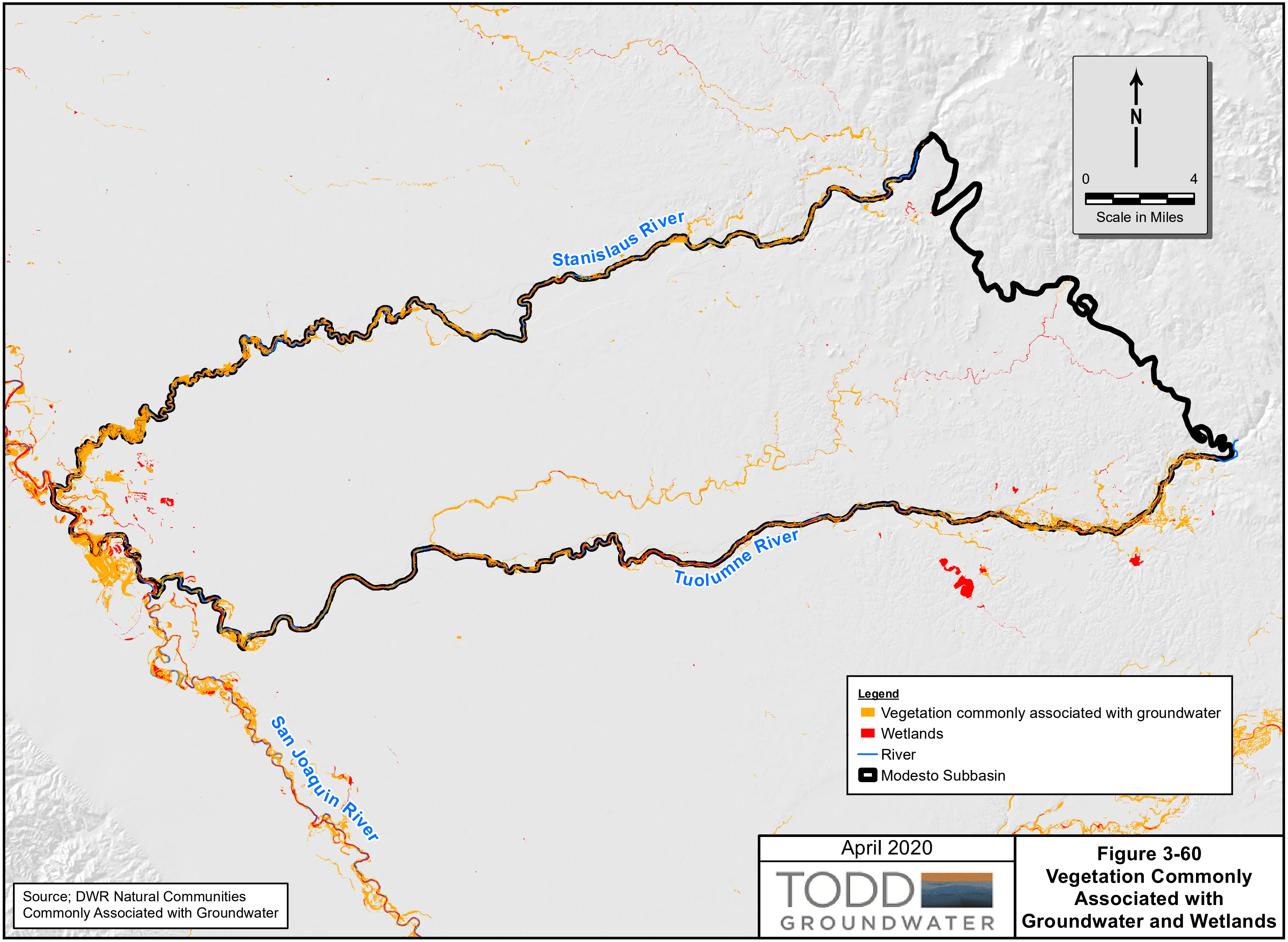

Figure 3-60
Vegetation Commonly Associated with Groundwater and Wetlands